

# Heat and Mass Transfer I

## Lecture



---

## “Heat and Mass Transfer I” (Lecture)

Edition of August 15, 2016

RWTH Aachen University  
Institute of Heat and Mass Transfer  
Univ.-Prof. Dr.-Ing. R. Kneer  
Augustinerbach 6  
D-52056 Aachen  
Fax 0241/80-95400  
Phone 0241/80-92143  
[www.wsa.rwth-aachen.de](http://www.wsa.rwth-aachen.de)  
[info@wsa.rwth-aachen.de](mailto:info@wsa.rwth-aachen.de)



---

# Contents

<b>1</b>	<b>Introduction</b>	<b>1</b>
1.1	Heat Radiation . . . . .	3
1.2	Heat Conduction . . . . .	4
1.3	Convection . . . . .	5
<b>2</b>	<b>Heat Radiation</b>	<b>9</b>
2.1	Radiation properties . . . . .	9
2.1.1	Wave/Quantum duality . . . . .	9
2.1.2	Intensity distribution of radiation and entire radiation intensity	12
2.1.2.1	Planck's distribution law . . . . .	12
2.1.2.2	Wien's Law of displacement . . . . .	13
2.1.2.3	Stefan-Boltzmann's law . . . . .	14
2.1.2.4	Radiation emissions in a specific spectral range . . . . .	14
2.1.3	Reflection, Absorption, Transmission . . . . .	17
2.1.4	Kirchhoff's law . . . . .	19
2.1.5	Radiation from a diffuse surface and direction-dependent radiation . . . . .	24
2.2	Radiation transfer . . . . .	25
2.2.1	Radiation flux - radiosity . . . . .	25
2.2.2	Radiation transfer between two bodies . . . . .	27
2.2.3	Radiation transfer between two grey surfaces . . . . .	32
2.2.4	Radiation transfer between two infinitely long grey plates . . . . .	32
2.2.5	Radiation transfer between two self-enclosed grey bodies . . . . .	34
<b>3</b>	<b>Conduction</b>	<b>37</b>
3.1	Differential equations of the temperature field . . . . .	37
3.2	Steady state, one-dimensional heat conduction without heat sources . . . . .	41
3.2.1	Plane walls with given surface temperatures . . . . .	41
3.2.2	Tube wall with predefined surface temperatures . . . . .	43
3.2.3	Plane walls with convective heat transfer . . . . .	46
3.2.4	Tube wall with convective heat transfer . . . . .	48
3.2.5	Heat conduction in fins . . . . .	49
3.3	Steady state, one-dimensional heat conduction with heat sources . . . . .	57
3.4	Steady state, multi-dimensional heat conduction without heat sources	59

3.5	Unsteady state heat conduction without heat sources . . . . .	64
3.5.1	Bodies with high values of thermal conductivity . . . . .	65
3.5.2	One-dimensional, unsteady state heat conduction examples . .	67
3.5.3	Dimensionless numbers and diagrams . . . . .	78
<b>4</b>	<b>Convection</b>	<b>91</b>
4.1	Conservation laws for laminar, steady state, two-dimensional flow . .	93
4.1.1	Equation of continuity . . . . .	94
4.1.2	Equations of momentum . . . . .	95
4.1.2.1	Equation of momentum in x-direction . . . . .	95
4.1.2.2	Equation of momentum in y-direction . . . . .	97
4.1.3	Equation of energy conservation . . . . .	98
4.2	Forced convection - boundary layer equations for laminar, steady state flow . . . . .	101
4.2.1	Exact solutions for the equations of boundary layers . . . . .	103
4.2.2	A simple approximation for the boundary layer equations . . . .	106
4.3	Natural convection - boundary layer equations for laminar, steady state flow . . . . .	111
4.4	Heat transfer in turbulent flows . . . . .	116
4.5	Application of dimensional analysis for heat transfer . . . . .	118
<b>5</b>	<b>Heat transfer laws</b>	<b>123</b>
5.1	Heat transfer laws for forced convection . . . . .	126
5.1.1	Forced convection at flows along surfaces . . . . .	126
5.1.1.1	Flat plate - laminar boundary layer flow . . . . .	126
5.1.1.2	Flat plate - turbulent boundary layer flow $Re_{x,crit} \approx 2 \cdot 10^5$ . . . . .	128
5.1.1.3	Cylinders in a flow parallel to their longitudinal axis .	131
5.1.1.4	Cylinders in a flow perpendicular to their longitudinal axis . . . . .	131
5.1.1.5	Bundles of smooth tubes in an orthogonal flow . . . .	134
5.1.1.6	Flow around spheres . . . . .	136
5.1.2	Forced convection in tubes . . . . .	137
5.1.2.1	Laminar flow in tubes, $Re_{d,crit} \approx 2300$ . . . . .	137
5.1.2.2	Turbulent flow in tubes, $Re_{d,crit} \approx 2300$ . . . . .	140
5.2	Heat transfer laws for natural convection . . . . .	141
5.2.1	Natural convection at circumflowed bodies . . . . .	141
5.2.1.1	Vertical plate - laminar boundary layer flow . . . .	141
5.2.1.2	Vertical plate - turbulent boundary layer flow . . . .	143
5.2.1.3	Vertical cylinder - laminar and turbulent boundary layer flow . . . . .	144

5.2.1.4	Horizontal cylinder - laminar and turbulent boundary layer flow, isothermal surface . . . . .	144
5.2.1.5	Horizontal plates - laminar and turbulent boundary layer flow, Holman (1976) . . . . .	145
5.2.2	Natural convection in enclosed volumes . . . . .	146
5.2.2.1	Fluid layers between isothermal, vertical walls . . . . .	146
5.2.2.2	Fluid layers between isothermal, horizontal walls . .	147
<b>6</b>	<b>Mass transfer</b>	<b>149</b>
6.1	Molecular concept of diffusion processes . . . . .	149
6.1.1	Diffusion in gases . . . . .	149
6.1.2	Diffusion in liquids . . . . .	151
6.2	Fundamentals . . . . .	153
6.3	Mass transfer in flows . . . . .	155
6.3.1	Examples for transient diffusion . . . . .	158
6.4	Transition laws in mass transfer . . . . .	159
6.4.1	Analogy between heat and mass transfer . . . . .	160
6.4.2	Solving the one-dimensional transient heat conduction and diffusion problem respectively . . . . .	161
6.5	Evaporation at a liquid surface . . . . .	163
6.5.1	Determining the mass transfer coefficient . . . . .	165
<b>Appendix</b>		<b>III</b>
Material properties . . . . .		III
Bessel function . . . . .		IX



---

# Chapter 1

## Introduction

This course focuses on the principles of heat transfer in different mediums or between two mediums. A short introduction in mass transfer is presented at the end of this lecture.

The terms “heat” and “heat flow” have already been introduced in the course *Thermodynamics*, in connection to the first law of thermodynamics.

Thermal equilibrium between the two heat containers A and B in an adiabatic system will be used to demonstrate the distinctions of these two courses.

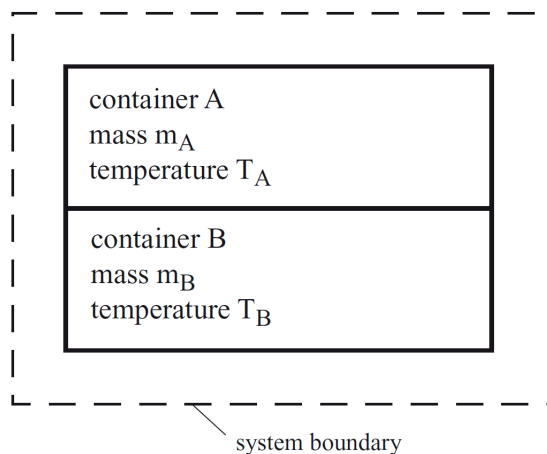


Figure 1.1: Thermal equilibrium between two heat containers

For the adiabatic system, with no external work and an unchanged external energy, the following equation, derived from the first law of thermodynamics is valid:

$$\underbrace{dQ}_0 + \underbrace{dW}_0 = dU + \underbrace{dE_a}_0$$

or

$$dU = 0$$

In other words, the internal energy of the system remains unchanged during the process of heat transfer leading to temperature equilibrium. Since the internal energy of the entire system consists of two components, there are at two different times  $t_0$  and  $t_1$

$$(U_A + U_B)_{t=t_0} = (U_A + U_B)_{t=t_1}$$

or, as long as no phase changes occur,

$$(m_A c_A T_A + m_B c_B T_B)_{t=t_0} = (m_A c_A T_A + m_B c_B T_B)_{t=t_1}$$

After a long period of time, when the temperature equilibrium concludes, the temperatures of both components will reach the following common final temperature:

$$T_{t \rightarrow \infty} = \frac{(m_A c_A T_A + m_B c_B T_B)_{t=t_0}}{m_A c_A T_A + m_B c_B T_B}$$

and the heat  $Q$  transferred over the dividing wall of the two containers can be calculated from the equilibrium of container A:

$$Q_A = (U_A)_{t \rightarrow \infty} - (U_A)_{t=t_0} = m_A c_A ((T_A)_{t \rightarrow \infty} - (T_A)_{t=t_0})$$

or

$$Q_A = -Q_B$$

So by using thermodynamics it is not possible to make conclusions about the mechanisms, which transfer the heat and hence about the temporal progress of the process. The necessary methods will be presented in this introductory course.

Mechanisms of heat transfer The methods of heat transfer in gaseous, liquid or solid media or between two media can be classified into:

- transfer through radiation
- transfer through conduction
- transfer through convection

The physical principles of these three methods will only be outlined in this introduction. An in-depth study will be carried out in later chapters of this lecture.

## 1.1 Heat Radiation

If two bodies of different temperatures are insulated in an evacuated container, we can expect temperature equilibrium after a certain period of time. This process of temperature equilibrium is based on heat transfer through electromagnetic waves, the heat radiation.

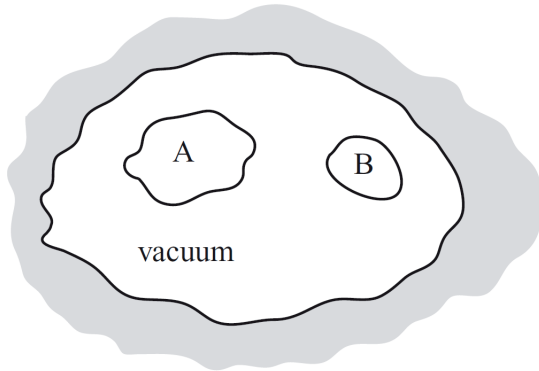


Figure 1.2: Heat transfer between two bodies through radiation

Thermodynamic considerations show that an ideal body, the so-called "black" body radiates heat, which is proportional to the fourth power of its absolute temperature. Thus, the net heat flow density is

$$\frac{\dot{Q}}{A} \propto (T_A^4 - T_B^4) \quad \text{oder} \quad \frac{\dot{Q}}{A} = \sigma (T_A^4 - T_B^4)$$

with  $\sigma$  as the Stefan-Boltzmann constant which has the value  $\sigma = 5,669 \cdot 10^{-8} \text{ W/m}^2\text{K}^4$ .

When radiation between technical surfaces takes place, the deviation from the emissivity of an ideal *black* body must be taken into account. This is done by introducing

the deviation factor,  $F_\epsilon$ . In addition another factor,  $F_A$ , will be introduced. It represents the deviations that occur by the fact that the emitted radiation from one body is not necessarily fully absorbed by the other due to their mutual orientation in space. Determining the values of these factors can be very complicated and will be discussed later on in detail. Much more elaborate are the processes of radiation that involve a gaseous atmosphere between the two bodies.

## 1.2 Heat Conduction

If there is a difference in temperature within a body then we expect heat to be transferred from one area of higher temperature to the area where the temperature is lower. The heat flow per area is proportional to the temperature gradient:

$$\frac{\dot{Q}}{A} \propto \frac{dT}{dx}.$$

The proportionality constant is substance-specific and is called thermal conductivity  $\lambda [W/mK]$

$$\frac{\dot{Q}}{A} = -\lambda \frac{dT}{dx}$$

The minus sign indicates that the heat flows in direction of the *temperature gradient*. In order to determine the heat flow quantitatively, the thermal conductivity must be known. In gases the thermal conductivity is determined by the collisions of gas molecules, where the kinetic energy of a gas molecule is presumed proportional to its temperature. Moving from one area of higher temperature to an area of lower temperature, the molecule loses part of its energy and momentum through collisions. Assuming the gas to be a continuum this process can be considered a process of heat conduction in gases.

For simple gas molecules and moderate temperatures thermal conductivity can be calculated on the basis of the kinetic theory.

Liquids and solids require more precise assumptions than the above theoretical premises, so that in general the values of the thermal conductivity are determined experimentally.

Table 1.1: Thermal conductivity of selected materials at 0°C

Material	Thermal Conductivity $\lambda$ [W/mK]
Metals	
Silver	410
Copper	385
Carbon-enriched steel	43
Chromium-Nickel-enriched steel	16
Non metallic solids	
Quartz	2,4
Sand rock	1,8
Window glass	0,8
Liquids	
Mercury	8,21
Water	0,56
Cooling agent R 12	0,07
Gases	
Hydrogen	0,175
Air	0,024
Water vapour	0,021

The table above lists a few thermal conductivity constants to show the order of their values for different mediums. A more detailed list can be found in Appendix A.

## 1.3 Convection

It is generally known that a hot object cools faster when it is being blown on instead of being left to cool down in stationary air. The heat conductivity mechanism on the air side of the system is additionally reinforced with the mechanism of heat transfer through the macroscopic air flow along the body. The intensity of this so-called convective heat transfer is proportional to the temperature difference between the body surface area and the cooling medium.

The proportionality constant - the convection heat-transfer coefficient  $\alpha$  - depends on many parameters such as the flow velocity, the medium type, etc. Even so, the convection heat-transfer coefficient can be determined theoretically in the simplest

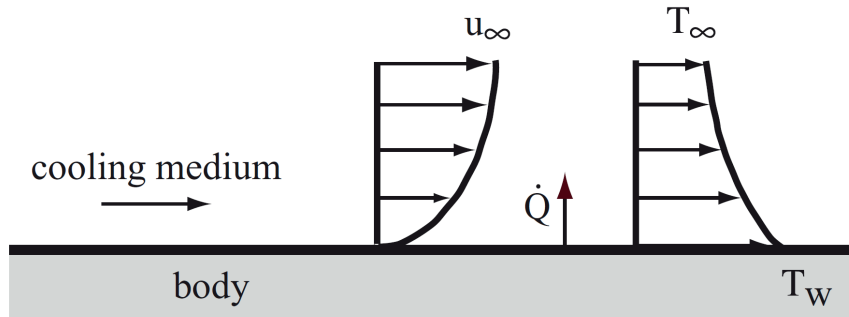


Figure 1.3: Heat flow of a body in the flow stream of the cooling medium

Table 1.2: Order of magnitude of the convection heat-transfer coefficient

Substance	convection heat-transfer coefficient $\alpha[\text{W}/\text{m}^2\text{K}]$
Natural convection, Gas	3 – 20
Natural convection, Water	100 – 600
Forced convection, Gas	10 – 100
Forced convection, Water	500 – 10.000
Boiling Water	2.000 – 25.000
Water vapour condensation	5.000 – 100.000

cases using the principles of fluid dynamics. Yet, in many real world situations, it can only be determined experimentally.

The order of magnitude of the convection heat-transfer coefficient is listed in the table above. In general, these three basic mechanisms of heat transfer occur simultaneously in real world problems. This can be shown for example in the steam generator of a power plant.

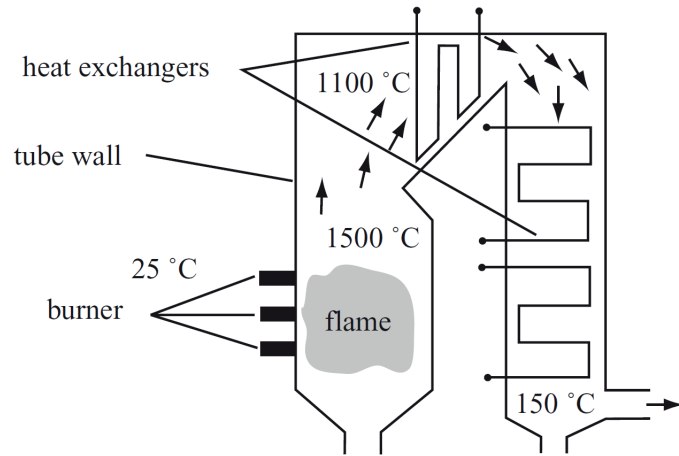


Figure 1.4: Diagram of a steam generator in a coal-fired power plant

In the heat chamber of the steam generator heat is transmitted from the heated gases to the pipe wall in order to vaporize the water in the pipes. The following diagram, a section view of the pipe wall, shows the heat transfer and the corresponding mechanisms.

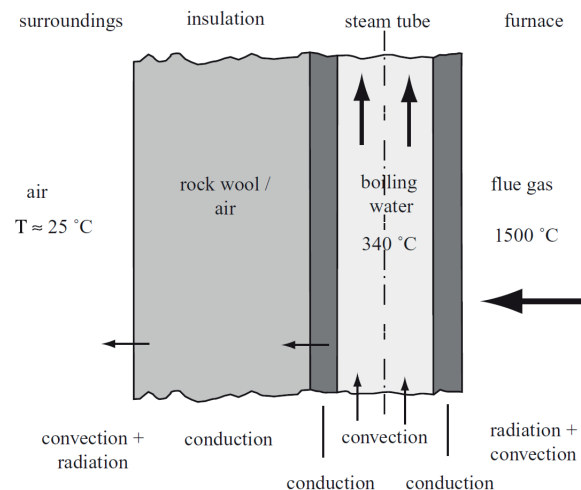


Figure 1.5: Heat transfer mechanisms at the tube wall of a steam generator



---

# **Chapter 2**

## **Heat Radiation**

Conduction and convection are heat transfer mechanisms, where energy is transported through molecular processes respectively macroscopic movement of fluids, whereas heat radiation does not require any medium, since it is based on electromagnetic processes. The intensity and the sort of radiation, emitted from a gaseous, liquid or solid body depends on the surface properties of the body and its temperature, yet they are independent of its surroundings. If not only the emitted radiation is to be considered, but also the heat exchange between the body and its surroundings, then the type, temperature and geometrical orientation in space of the surrounding bodies must be taken into account. In spite of the fact that in most heat transfer problems energy is simultaneously transported through conduction and/or convection and radiation, henceforth only radiation will be regarded, as far as possible.

### **2.1 Radiation properties**

#### **2.1.1 Wave/Quantum duality**

Physics teaches us that radiation can be explained both using the wave as well as the quantum mechanics theory. This dual character has been impressively proven experimentally, see fig. 2.1, Whitaker (1977). Exposing a photographic plate with low light intensity through an aperture with two thin slits, the following interference

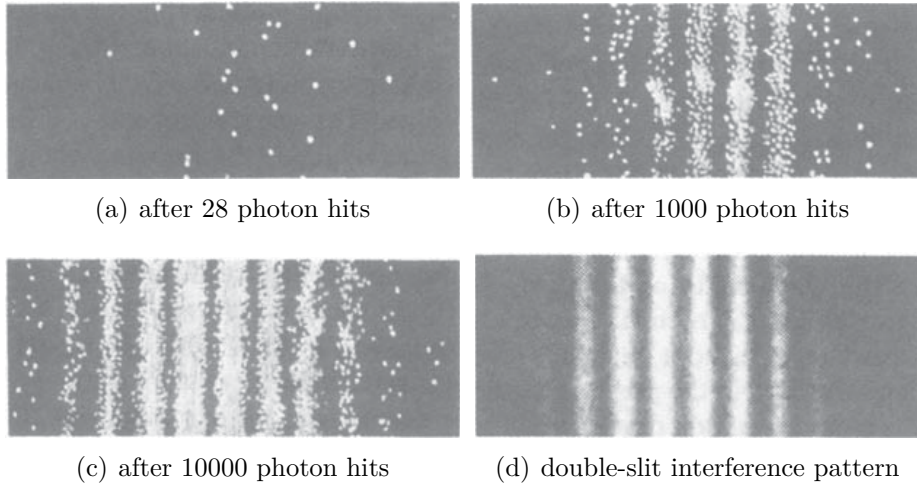


Figure 2.1: Double-slit experiment by E.R. Huggins, Physics I, W.A. Benjamin, Inc., Menlo Park, California, USA, 1968, from Whitaker (1977)

patterns, Fig. 2.1(a), 2.1(b), 2.1(c) and 2.1(d), which depend on the exposure time can be observed.

After a very short time interval, Fig. 2.1(a), distinct light points can be recognized, which lead to the conclusion that individual light quanta - photons - hit the plate. At longer time periods it happens that the photons do not hit the screen at random, but form a striped pattern, Fig. 2.1(b) and 2.1(c). These stripes form an interference pattern, which can also be observed during superposition of circular waves passing through a diffraction grating and striking a dark screen behind it, Fig. 2.1(d). This demonstrates the wave character of radiation. The following figure shows the electromagnetic spectrum and the wavelengths at which heat radiation takes place Fig. 2.2.

The wavelength  $\lambda$ , usually given in the unit  $[\mu\text{m}]$  is related to the frequency  $\nu$  through the speed of light  $c$  as shown in the following equation

$$\lambda = \frac{c}{\nu} \quad (2.1)$$

The wave-like nature of radiation shows its character when the size of the "slits" through which the rays are refracted has the same order of magnitude as the wavelength of the radiation.

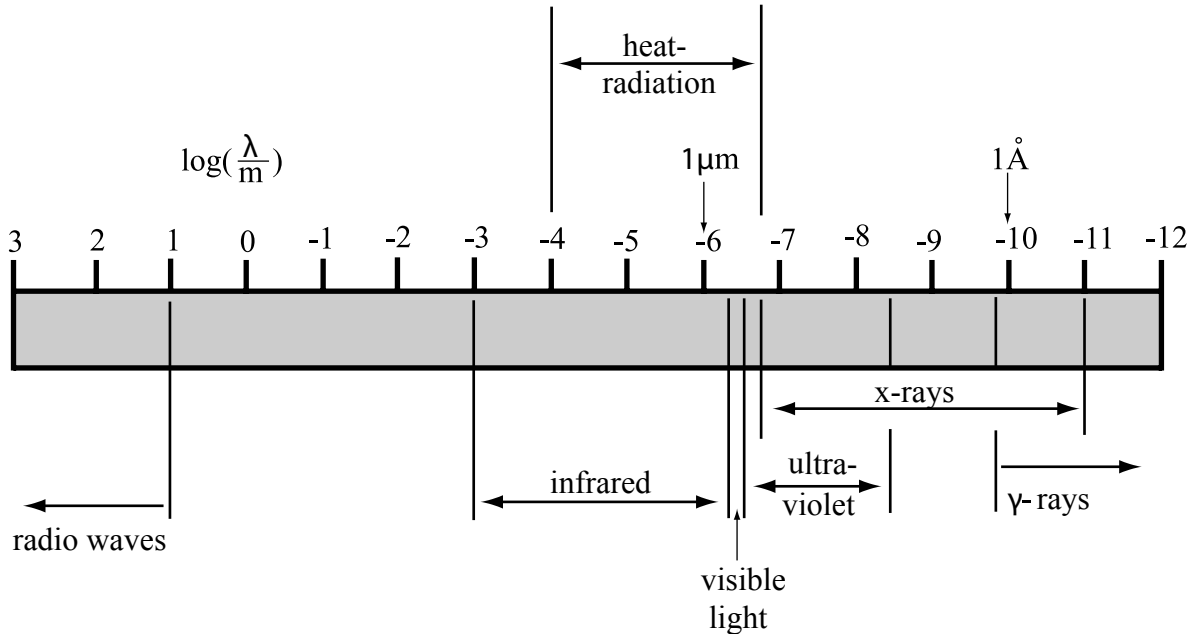


Figure 2.2: Electromagnetic spectrum

The spectrum shown above shows clearly that the radiation wavelengths are much smaller than the size of a typical "slit". Thus, the quantum character dominates during heat radiation. According to Planck, each quantum or photon has the energy

$$E = h \nu = \frac{hc}{\lambda} \quad (2.2)$$

where Planck's constant is  $h = 6,626 \cdot 10^{-34} [Js]$ .

Regarding equation (2.2) it is obvious that the transported energy of each quantum relates inversely proportional to the wavelength  $\lambda$ . This relation leads to the definition of the wavenumber  $\eta$ :

$$\eta = \frac{1}{\lambda} \quad (2.3)$$

In contrast to the wavelength, the wavenumber offers the advantage of a proportional relation to the transported energy of a quantum. This is only valid if the propagation velocity of the radiation does not change, see equation (2.2). If the velocity changes - e.g. by entering into a medium with a different refraction index - the wavelength changes as well as the wavenumber, see equation (2.2). So, for

problems with different refraction indexes it is better to consider the frequency  $\nu$ , because it does not depend on the refraction index.

### 2.1.2 Intensity distribution of radiation and entire radiation intensity

The radiation emitted from a body surface covers the whole spectrum of wavelengths. The intensity of radiation depends on the absolute temperature of a body. A simple model defines the so-called "black body": this body absorbs all the radiation falling upon it.

#### 2.1.2.1 Planck's distribution law

Max Planck derived from the theory of quantum mechanics a relationship for the distribution of radiation intensity over the wavelength of a black body. **Planck's distribution law** describes the emitted radiation intensity  $\dot{q}_{b\lambda}''$  in an infinitesimal wavelength range  $d\lambda$ , the so-called monochrome or spectral emissive power. It is defined as follows:

$$\dot{q}_{b\lambda}'' = \frac{c_1 \lambda^{-5}}{\exp\left[\frac{c_2}{\lambda T}\right] - 1} \left[ \frac{W}{m^2} \frac{1}{m} \right] \quad (2.4)$$

where b indicates the black body. The spectral emissive power is a function of temperature of the emitting body.

The constants  $c_1$  and  $c_2$  can be determined using Planck's constant  $h$ , the Boltzmann constant  $k$  and the value for the speed of light in vacuum  $c_o$ . Hence, their values are

$$c_1 = 2\pi h c_o^2 = 2\pi 6,6256 10^{-34} (2,9979 10^8)^2 = 3,741 10^{-16} \text{ Wm}^2$$

and

$$c_2 = h \frac{c_o}{k} = 6,6256 10^{-34} \frac{2,9979 10^8}{1,3805 10^{-23}} = 1,439 10^{-2} \text{ mK}$$

with

$$k = \frac{R_m}{N_L} = \frac{8,3143}{6,0225 10^{23}} = 1,3805 10^{-23} \text{ J/K},$$

and  $N_L$  as the Loschmidt number.

The following diagram 2.3 shows Planck's distribution law for selected temperatures and radiation wavelengths.

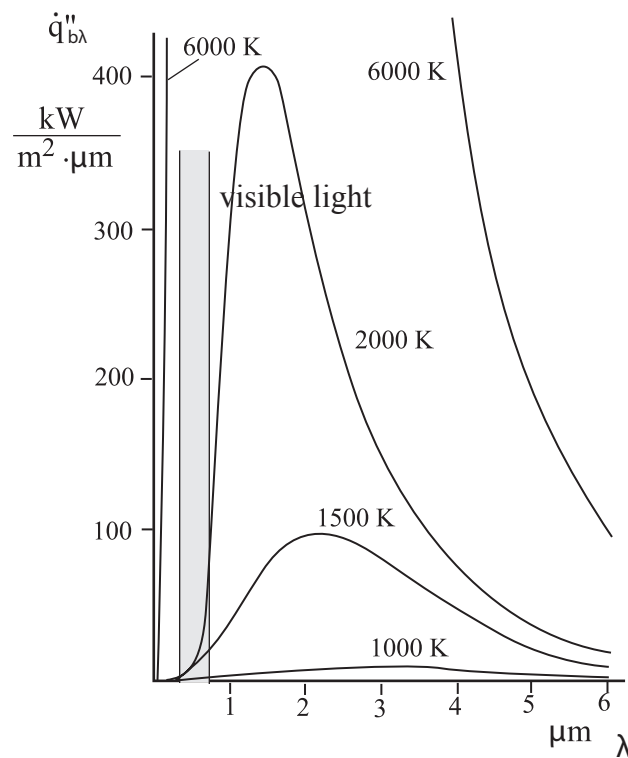


Figure 2.3: Spectral radiant flux density of a black body

Apparently the emitted radiation intensity increases with increasing temperature and the corresponding maximum shifts to smaller wavelengths as the temperature increases.

### 2.1.2.2 Wien's Law of displacement

The derivative of equation (2.4) gives the position of the maxima of the curve. This is the so-called **Wien's Law of displacement**

$$\lambda_{max} = \frac{2898 \mu\text{m}K}{T} \quad (2.5)$$

### 2.1.2.3 Stefan-Boltzmann's law

In order to determine the entire emitted radiation power per area, Planck's distribution law (2.4) will be integrated over the entire wavelength range. An illustrative example is given in Figure 2.4, with the area below the intensity curve being equal to the emitted radiation power. This integration leads to the **Stefan-Boltzmann law**.

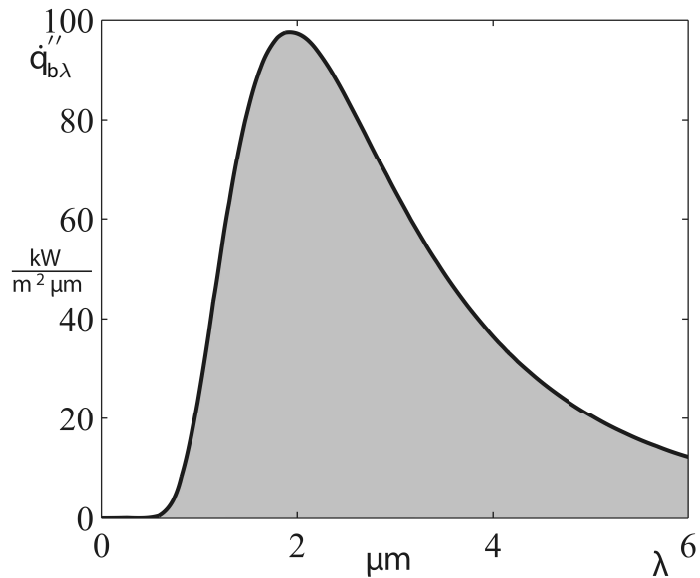


Figure 2.4: Entire emitted radiation, shown as the integral of the Planck-distribution

$$\dot{q}_b'' = \int_{\lambda=0}^{\infty} \dot{q}_{b\lambda}'' d\lambda = \int_{\lambda=0}^{\infty} \frac{c_1 \lambda^{-5}}{\exp\left[\frac{c_2}{\lambda T}\right] - 1} d\lambda = \sigma T^4 \quad (2.6)$$

The Stefan-Boltzmann constant  $\sigma$  has the value  $\sigma = 5,67 \cdot 10^{-8} \left[ \frac{\text{W}}{\text{m}^2 \text{K}^4} \right]$ .

### 2.1.2.4 Radiation emissions in a specific spectral range

Occasionally, instead of considering the radiation emissions of the entire spectrum, it is necessary to consider the emissions only in a specific range between the wave-

lengths  $\lambda_1$  and  $\lambda_2$ . The radiation density of this interval can be determined by integration of the Planck-distribution:

$$\dot{q}_{b,\lambda_1 \rightarrow \lambda_2}'' = \int_{\lambda_1}^{\lambda_2} \dot{q}_{b\lambda}'' d\lambda \quad (2.7)$$

The solution of this integral can be described by the following series approach:

$$F_{0 \rightarrow \lambda T} = \frac{15}{\pi^4} \sum_{n=1}^{\infty} \left[ \frac{e^{-n\xi}}{n} \left( \xi^3 + \frac{3\xi^2}{n} + \frac{6\xi}{n^2} + \frac{6}{n^3} \right) \right] \quad (2.8)$$

with

$$\xi = \frac{c_2}{\lambda T}$$

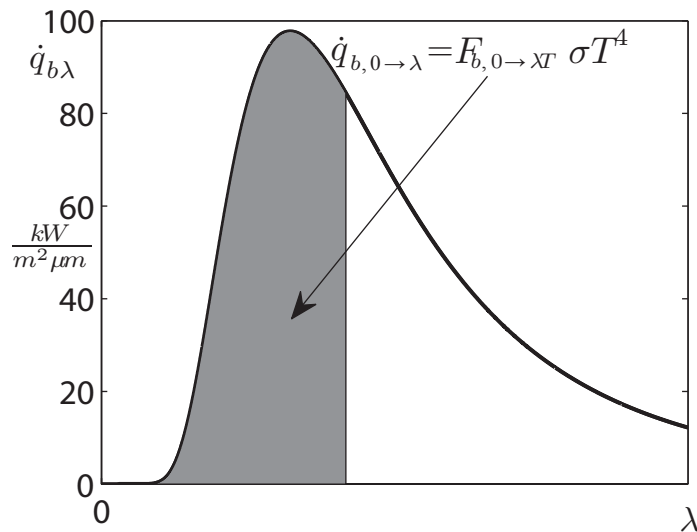
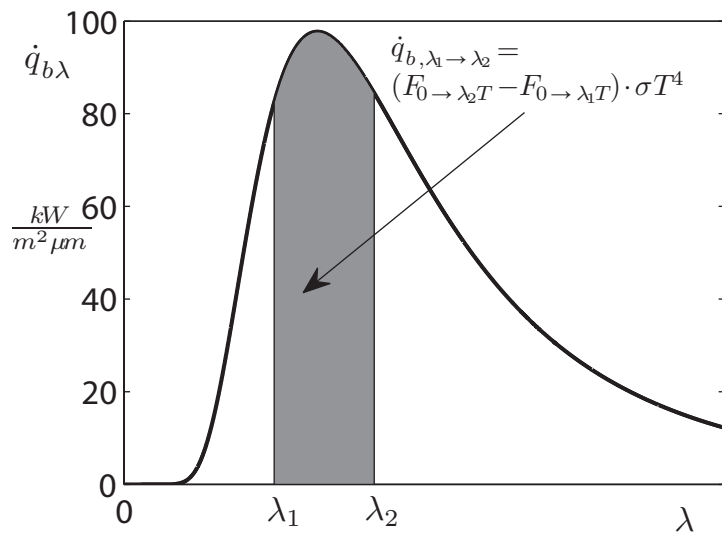
The factor  $F_{0 \rightarrow \lambda T}$  describes the ratio between the entire emitted radiation intensity and the emitted radiation intensity in the spectral range between 0 and  $\lambda$ . By using Stefan-Boltzmann law the actual emitted radiation intensity, shown in Figure 2.5 can be calculated:

$$\dot{q}_{b,0 \rightarrow \lambda}'' = F_{0 \rightarrow \lambda T} \cdot (\sigma T^4) \quad (2.9)$$

The radiation intensity between any interval of the spectrum - shown in Figure 2.6 - can be described as follows:

$$\dot{q}_{b,\lambda_1 \rightarrow \lambda_2}'' = (F_{0 \rightarrow \lambda_2 T} - F_{0 \rightarrow \lambda_1 T}) \cdot \sigma T^4 \quad (2.10)$$

For simple calculations the series approach, equation (2.8), is not practical; therefore tables with exemplary values for the factor  $F_{0 \rightarrow \lambda T}$  are used. The series approach is more common for computer-based calculations. Even with a small number of links  $n$ , results of sufficient accuracy can be obtained.

Figure 2.5: Emitted radiation power between  $0 \rightarrow \lambda$ Figure 2.6: Emitted radiation power between  $\lambda_1 \rightarrow \lambda_2$

### 2.1.3 Reflection, Absorption, Transmission

When radiation of a specific wavelength falls upon the surface of a (non black) body, this radiation is either reflected off the surface, absorbed by the body or transmitted through it, whereas in case of reflection, it can be distinguished between fully reflective (angle of incidence is equal to the angle of reflection) or diffuse, in which case the radiation is equally distributed in all directions. The reflected component

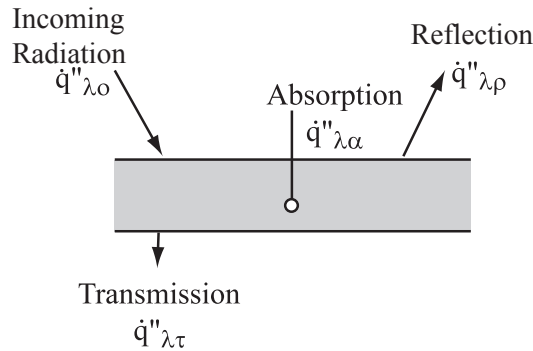


Figure 2.7: Contributions to radiation transport

of the radiation is called reflectivity  $\rho(\lambda)$ , the absorbed portion absorptivity  $\alpha(\lambda)$  and the transmitted part of radiation transmissivity  $\tau(\lambda)$ .

$$\rho(\lambda) \equiv \frac{\dot{q}_{\lambda\rho}''}{\dot{q}_{\lambda o}''}; \quad \alpha(\lambda) \equiv \frac{\dot{q}_{\lambda\alpha}''}{\dot{q}_{\lambda o}''}; \quad \tau(\lambda) \equiv \frac{\dot{q}_{\lambda\tau}''}{\dot{q}_{\lambda o}''} \quad (2.11)$$

So that

$$\rho(\lambda) + \alpha(\lambda) + \tau(\lambda) = 1 \quad (2.12)$$

We can distinguish between the following special cases:

- Since most solids are opaque to radiation, the incident radiation is partly reflected and partly absorbed in thin layers of a few  $\mu m$  (electric conductors) up to  $2 mm$  (electric insulators)

$$\rho(\lambda) + \alpha(\lambda) = 1 \quad (2.13)$$

- Solids, which fully absorb all radiation have already been defined as “black bodies”

$$\alpha(\lambda) = \alpha = 1 \quad (2.14)$$

- “Grey” bodies, on the other hand, are bodies with radiation properties that are independent of the wavelength and which radiate in all directions (diffuse radiation) ( $\alpha(\lambda) = \alpha$ ,  $\rho(\lambda) = \rho$ ,  $\tau(\lambda) = \tau$ )

$$\rho + \alpha + \tau = 1 \quad (2.15)$$

- Gases normally do not reflect radiation, hence

$$\alpha(\lambda) + \tau(\lambda) = 1 \quad (2.16)$$

The following diagram shows experimental results of measurements of the spectral absorptivity of a polished and an anodised aluminium plate for wavelengths in the range of heat radiation, as used in Whitaker (1977) .

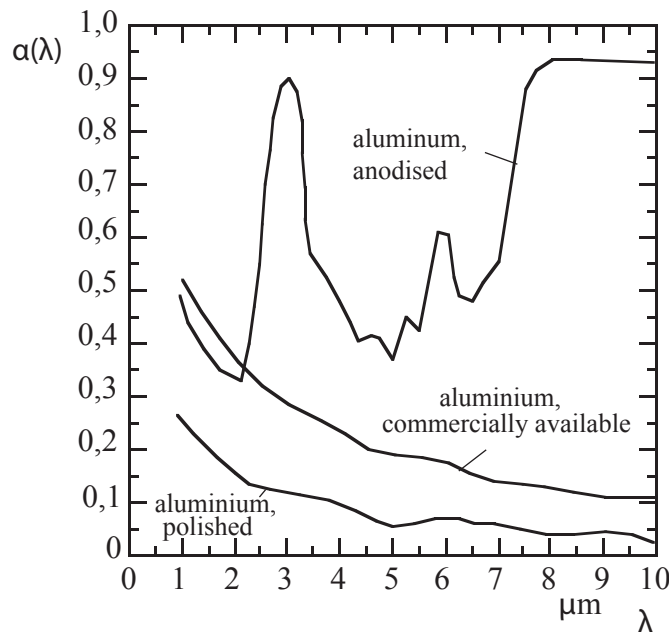


Figure 2.8: Absorptivity of a polished and an anodised aluminium plate, Whitaker (1977) at 0°C

The reduction of the absorptivity at increasing wavelengths of both the polished and the typical (commercially available) aluminium is characteristic for all electric conductors. Isolators, such as the surface layer of the anodised aluminium, show the opposite trend.

In correspondence to the spectral properties of a body, the total reflectivity, the total absorptivity and the total transmissivity can be defined as mean over all wavelengths, respectively

$$\rho = \frac{\int_0^{\infty} \dot{q}_{\lambda\rho}'' d\lambda}{\int_0^{\infty} \dot{q}_{\lambda o}'' d\lambda}, \quad (2.17)$$

$$\alpha = \frac{\int_0^{\infty} \dot{q}_{\lambda\alpha}'' d\lambda}{\int_0^{\infty} \dot{q}_{\lambda o}'' d\lambda}, \quad (2.18)$$

$$\tau = \frac{\int_0^{\infty} \dot{q}_{\lambda\tau}'' d\lambda}{\int_0^{\infty} \dot{q}_{\lambda o}'' d\lambda}, \quad (2.19)$$

which again yields

$$\rho + \alpha + \tau = 1. \quad (2.20)$$

Unlike the spectral values, the total values are not only dependent on the temperature of the body in question, but they also depend on the body that emits the incident radiation. Since usually very little is known about the dependence of the radiation properties on the wavelength and, in general, their determination proves to be very difficult, normally only constant mean values are used in practice.

#### 2.1.4 Kirchhoff's law

Kirchhoff's law states the relationship between the absorbed and the emitted radiation of a body. As shown in the following experiment (see figure below), two bodies with evacuated cavities and of different materials, adiabatic to the outside, have been positioned so that a small opening connects the cavities. Radiation coming from cavity 1 passes through the orifice into cavity 2, where it is being absorbed

after a number of reflections. The same applies for radiation coming from cavity 2

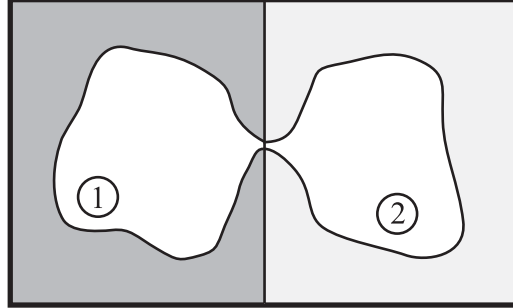


Figure 2.9: Radiation exchange between two evacuated cavities

and arriving in cavity 1. In thermal equilibrium, i.e. when temperature compensation between the two bodies has reached, the following must apply according to the second law of thermodynamics

$$\dot{q}_{1 \rightarrow 2}'' = \dot{q}_{2 \rightarrow 1}''$$

Therefore, it can be concluded that the difference of the wall properties of the cavities does not influence the radiation flow between them.

If, for example, one of the two cavities is a black body, then the above stated still applies. This yields

$$\dot{q}_{1 \rightarrow 2}'' = \dot{q}_b'' \text{ or in general } \dot{q}_C'' = \dot{q}_b''$$

hence, it can be stated that the radiation of any cavity is equivalent to the radiation of a black body.

If in one of the cavities C a small, non-black body 1 with the surface area  $A_1$  is placed, then in thermal equilibrium, the absorbed portion of radiation from the cavity by body 1 has to be equal to the emitted radiation of the cavity. Furthermore, having in mind that the cavity radiates as a black body, it follows

$$\alpha_1 \dot{q}_b'' A_1 = \dot{q}_{\epsilon 1}'' A_1 \quad (2.21)$$

Which yields

$$\alpha = \frac{\dot{q}_{\epsilon 1}''}{\dot{q}_b''} \quad (2.22)$$

which is a restatement of Kirchhoff's law that the absorptivity of a body is equal to the relationship of the emitted radiation to that of a black body with the same temperature. This relationship is defined as emissivity  $\epsilon$

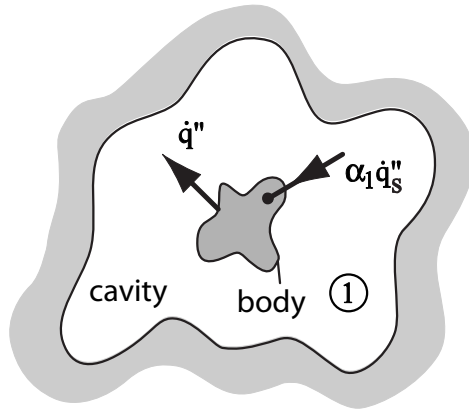


Figure 2.10: Radiation exchange between a body and a cavity

$$\epsilon \equiv \frac{\dot{q}_\epsilon''}{\dot{q}_b''} \quad (2.23)$$

Or rewritten in terms of Kirchhoff's law

$$\alpha = \epsilon. \quad (2.24)$$

Strictly speaking, Kirchhoff's law is valid only for monochromatic radiation, i.e.

$$\alpha(\lambda) = \epsilon(\lambda). \quad (2.25)$$

Yet, for many practical purposes equation (2.24) must be employed to avoid unnecessary complex computations or also because of the absence of spectral data. The necessary requirements for the validity of Kirchhoff's law will be discussed next. For this purpose the total emissivity  $\epsilon$  has to be determined by integrating over the spectral radiation power.

$$\epsilon = \frac{\dot{q}_\epsilon''}{\dot{q}_b''} = \frac{\int_0^\infty \dot{q}_{\lambda\epsilon}'' d\lambda}{\int_0^\infty \dot{q}_{\lambda b}'' d\lambda}. \quad (2.26)$$

Defining the corresponding spectral emissivity as in equation (2.23)

$$\epsilon(\lambda) \equiv \frac{\dot{q}_{\lambda\epsilon}''}{\dot{q}_{\lambda b}''}, \quad (2.27)$$

equation (2.26) yields a relationship that depends on the type of the body and its temperature

$$\epsilon = \frac{\int_0^\infty \epsilon(\lambda) \dot{q}_{\lambda b}'' d\lambda}{\int_0^\infty \dot{q}_{\lambda b}'' d\lambda} = \epsilon(T_{body}). \quad (2.28)$$

The total absorption  $\alpha$  can be written as

$$\alpha = \frac{\dot{q}_\alpha''}{\dot{q}_o''} = \frac{\int_0^\infty \dot{q}_{\lambda\alpha}'' d\lambda}{\int_0^\infty \dot{q}_{\lambda o}'' d\lambda}. \quad (2.29)$$

$$\alpha \equiv \frac{\dot{q}_{\lambda\alpha}''}{\dot{q}_{\lambda o}''} \quad (2.30)$$

Equation (2.29) leads to the following relationship, which depends on the type of both radiating bodies under investigation and their corresponding temperatures

$$\alpha = \frac{\int_0^\infty \alpha(\lambda) \dot{q}_{\lambda o}'' d\lambda}{\int_0^\infty \dot{q}_{\lambda o}'' d\lambda} = \alpha(T_{body}, T_{rad}). \quad (2.31)$$

Comparison of equation (2.28) and (2.31) makes clear that Kirchhoff's law (2.24), defined for the total emissivity  $\epsilon$  and total absorptivity  $\alpha$ , may not always be valid since the incident and emitted radiation are not equally dependent on the temperature and spectral distribution.

Two special cases should be mentioned for which Kirchhoff's law for the total radiation properties remains valid and which can be derived from equation (2.28) and (2.31)

- The radiating body is a black or grey body whose temperature is equal to that of the investigated body,  $T_{rad} = T_{body}$

- The surfaces of the body are grey, i.e. their absorptivity is independent from the wavelength.

Especially the second case is important, since it is valid for many practical cases.

If a high level of accuracy is required, then the exact knowledge of the monochromatic radiation properties is necessary.

The following diagram, Figure 2.11 shows the radiant flux density of an actual real body at  $T = 2000\text{K}$ . The results of Planck's distribution law, equation (2.4), for a black and a grey body are shown as a comparison. A detailed summary of emissivity values of different materials is given in the Appendix A6.

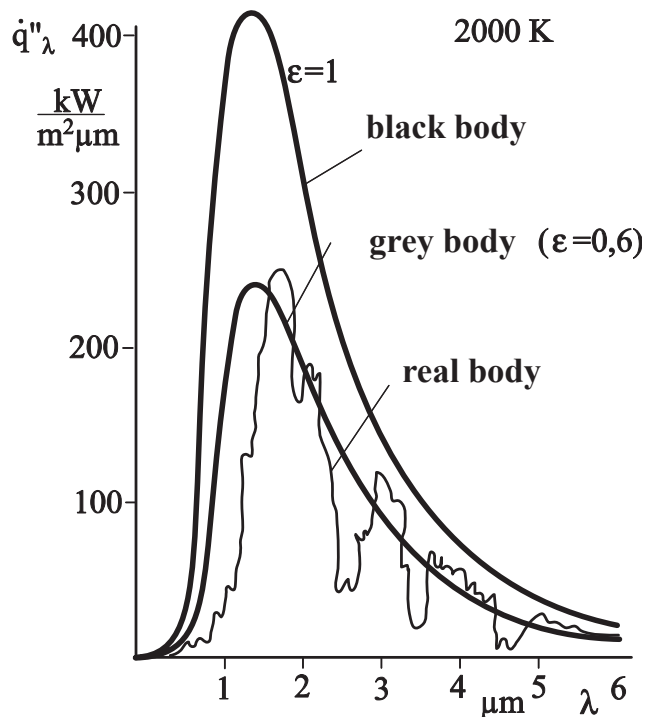


Figure 2.11: Spectral radiant flux density of a black, grey and a real body surface

### 2.1.5 Radiation from a diffuse surface and direction-dependent radiation

Emissivity data for different materials, see e.g. tables in Appendix, are usually determined by measurements in the entire hemisphere. Most of the real surfaces used in practice have an direction dependent emissivity, so that only ideal surfaces as that of the black or grey body can be considered diffuse, i.e. independent of the direction.

Measurement results, as shown in the following figure, show that for example electric conductors have direction-dependent emissivity, which increases with increasing viewing angle  $\varphi$ . On the other hand, insulators possess nearly constant and relatively large emissivity over a wide range of viewing angles.

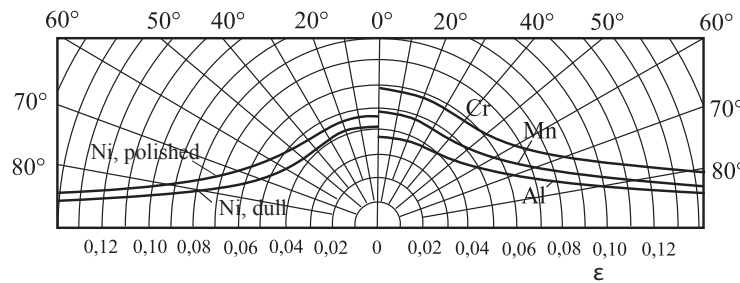


Figure 2.12: Electric conductors

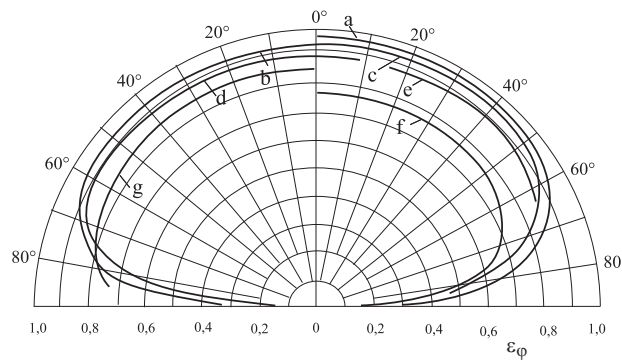


Figure 2.13: Isolators: (a) Wet ice, (b) wood, (c) glass, (d) paper, (e) chalk, (f) copper oxide, (g) aluminium oxide at room temperature

## 2.2 Radiation transfer

### 2.2.1 Radiation flux - radiosity

The radiation properties necessary to describe the heat flow from a body have been discussed so far. If not the total emitted heat flow from a body, but the heat exchange between the body and a nearby object is regarded, it is necessary to know the exact radiation amount in direction to the object as well as the radiation absorbed by this object.

To gain better insight, we imagine a hemisphere of radius  $r$  over a small surface element  $dA$ , positioned at the centre of the hemisphere. In this case the entire heat flow emitted from the surface element passes through the hemisphere.

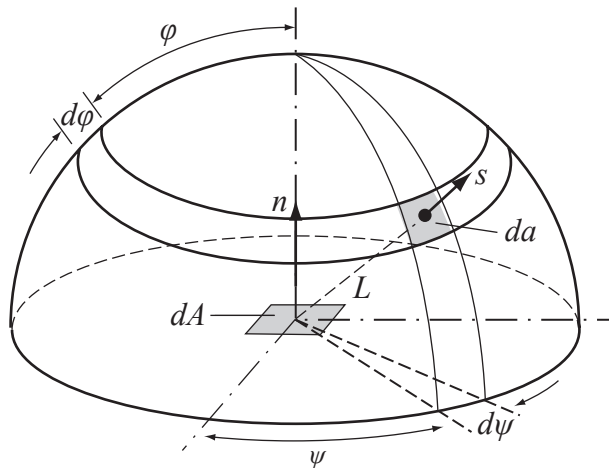


Figure 2.14: Radiation between a surface element and a hemisphere

Considering a surface element on the hemisphere  $da$ , then the energy flow from  $dA$  to  $da$  is defined as radiation flux or radiosity  $L$  by the following equation

$$d\dot{Q}(\varphi, \psi) = L d\Omega dA \cos \varphi, \quad (2.32)$$

The radiosity  $L$  is thus that portion of the energy flux that is emitted from the projected area  $dA \cos \varphi$  in direction of the radiation per unit angle  $d\Omega$ , where the

solid angle  $d\Omega$  is measured in units of “steradian” [sr] and describes the ratio of the surface element on the hemisphere to the radius of the sphere squared

$$d\Omega = \frac{da(\varphi, \psi)}{r^2} \quad (2.33)$$

Diffuse surfaces, i.e. surfaces whose radiation is direction-independent, such as a grey or black body, have constant radiation density. The energy flux to the solid angle  $d\dot{Q}(\varphi, \psi)$  is thus proportional to the projected area  $dA \cos \varphi$ . The radiation density  $L$  is that intensity of the radiation of a surface that is readily perceived by the eye, which in turn is independent of the viewing angle in the case of diffusely radiating bodies. The radiation can have its origin both in the emissive body or can also consist of reflected or transmitted parts of another radiation source. The solid angle, which describes the surface element  $da$  can also be expressed in geometrical terms as

$$d\Omega = \frac{da(\phi, \psi)}{r^2} = \frac{r \sin \varphi d\psi r d\varphi}{r^2} = \sin \varphi \, d\varphi \, d\psi \quad (2.34)$$

Using equation (2.32) leads to

$$d\dot{Q}(\varphi, \psi) = L \sin \varphi \cos \varphi d\phi d\psi dA \quad (2.35)$$

which after integration over the hemisphere yields the relationship between the radiation density and the emissive power of the surface element

$$\dot{q}'' = \pi L \quad (2.36)$$

This particular form of the emissive power is often called “surface brightness”.

### 2.2.2 Radiation transfer between two bodies

If radiation transfer between two diffusely radiating surfaces of two bodies with different temperatures occurs, then the hotter body emits more heat to the colder one, so that the net heat flow is from the hotter to the colder body. In an arbitrary orientation in space, heat  $d\dot{Q}_{1 \rightarrow 2}$  flows from the surface area  $dA_1$  of body 1 to the surface area  $dA_2$  of body 2.

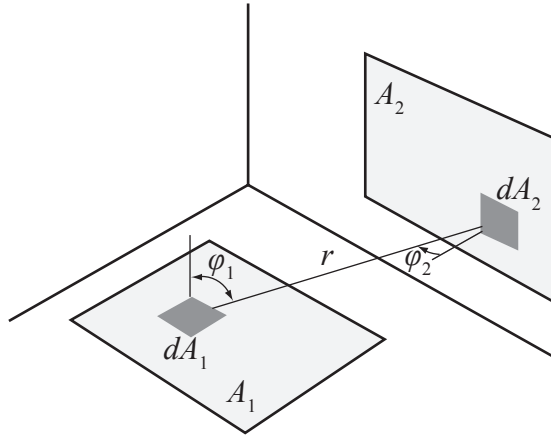


Figure 2.15: Radiation transfer between two surfaces

Using equation (2.32), it is

$$d\dot{Q}_{1 \rightarrow 2} = L_1 \cos \varphi_1 d\Omega_1 dA_1 \quad (2.37)$$

Since the surface element  $dA_2$  is not perpendicular to the connecting line  $r$ , only the projected portions of the area  $dA_2$  should be used to determine the solid angle, i.e.

$$d\Omega_1 = \frac{dA_2 \cos \varphi_2}{r^2} \quad (2.38)$$

Which yields

$$d\dot{Q}_{1 \rightarrow 2} = L_1 \frac{\cos \varphi_1 \cos \varphi_2}{r^2} dA_1 dA_2 \quad (2.39)$$

We get the corresponding relationship for the heat  $d\dot{Q}_{2 \rightarrow 1}$  from the surface element  $dA_2$  radiated to the surface element  $dA_1$ .

$$d\dot{Q}_{2 \rightarrow 1} = L_2 \frac{\cos \varphi_1 \cos \varphi_2}{r^2} dA_1 dA_2 \quad (2.40)$$

Hence, the net radiation transfer between the two bodies is

$$d\dot{Q}_{1 \leftarrow 2} = \int_{A_2} \int_{A_1} (L_1 - L_2) \frac{\cos \varphi_1 \cos \varphi_2}{r^2} dA_1 dA_2 \quad (2.41)$$

Since only diffusely radiating surfaces with homogeneous radiation properties over the body surface are considered, it can be simplified to

$$d\dot{Q}_{1 \leftarrow 2} = (L_1 - L_2) \int_{A_2} \int_{A_1} \frac{\cos \varphi_1 \cos \varphi_2}{r^2} dA_1 dA_2 \quad (2.42)$$

Replacing the radiosity  $L$  by the radiation power  $\dot{q}''$  using equation (2.36)

$$d\dot{Q}_{1 \leftarrow 2} = (\dot{q}_1'' - \dot{q}_2'') \int_{A_2} \int_{A_1} \frac{\cos \varphi_1 \cos \varphi_2}{\pi r^2} dA_1 dA_2 \quad (2.43)$$

The double integration over the surfaces of the two bodies gives an expression which contains only geometrical quantities and none of the radiation properties, but on the other hand such integration is normally too complex and is usually replaced by numerical, graphic or photographic methods. The results of the integration are readily available for a number of typical geometrical orientations in space and can be found in other literature. Usually, these results are given as the so-called "view factors".

The view factor  $\Phi_{12}$  is that portion of radiation that originates from the area  $A_1$  and hits the surface area  $A_2$

$$\Phi_{12} = \frac{\dot{Q}_{1 \rightarrow 2}}{\dot{q}_1'' A_1} \quad (2.44)$$

If a direct radiation transfer between the surface area  $A_1$  and  $n$  other surfaces exists,

$$\Phi_{11} + \Phi_{12} + \Phi_{13} + \dots + \Phi_{1n} = 1 \quad (2.45)$$

is valid.

Integrating equation (2.39) and (2.44) yields a relationship for the view factor  $\Phi_{12}$ , which depends only on the geometric values

$$\Phi_{12} = \frac{1}{A_1} \int_{A_2} \int_{A_1} \frac{\cos \varphi_1 \cos \varphi_2}{\pi r^2} dA_1 dA_2 \quad (2.46)$$

And for  $\Phi_{21}$

$$\Phi_{21} = \frac{1}{A_2} \int_{A_2} \int_{A_1} \frac{\cos \varphi_1 \cos \varphi_2}{\pi r^2} dA_1 dA_2 \quad (2.47)$$

Thus, the double integrals of equation (2.46) and (2.47) are equal, which in turn leads to the reciprocal rule

$$A_1 \Phi_{12} = A_2 \Phi_{21} \quad (2.48)$$

and finally, using equation (2.43)

$$\dot{Q}_{1 \Rightarrow 2} = A_1 \Phi_{12} (\dot{q}_1'' - \dot{q}_2'') \quad (2.49)$$

$$= A_2 \Phi_{21} (\dot{q}_1'' - \dot{q}_2'') \quad (2.50)$$

If only black bodies are involved, then the emissive power consists only of emitted radiation, for which the Stefan-Boltzmann law equation (2.6), is valid. Hence

$$\dot{Q}_{1 \Rightarrow 2} = A_1 \Phi_{12} \sigma [(T_1)^4 - (T_2)^4] \quad (2.51)$$

$$= A_2 \Phi_{21} \sigma [(T_1)^4 - (T_2)^4] \quad (2.52)$$

As an example, the following diagram shows how the view factors can be determined for radiation transfer between parallel or perpendicular plates, according to Holman, 1976. This may be used for example, in the determination of direct radiation transfer between two walls of a room.

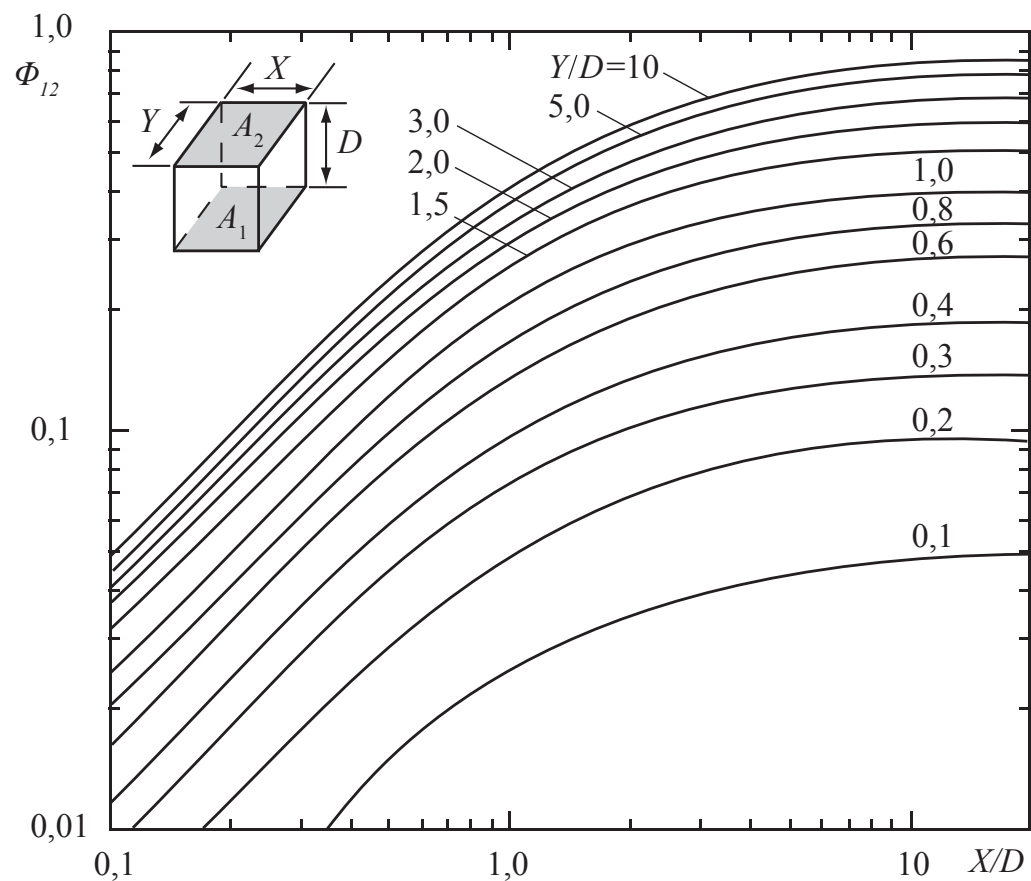


Figure 2.16: View factor of the radiation transfer between parallel, rectangular plates by Holman (1976)

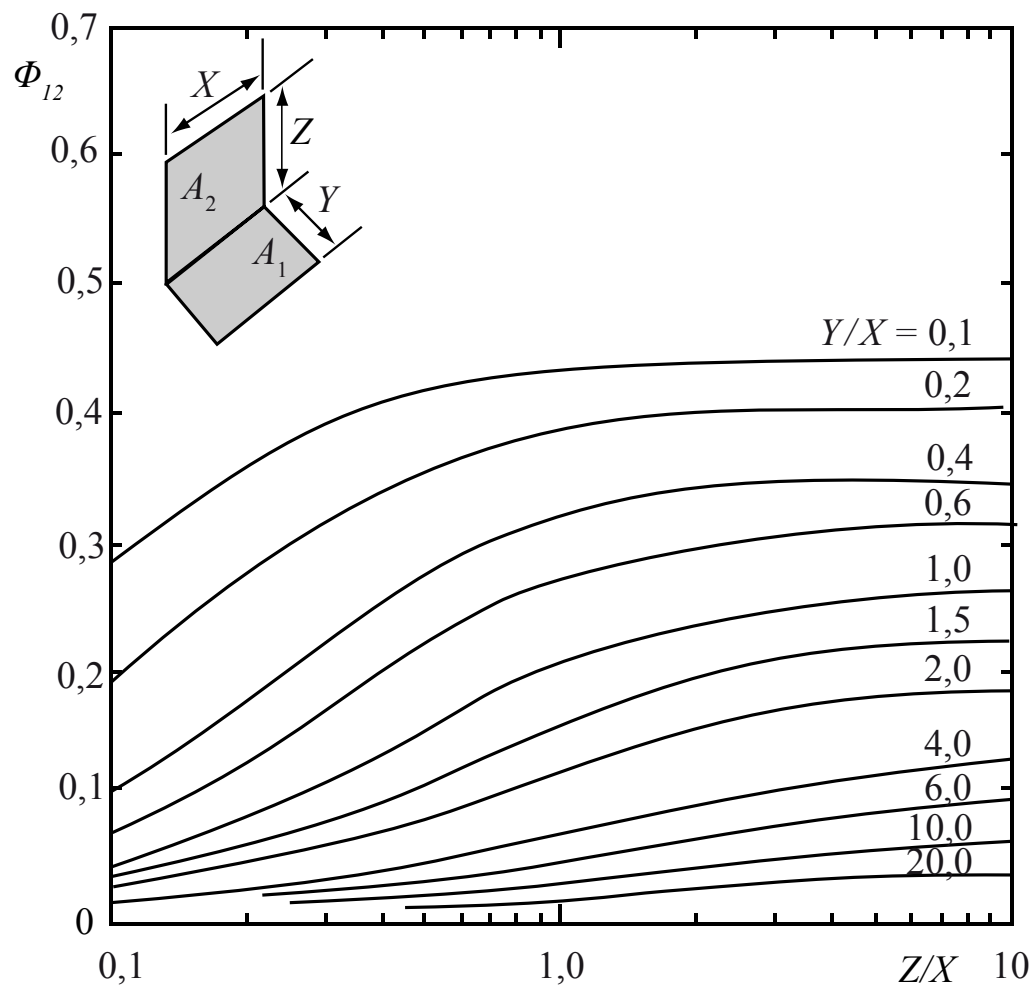


Figure 2.17: View factor of the radiation transfer between perpendicular, rectangular plates by Holman (1976)

### 2.2.3 Radiation transfer between two grey surfaces

If, as a special case, radiation transfer between two black bodies occurs, then knowing the view factor and introducing Stefan-Boltzmann's law in equation (2.49) and (2.50), the relationship of the net radiation transfer as a function of the temperature of the bodies, equation (2.51) and (2.52) can be determined.

For grey bodies on the other hand, the surface brightness includes not only the emitted, but also portions of the reflected and transmitted radiation, since unlike black bodies, the incident radiation is not fully absorbed.

Thus, for the radiation transfer between two non-transmissive solids

$$\dot{Q}_{1 \leftarrow 2} = \Phi_{12} \dot{Q}_1 - \Phi_{21} \dot{Q}_2, \quad (2.53)$$

where e.g.  $\dot{Q}_1 = A_1 \dot{q}_1'' = \dot{Q}_{1,\epsilon} + \dot{Q}_{1,\rho}$  is valid.

The solution methods for these equations are usually rather complex. Yet, for a number of simple, often encountered geometries, complete relationships for the radiation transfer can be derived.

### 2.2.4 Radiation transfer between two infinitely long grey plates

By using the already derived equations, the heat radiation of a plate can be expressed

$$\dot{Q}_1 = A_1 \dot{q}_1'' = \dot{Q}_{1,\epsilon} + \dot{Q}_{1,\rho} = \epsilon_1 A_1 \dot{q}_{b1}'' + \rho_1 A_2 \dot{q}_2'' \quad (2.54)$$

With  $\rho + \alpha = 1$  and applying Kirchhoff's law,  $\alpha = \epsilon$ , yields

$$\dot{q}_1'' = \epsilon_1 \dot{q}_{b1}'' + (1 - \epsilon_1) \dot{q}_2'' \quad (2.55)$$

and

$$\dot{q}_2'' = \epsilon_2 \dot{q}_{b2}'' + (1 - \epsilon_2) \dot{q}_1''. \quad (2.56)$$

respectively.

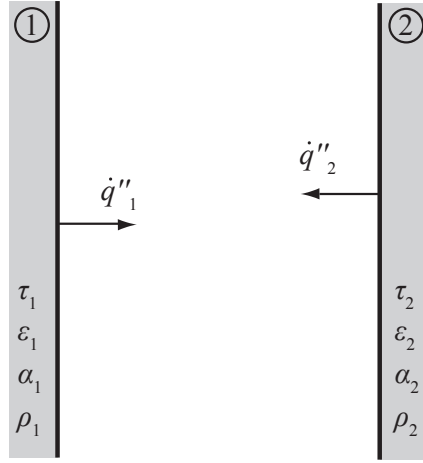


Figure 2.18: Radiation transfer between respectively. two grey surfaces

From equation (2.55) and (2.56) the surface brightnesses  $\dot{q}''_1$  and  $\dot{q}''_2$  are

$$\dot{q}''_1 = \frac{\epsilon_1 \dot{q}_{b1}'' + (1 - \epsilon_1)\epsilon_2 \dot{q}_{b2}''}{1 - (1 - \epsilon_1)(1 - \epsilon_2)}, \quad (2.57)$$

$$\dot{q}''_2 = \frac{\epsilon_2 \dot{q}_{b2}'' + (1 - \epsilon_2)\epsilon_1 \dot{q}_{b1}''}{1 - (1 - \epsilon_1)(1 - \epsilon_2)}. \quad (2.58)$$

Substituting in equation (2.42) and knowing that  $\Phi_{12} = \Phi_{21} = 1$  we get the following relationship for the net radiation transfer,

$$\dot{q}_{1 \rightarrow 2}'' = \frac{1}{\frac{1}{\epsilon_1} + \frac{1}{\epsilon_2} - 1} (\dot{q}_{b1}'' - \dot{q}_{b2}''), \quad (2.59)$$

which can also be written as a function of the body temperature using the Stefan-Boltzmann law, equation (2.6)

$$\dot{q}_{1 \rightarrow 2}'' = \frac{1}{\frac{1}{\epsilon_1} + \frac{1}{\epsilon_2} - 1} \sigma (T_1^4 - T_2^4). \quad (2.60)$$

### 2.2.5 Radiation transfer between two self-enclosed grey bodies

In this case, it holds

$$\dot{Q}_1 = A_1 \dot{q}_1'' = \dot{Q}_{1,\epsilon} + \dot{Q}_{1,\rho} = \epsilon_1 A_1 \dot{q}_{b1}'' + \rho_1 (\Phi_{21} \dot{q}_2'' A_2) \quad (2.61)$$

or using Kirchhoff's law and the reciprocal rule  $\Phi_{12}A_1 = \Phi_{21}A_2$

$$\dot{Q}_1 = A_1 \dot{q}_1'' = A_1 (\epsilon_1 \dot{q}_{b1}'' + (1 - \epsilon_1) \Phi_{12} \dot{q}_2'') . \quad (2.62)$$

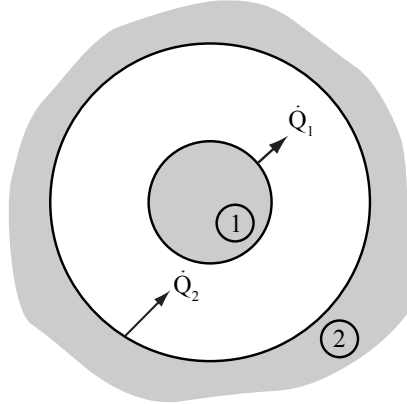


Figure 2.19: Radiation Transfer between two enclosed bodies

In the case of enclosed bodies, the view factor  $\Phi_{12}$  has the value 1 and thus

$$A_1 \dot{q}_1'' = A_1 (\epsilon_1 \dot{q}_{b1}'' + (1 - \epsilon_1) \dot{q}_2'') . \quad (2.63)$$

For the heat emitted from body 2 we get additionally parts of the reflected radiation, which originate from the surface brightness of the body itself - in other words “the body sees itself”.

$$\dot{Q}_2 = A_2 \dot{q}_2'' = \epsilon_2 A_2 \dot{q}_{b2}'' + \rho_2 (\Phi_{12} \dot{q}_1'' A_1) + \rho_2 (\Phi_{22} \dot{q}_2'' A_2) \quad (2.64)$$

Knowing that  $\Phi_{12} = 1$  and  $\Phi_{21} = \frac{A_1 \Phi_{12}}{A_2} = \frac{A_1}{A_2}$  yields,

$$A_2 \dot{q}_2'' = \epsilon_2 A_2 \dot{q}_{b2}'' + (1 - \epsilon_2) \dot{q}_1'' A_1 + (1 - \epsilon_2) \left(1 - \frac{A_1}{A_2}\right) \dot{q}_2'' A_2 . \quad (2.65)$$

Equation (2.63) and (2.65) are used to determine the surface brightness of both bodies, which after substituting in equation (2.53) and several transformations yield a relationship for the radiation transfer

$$\dot{Q}_{1 \Rightarrow 2} = \frac{1}{\frac{1}{\epsilon_1} + \frac{A_1}{A_2} \left( \frac{1}{\epsilon_2} - 1 \right)} A_1 \sigma (T_1^4 - T_2^4). \quad (2.66)$$



---

# Chapter 3

## Conduction

This section deals with the simplest heat transport mechanism, heat conduction, excluding the discussion on the additional combined influence of convection and radiation. The thermal conductivity  $\lambda \left[ \frac{W}{mK} \right]$ , already known from previous chapters, defines the material properties, so that knowing the molecular structure of the body or fluid transporting heat through conduction is not necessary. It is sufficient to assume the medium to be homogenous in structure.

### 3.1 Differential equations of the temperature field

The following experiment will be examined: if the surface temperatures of a flat plate with thickness  $\delta$  were adjust to  $T_1$  and  $T_2$  by heating or cooling, then a linear relationship between the rate of heat flow per unit area  $\frac{\dot{Q}}{A}$  and the temperature difference  $(T_1 - T_2)$  per plate thickness  $\delta$  can be observed. The temperature shape in the plate is thus linear progressive and the heat flow rate per unit area can be derived

$$\frac{\dot{Q}}{A} \equiv \dot{q}'' = \lambda \frac{T_1 - T_2}{\delta} \left[ \frac{W}{m^2} \right] \quad (3.1)$$

The experiment above shows that a general relationship, determined by Fourier in 1822, can be also expressed in the form

$$\dot{q}'' = -\lambda \frac{\partial T}{\partial n} \quad (3.2)$$

(Fourier's equation)

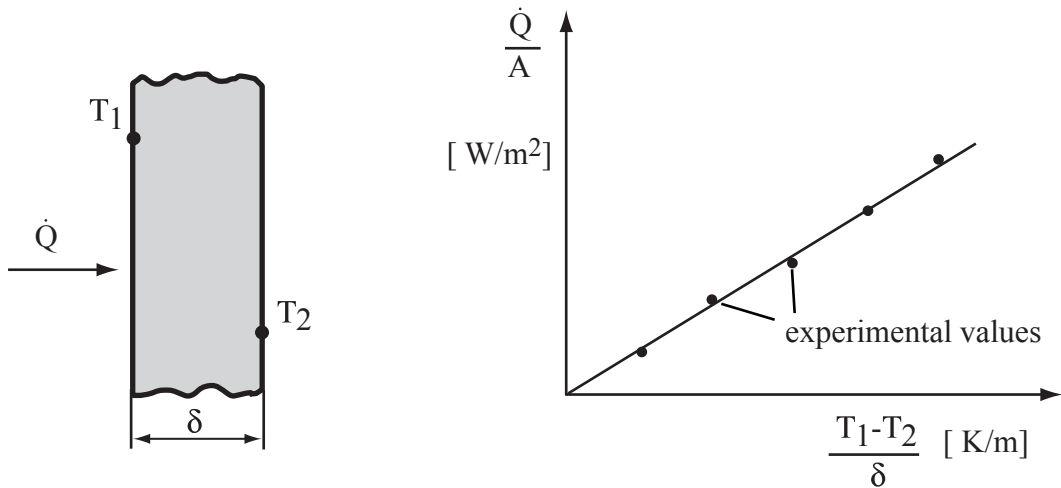


Figure 3.1: Heat flow rate per unit area as a function of the temperature difference

where  $\frac{\partial T}{\partial n}$  is the temperature gradient perpendicular to a surface of constant temperature.

The negative sign, as implied by the second law of thermodynamics, indicates that heat can only flow from regions of higher to regions of lower temperature.

The temperature field of a body, which can include heat sources, such as Joule's heat or reaction heat, is described by equations of energy conservation on a control volume.

**Theorem:** The increase of inner energy in time of a control volume is the difference between the incoming and outflowing energy fluxes and the heat produced within the body.

The incoming energy flow at the surface area  $dydz$  is solely a conductive heat flux, since we exclude convection. Using Fourier's equation (3.2) the incoming conductive heat flow rate in x-direction  $d\dot{Q}_x$  is:

$$d\dot{Q}_x = -\lambda \frac{\partial T}{\partial x} dy dz \quad (3.3)$$

and for the outflowing rate of conductive heat flow in x-direction

$$\begin{aligned} d\dot{Q}_{x+dx} &= d\dot{Q}_x + \frac{\partial}{\partial x} (d\dot{Q}_x) dx \\ &= d\dot{Q}_x + \frac{\partial}{\partial x} \left( -\lambda \frac{\partial T}{\partial x} \right) dx dy dz \end{aligned} \quad (3.4)$$

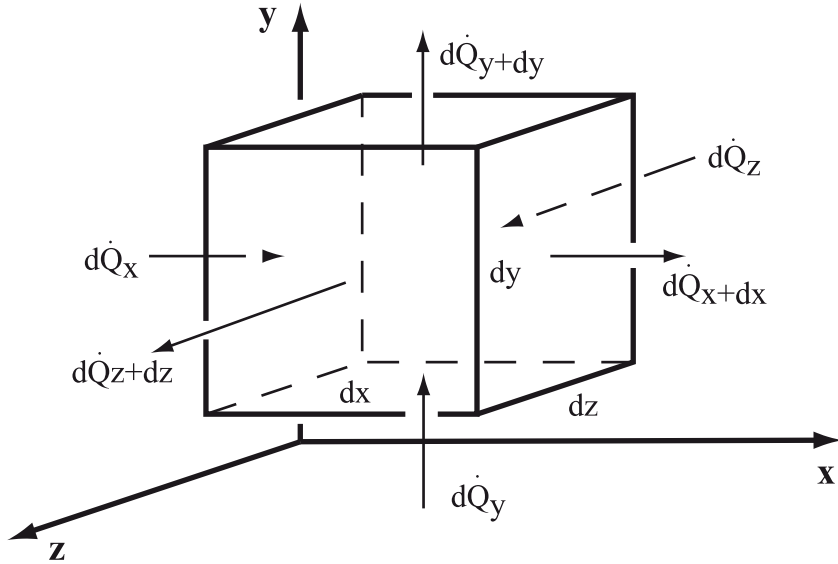


Figure 3.2: Energy balance of a static control volume

Similar expressions are obtained for the other two axes, respectively. The heat produced in the volume element is

$$\dot{\Phi}''' dx dy dz \quad (3.5)$$

with the source strength

$$\dot{\Phi}''' \left[ \frac{W}{m^3} \right] \quad (3.6)$$

The rate of change of inner energy of the element, assuming negligible changes of mass in the volume element, can be written as

$$\frac{dU}{dt} = \frac{d(mu)}{dt} = \rho c_v dx dy dz \frac{\partial T}{\partial t} \quad (3.7)$$

where  $\rho$  [ $kg/m^3$ ] is the density and  $c_v$  [ $J/kgK$ ] the specific heat capacity at constant volume (the index v can be neglected for solids).

The law of conservation of energy gives the differential equation for the temperature field in cartesian coordinates. Similar differential equations can be derived for cylindrical and spherical coordinates.

$$\rho c \frac{\partial T}{\partial t} = \frac{\partial}{\partial x} \left( \lambda \frac{\partial T}{\partial x} \right) + \frac{\partial}{\partial y} \left( \lambda \frac{\partial T}{\partial y} \right) + \frac{\partial}{\partial z} \left( \lambda \frac{\partial T}{\partial z} \right) + \dot{\Phi}''' \quad (3.8)$$

(Cartesian coordinates (x,y,z,t))

$$\rho c \frac{\partial T}{\partial t} = \frac{1}{r} \frac{\partial}{\partial r} \left( r \lambda \frac{\partial T}{\partial r} \right) + \frac{1}{r^2} \frac{\partial}{\partial \theta} \left( \lambda \frac{\partial T}{\partial \theta} \right) + \frac{\partial}{\partial z} \left( \lambda \frac{\partial T}{\partial z} \right) + \dot{\Phi}''' \quad (3.9)$$

(Cylindrical coordinates (r,θ,z,t))

$$\rho c \frac{\partial T}{\partial t} = \frac{1}{r^2} \frac{\partial}{\partial r} \left( r^2 \lambda \frac{\partial T}{\partial r} \right) + \frac{1}{r^2 \sin^2 \theta} \frac{\partial}{\partial \theta} \left( \lambda \sin \theta \frac{\partial T}{\partial \theta} \right) + \frac{1}{r^2 \sin^2 \theta} \frac{\partial}{\partial \phi} \left( \lambda \frac{\partial T}{\partial \phi} \right) + \dot{\Phi}''' \quad (3.10)$$

(Spherical coordinates (r,θ,ϕ,t))

In section 4 “Convection” it will be shown in detail that the equations (3.8) - (3.10) are also valid in cases where mass changes are considered, i.e. density changes, if the value of the specific heat  $c$  will be substituted with that at constant pressure  $c_p$ .

In most cases, the thermal conductivity  $\lambda$  is regarded as constant, which simplifies equations (3.8) - (3.10). Hence, (3.8) can be written as follows

$$\frac{\rho c}{\lambda} \frac{\partial T}{\partial t} = \frac{\partial^2 T}{\partial x^2} + \frac{\partial^2 T}{\partial y^2} + \frac{\partial^2 T}{\partial z^2} + \frac{\dot{\Phi}'''}{\lambda}$$

or

$$\frac{1}{a} \frac{\partial T}{\partial t} = \frac{\partial^2 T}{\partial x^2} + \frac{\partial^2 T}{\partial y^2} + \frac{\partial^2 T}{\partial z^2} + \frac{\dot{\Phi}'''}{\lambda} \quad (3.11)$$

where  $a$  is the so-called *thermal diffusivity*  $a \equiv \frac{\lambda}{\rho c}$ , and has the unit [ $\text{m}^2/\text{s}$ ] . The solution of Fourier's differential equation (3.11) including the boundary conditions gives the temperature field of the body. It is clear from equation (3.11) that the ability of a material to ‘let heat pass through it’ increases with increasing thermal

diffusivity. This can be due to a high thermal conductivity  $\lambda$  or a low heat capacity  $\rho c$  of the material.

The following layers discuss solutions of the differential equation (3.8) - (3.10) for specific applications. The temperature field determined for a specific problem under consideration of its boundary conditions is used in equation (3.2) to determine the heat flux through a surface.

Fourier's differential equation (3.11) can also be found in the literature termed as

a) Poisson's equation when the unsteady state term  $\frac{1}{a} \frac{\partial T}{\partial t}$  is not considered

$$\frac{\partial^2 T}{\partial x^2} + \frac{\partial^2 T}{\partial y^2} + \frac{\partial^2 T}{\partial z^2} + \frac{\dot{\Phi}'''}{\lambda} = 0$$

b) Laplace equation, when additional heat sources are not present  $\frac{\dot{\Phi}'''}{\lambda}$

$$\frac{\partial^2 T}{\partial x^2} + \frac{\partial^2 T}{\partial y^2} + \frac{\partial^2 T}{\partial z^2} = 0 \quad (3.12)$$

## 3.2 Steady state, one-dimensional heat conduction without heat sources

### 3.2.1 Plane walls with given surface temperatures

For steady state, one-dimensional problems, without heat sources and constant heat conductivity  $\lambda$ , equation (3.8) simplifies to

$$\frac{d^2 T}{dx^2} = 0 \quad (3.13)$$

Integrating yields  $T = Ax + B$ , and hence, the already mentioned linear temperature profile. The constants  $A$  and  $B$  are determined from the boundary conditions

$$\begin{aligned} x = 0 & : T = T_1 \\ \text{and } x = \delta & : T = T_2 \end{aligned}$$

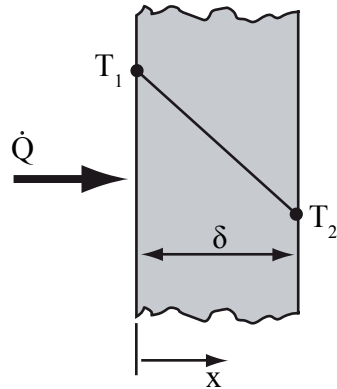


Figure 3.3: Conduction through a flat wall

The temperature profile in the plate is thus

$$T = T_1 + \frac{T_2 - T_1}{\delta} x \quad (3.14)$$

and using equation (3.2) the heat flux is

$$\dot{Q} = -\lambda A \frac{dT}{dx} = \lambda A \frac{T_1 - T_2}{\delta} \quad [\text{W}] \quad (3.15)$$

In case of a composite wall, i.e. consisting of many layers with different thicknesses and materials, equation (3.15) must be calculated for each section in turn. The heat entering section 1, flows unchanged out of section 3 for steady state, one-dimensional cases.

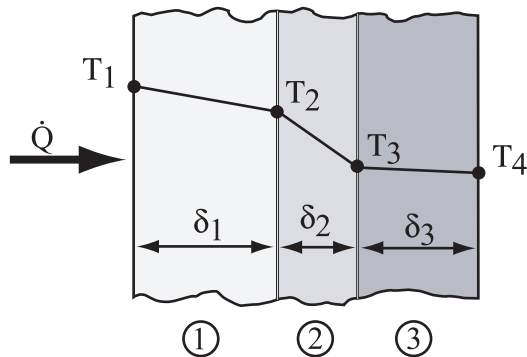


Figure 3.4: Conduction through a composite wall

$$\dot{Q} = \lambda_1 \frac{A}{\delta_1} (T_1 - T_2) = \lambda_2 \frac{A}{\delta_2} (T_2 - T_3) = \lambda_3 \frac{A}{\delta_3} (T_3 - T_4)$$

Hence,

$$\dot{Q} = \frac{A}{\frac{\delta_1}{\lambda_1} + \frac{\delta_2}{\lambda_2} + \frac{\delta_3}{\lambda_3}} (T_1 - T_4)$$

or in general for  $n$  layers,

$$\dot{Q} = \frac{1}{\sum_{i=1}^n \frac{\delta_i}{A\lambda_i}} (T_1 - T_{n+1}) = \frac{1}{W_L} (T_1 - T_{n+1}) \quad (3.16)$$

The heat flow is equal to a temperature potential divided by the sum of the thermal resistances  $W_{L_i}$  of each layer, where

$$W_L = \sum_{i=1}^n W_{L_i} = \sum_{i=1}^n \left( \frac{\delta_i}{A\lambda_i} \right) \left[ \frac{\text{K}}{\text{W}} \right]$$

Equation (3.16) is thus in a form matching that of Ohm's law for electric conductors.

### 3.2.2 Tube wall with predefined surface temperatures

Within the control volume,  $2\pi r dr L$ , the heat flowing through the surface  $2\pi r L$  is

$$\dot{Q}_r = -\lambda 2\pi r L \frac{dT}{dr}$$

and the leaving heat flow through the area  $2\pi(r + dr)L$  is

$$\begin{aligned} \dot{Q}_{r+dr} &= \dot{Q}_r + \frac{d\dot{Q}_r}{dr} dr \\ &= \dot{Q}_r - 2\pi L \lambda \frac{d}{dr} \left( r \frac{dT}{dr} \right) dr \end{aligned}$$

The heat flow remains constant for steady state, one-dimensional case

$$\dot{Q}_r - \dot{Q}_{r+dr} = 0 \quad (3.17)$$

Which yields

$$\frac{d}{dr} \left( r \frac{dT}{dr} \right) = 0 \quad (3.18)$$

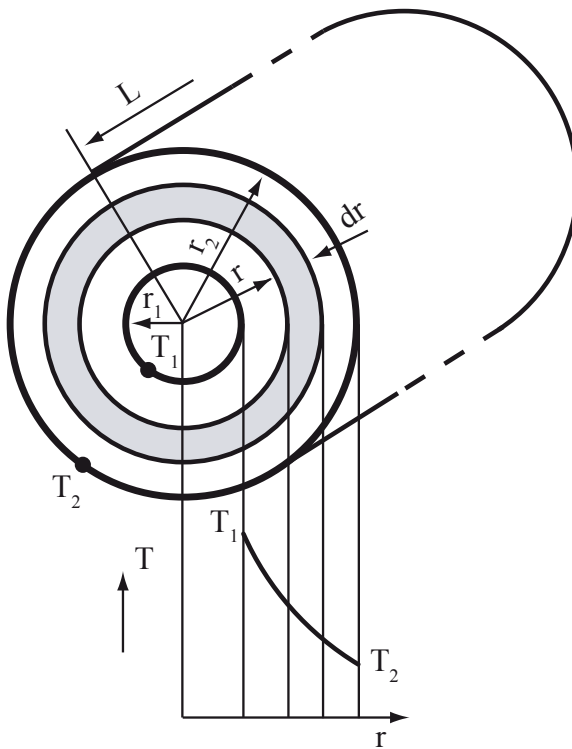


Figure 3.5: Conduction through a tube wall

or

$$\frac{d^2T}{dr^2} + \frac{1}{r} \frac{dT}{dr} = 0 \quad (3.19)$$

The relationship (3.18) can also be obtained directly from equation (3.9).

The solution of Laplace's equation (3.18),

$$T = A \ln\left(\frac{r}{r_0}\right) + B \quad (3.20)$$

where  $r_0$  is the reference radius.

Using boundary conditions  $r = r_1: T = T_1$  und  $r = r_2: T = T_2$  the constants A and B from equation (3.20) can be determined

$$A = \frac{T_2 - T_1}{\ln\left(\frac{r_2}{r_1}\right)} ; \quad B = T_1 - \frac{\ln\left(\frac{r_1}{r_0}\right)(T_2 - T_1)}{\ln\left(\frac{r_2}{r_1}\right)}$$

The temperature in the wall of the tube proves to have logarithmic character, which is given by

$$T = T_1 + \ln\left(\frac{r}{r_1}\right) \frac{T_2 - T_1}{\ln\left(\frac{r_2}{r_1}\right)} \quad (3.21)$$

or

$$T = T_2 + \ln\left(\frac{r}{r_2}\right) \frac{T_2 - T_1}{\ln\left(\frac{r_2}{r_1}\right)} \quad (3.22)$$

By using Fourier's equation, (3.2), the heat flux through the walls can be described

$$\dot{Q} = -\lambda A \frac{dT}{dr} = -\lambda 2\pi r L \frac{dT}{dr}$$

and with equation (3.21)

$$\dot{Q} = +2\pi\lambda L \frac{T_1 - T_2}{\ln\left(\frac{r_2}{r_1}\right)} \quad (3.23)$$

Introducing again, as stated in equation (3.16), the thermal resistance, then equation (3.23) transforms into

$$\dot{Q} \equiv \frac{T_1 - T_2}{W_L} \quad \text{with} \quad W_L = \frac{\ln\left(\frac{r_2}{r_1}\right)}{2\pi\lambda L} \quad (3.24)$$

In analogy to the composite wall multiple layer tubes or shells can also be considered. The heat flow can be written as:

$$\dot{Q} = \frac{T_1 - T_{n+1}}{\sum_{i=1}^n W_{L_i}} = \frac{T_1 - T_{n+1}}{\frac{1}{2\pi L} \sum_{i=1}^n \frac{1}{\lambda_i} \ln \frac{r_{i+1}}{r_i}} \quad (3.25)$$

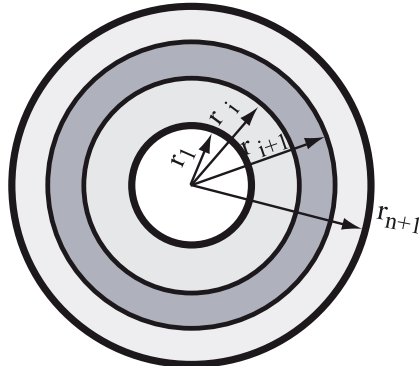


Figure 3.6: Conduction through a spherical shell

### 3.2.3 Plane walls with convective heat transfer

Although chapter 3 discusses only heat transfer through conduction, the convective heat transfer will be introduced in this section, since the latter is of importance and related by its boundary conditions to conduction. It has already been mentioned in the introduction that the energy transport from a flowing fluid to the neighbouring wall is not solely taken over by conduction. Only in the direct proximity of the wall, where due to the viscosity of the fluid the velocity can be neglected, it is able to calculate the heat flow as usual according to equation (3.2)

$$\dot{Q} = -A \left( \lambda \frac{dT}{dx} \right)_{\text{fluid,wall}} \quad (3.26)$$

using the temperature gradient in the fluid and the thermal conductivity  $\lambda_f$  as parameters. The temperature gradient on the wall depends, in addition, on the flow velocity of the fluid, so that a theoretical solution is possible only in a limited number of situations, described in chapter 4.

Therefore, instead of equation (3.26), we normally use an empirical assumption for the convective heat transfer, e.g. on the side of the fluid A,

$$\dot{Q} = A\alpha_A (T_A - T_1) \quad (3.27)$$

where the heat transfer coefficient  $\alpha$   $\left[ \frac{\text{W}}{\text{m}^2 \text{K}} \right]$  is assumed to be known.

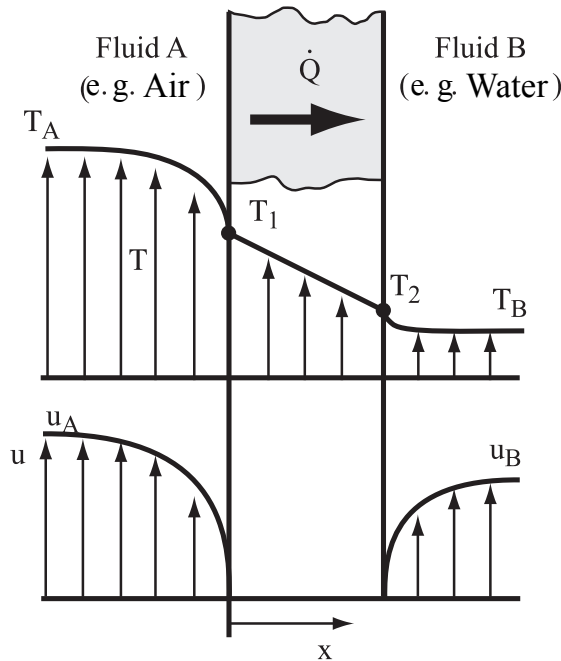


Figure 3.7: Heat transfer through a wall at convective boundary conditions

For the above case of a fluid flowing over a wall, we get the heat flux

- from fluid A to the wall by convection

$$\dot{Q}_{\text{conv}_A} = A \alpha_A (T_A - T_1)$$

- through the wall by conduction

$$\dot{Q}_{\text{cond}} = A \frac{\lambda}{\delta} (T_1 - T_2)$$

- from the wall to fluid B by convection

$$\dot{Q}_{\text{conv}_B} = A \alpha_B (T_2 - T_B)$$

In steady state it is,

$$\dot{Q}_{\text{conv}_A} = \dot{Q}_{\text{cond}} = \dot{Q}_{\text{conv}_B} = \dot{Q}$$

and thus

$$\dot{Q} = \frac{A}{\frac{1}{\alpha_A} + \sum_{i=1}^n \frac{\delta_i}{\lambda_i} + \frac{1}{\alpha_B}} (T_A - T_B) \quad (3.28)$$

The denominator in equation (3.28) may be substituted by defining the overall heat transfer coefficient  $k \left[ \frac{W}{m^2 K} \right]$

$$\frac{1}{k} = \frac{1}{\alpha_A} + \sum_{i=1}^n \frac{\delta_i}{\lambda_i} + \frac{1}{\alpha_B} \quad (3.29)$$

We get

$$\dot{Q} = kA(T_A - T_B) \quad (3.30)$$

or also by introducing the ‘heat transfer resistance’ for convection

$$W_{\text{conv}} \equiv \frac{1}{A\alpha} \left[ \frac{K}{W} \right]$$

$$\dot{Q} = \frac{1}{W_{\text{conv}_A} + W_{\text{cond}} + W_{\text{conv}_B}} (T_A - T_B) = \frac{1}{\sum W_i} (T_A - T_B) \quad (3.31)$$

By adding additional thermal resistances of conduction  $W_{\text{cond}} = W_{L_i}$ , equation 3.31 can be expanded to include cases of composite walls.

### 3.2.4 Tube wall with convective heat transfer

The derived relationships from the previous section can be used to solve problems where single or composite tube wall are used. As a practical example the calculation of the heat loss of an insulated hot water pipe is given.

The thermal resistances  $W_{L_i}$  from equation (3.25) have to be modified in order to include the heat transfer resistances on the tube’s inner and outer side  $W_{\text{conv}_A} = \frac{1}{\alpha_A A_A}$  and  $W_{\text{conv}_B} = \frac{1}{\alpha_B A_B}$ , respectively, where  $A_A = 2\pi r_1 L$  and  $A_B = 2\pi r_{n+1} L$ .

Hence, we get for the heat flux

$$\dot{Q} = \frac{2\pi L}{\frac{1}{\alpha_A r_1} + \sum_{i=1}^n \frac{1}{\lambda_i} \ln \frac{r_{i+1}}{r_i} + \frac{1}{\alpha_B r_{n+1}}} (T_A - T_B) \quad (3.32)$$

or instead of using the radii, using the diameters

$$\dot{Q} = \frac{\pi L}{\frac{1}{\alpha_A d_1} + \frac{1}{2} \sum_{i=1}^n \frac{1}{\lambda_i} \ln \frac{d_{i+1}}{d_i} + \frac{1}{\alpha_B d_{n+1}}} (T_A - T_B)$$

Comparing the equation above to the form where the overall heat transfer coefficient  $k$  is used

$$\dot{Q} = kA(T_A - T_B) = k\pi dL(T_A - T_B) \quad (3.33)$$

we get

$$\frac{1}{k} = \frac{1}{\alpha_A} \frac{d}{d_1} + \frac{d}{2} \sum_{i=1}^n \frac{1}{\lambda_i} \ln \frac{d_{i+1}}{d_i} + \frac{1}{\alpha_B} \frac{d}{d_{n+1}} \quad (3.34)$$

Where any surface area  $A$  or any diameter  $d$  may be used in equation (3.33) and equation (3.34), respectively. Normally, in practice, the outer diameter  $d_{n+1}$  is used as reference. For thin-walled tubes the relationship for flat plates (3.28) may be used, if the area will be substituted with  $A = \pi d_m L$ , where  $d_m$  describes the arithmetic mean diameter. Thus, for problems with heat transfer coefficients of equal order of magnitude on both sides of the fluid, it is good practice to use the mean value of the inner and outer diameter for calculations. If the heat transfer coefficients greatly deviate from each other, then it is recommended to select the diameter with the lower heat transfer coefficient

### 3.2.5 Heat conduction in fins

The above stated relationships are of special technical importance to predict the temperature distribution and heat flux in fins. Fins are usually placed in the form of cylindrical rod fins, plane fins, circular fins, etc. on the surface of a heat emitting (or heat absorbing) body in areas where the greatest heat transfer resistances are located. The efficiency of a fin is given by the fin efficiency  $\eta_F$ , which is defined as

$$\eta_F = \frac{\text{transferred heat}}{\text{maximum transferable heat}} \quad (3.35)$$

where the ‘maximal transferable heat’ is the heat that can be transferred by the fin if its total surface area reached the temperature of the fin base. In the following we will discuss those fin geometries, which approximately can be regarded one-dimensional

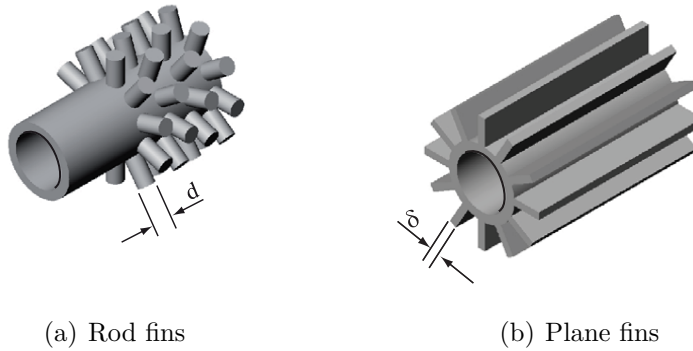


Figure 3.8: Tubes with finned surfaces

and thus allow an analytical approach. Two-dimensional and three-dimensional fins can only be described by using numerical methods.

Rod fins and plane fins Allowing the simplified assumptions that

- the temperature shape in a fin is one-dimensional, i.e. the temperature changes only as a function of the length of the fin, but not its radius
- the heat transfer coefficient is known,

we get from the heat balance on the fin element with cross section area  $A_c$ , that the difference between the incoming and outgoing heat flux must be dissipated by convection to the surroundings.

$$\dot{Q}_x - \dot{Q}_{x+dx} = d\dot{Q}_{\text{conv}}$$

Using equation (3.2) the heat fluxes are

$$\dot{Q}_x = -\lambda A_c \frac{dT}{dx}$$

$$\dot{Q}_{x+dx} = \dot{Q}_x + \frac{d\dot{Q}_x}{dx} dx = -\lambda A_c \left( \frac{dT}{dx} + \frac{d^2T}{dx^2} dx \right)$$

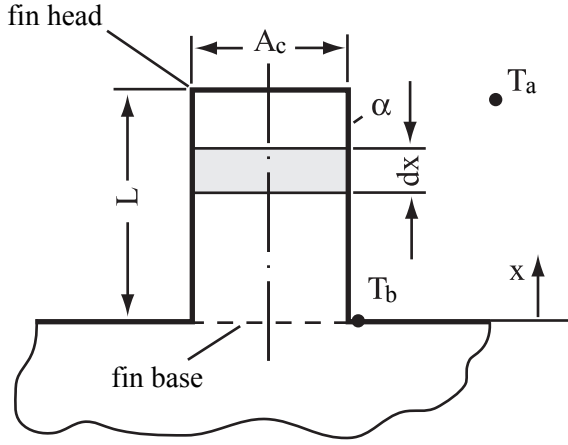


Figure 3.9: Energy balance of a fin

and with equation (3.27) the convection flux from the element with circumference  $U$  and length  $dx$  to the surrounding

$$d\dot{Q}_{\text{conv}} = \alpha U (T - T_u) dx$$

The balance yields, after introducing a temperature difference  $\theta \equiv T - T_a$  the differential equation for the temperature of the fin

$$\frac{d^2\theta}{dx^2} - \underbrace{\frac{\alpha U}{\lambda A_c}}_{\text{m}^2} \theta = 0 \quad (3.36)$$

Which has the general solution with

$$\theta = A e^{mx} + B e^{-mx} = A^* \sinh(mx) + B^* \cosh(mx) \quad (3.37)$$

with

$$m \equiv \left( \frac{\alpha U}{\lambda A_c} \right)^{\frac{1}{2}} \left[ \frac{1}{m} \right],$$

For the rod fin with circular cross section  $m = \left( \frac{4\alpha}{\lambda d} \right)^{\frac{1}{2}}$  and for the plane fin  $m = \left( \frac{2\alpha}{\lambda d} \right)^{\frac{1}{2}}$

Boundary conditions

1.  $x = 0: \theta = \theta_b$

2.  $x = L:$

At the top of the fin many combinations of boundary conditions are possible

- a) The heat flow out of the top of the fin is negligible in comparison to the total dissipated heat, hence the top of the fin (which also can be called ‘head’) can be regarded as adiabatic

$$\left(\frac{d\theta}{dx}\right)_{x=L} = 0$$

- b) The fin is very long, thus the temperature of the top is approximately equal to the surrounding temperature

$$(\theta)_{x=L} = 0$$

- c) The fin has a finite height and transfers heat from the head as well

$$(Q)_{x=L} = \alpha A_c \theta_{\text{head}}$$

In the following the boundary condition 2a will be considered.

Then, from equation (3.37) the temperature over the height of the fin is

$$\theta = \theta_F \frac{e^{m(L-x)} + e^{-m(L-x)}}{e^{mL} + e^{-mL}} \quad (3.38)$$

or

$$\theta = \theta_F \frac{\cosh[m(L-x)]}{\cosh(mL)} \quad (3.39)$$

The following diagram shows the dimensionless temperature shape of a rod fin with circular cross section, for different fin materials with  $m = \left(\frac{4\alpha}{\lambda d}\right)^{\frac{1}{2}}$ .

The fin’s diameter is  $d = 8\text{mm}$ , its length  $L = 40\text{mm}$  and a heat transfer coefficient against surrounding air  $\alpha = 10 \frac{\text{W}}{\text{m}^2 \text{K}}$ .

From the temperature curve above the total heat transferred to the surroundings by the fin can be determined. Energy balance along the fin shows that in steady state the heat, entering the fin base by conduction, is equal to the heat transferred to the surroundings by convection

$$\dot{Q} = \dot{Q}_b = -\lambda A_c \left(\frac{d\theta}{dx}\right)_{x=0}$$

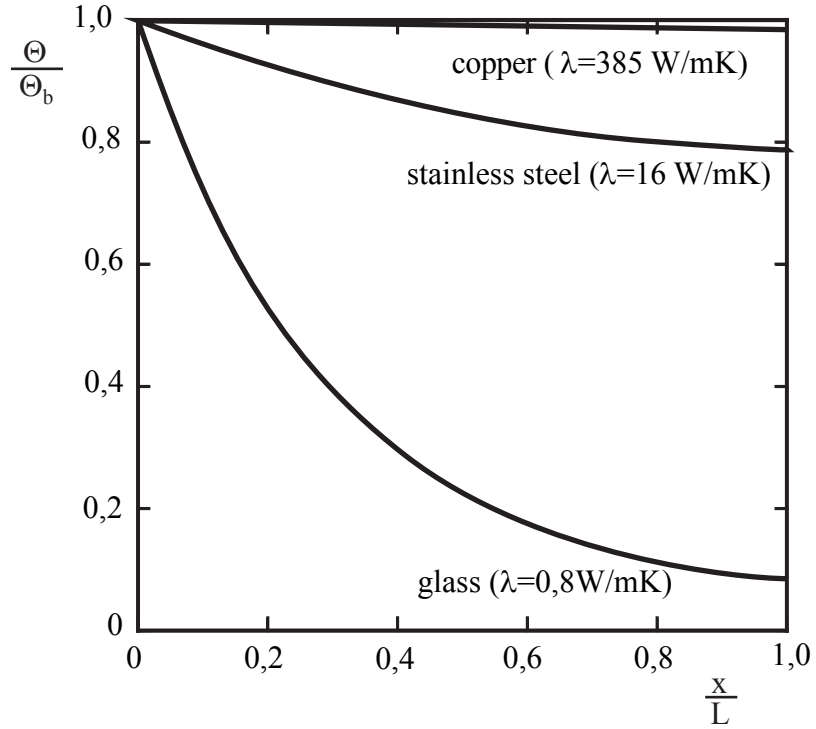


Figure 3.10: Change of temperature over the length of a rod fin

Using equation (3.38)

$$\dot{Q} = \lambda A_c m \theta_b \left( \frac{e^{mL} - e^{-mL}}{e^{mL} + e^{-mL}} \right) \quad (3.40)$$

or

$$\dot{Q} = \lambda A_b m \theta_b \tanh(mL) \quad (3.41)$$

To determine the efficiency of the fin, the calculated heat flux from equation (3.41) is rated over the maximum possible heat flux of that particular fin geometry, see equation (3.35),

$$\eta_F \equiv \frac{\dot{Q}}{\dot{Q}_{\max}} = \frac{\lambda A_c m \theta_b \tanh(mL)}{\alpha U L \theta_b} \quad (3.42)$$

$$\eta_F = \frac{\tanh(mL)}{mL}$$

This function is shown in fig. 3.11

As can be seen from the curve, the efficiency cannot be optimised solely over the

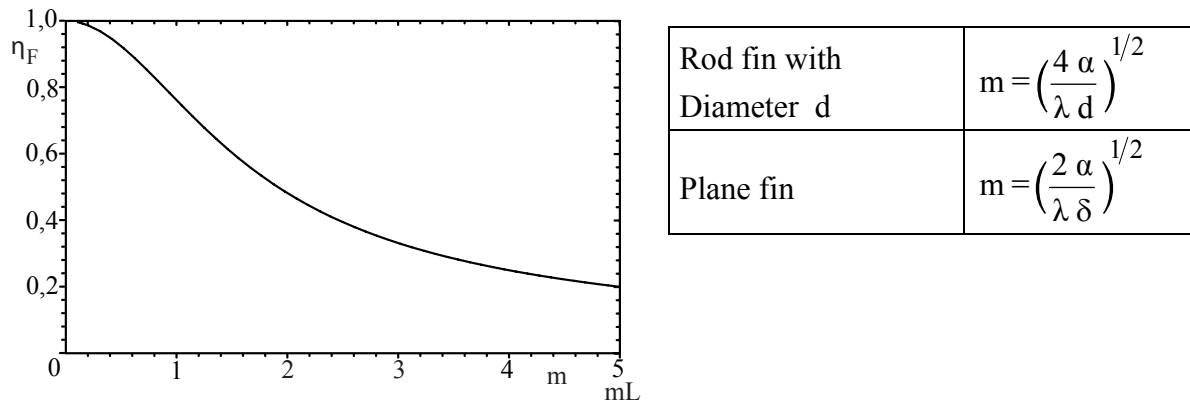


Figure 3.11: Efficiency coefficient of a rod fin

length of the fin, since factors like mass of the fin or volume must also be considered.

Equations (3.38) - (3.42) have been derived for the boundary condition 2a). For cases 2b) and 2c) the solutions can be derived in the same manner.

Circular fins This kind of fin geometry is often used in the cooling elements industry, therefore the appropriate solutions will be indicated.

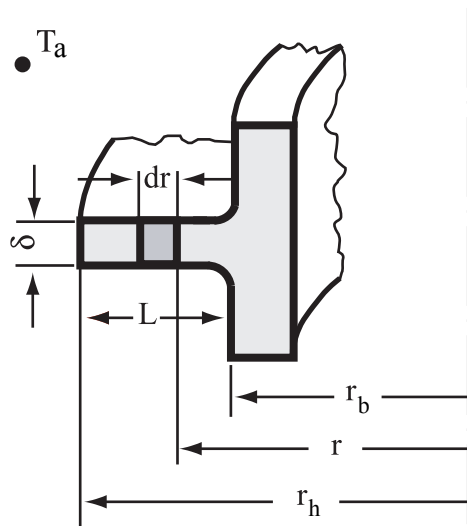


Figure 3.12: Heat transfer through circular fins

Heat balance for the fin element  $2\pi r dr$  yields the differential equation

$$\frac{d^2\theta}{dr^2} + \frac{1}{r} \frac{d\theta}{dr} - \frac{2\alpha}{\lambda\delta} \theta = 0 \quad (3.43)$$

This is the Bessel differential equation of zero order. The solution is given by elements of the modified Bessel function  $I_o$  and  $K_o$  (see table 2 in appendix)

$$\theta = A I_o(mr) + B K_o(mr) \quad (3.44)$$

where  $m = \left(\frac{2\alpha}{\lambda\delta}\right)^{\frac{1}{2}}$ . The constants  $A$  and  $B$  have to be determined from the boundary conditions.

With the boundary conditions

1.  $r = r_b : \theta = \theta_b$
2.  $r = r_h : \left(\frac{d\theta}{dr}\right)_{r=r_h} = 0$

the temperature in the fin is

$$\theta = \theta_b \frac{I_o(m r)K_1(m r_h) + I_1(m r_h)K_o(m r)}{I_o(m r_b)K_1(m r_h) + I_1(m r_h)K_o(m r_b)} \quad (3.45)$$

and for the total dissipated heat

$$\dot{Q} = 2\pi r_b \lambda \delta m \theta_b \frac{I_1(m r_h)K_1(m r_b) - I_1(m r_b)K_1(m r_h)}{I_o(m r_b)K_1(m r_h) + I_1(m r_h)K_o(m r_b)} \quad (3.46)$$

and finally for the efficiency coefficient of the fin

$$\eta_F \equiv \frac{\dot{Q}}{\dot{Q}_{\max}} = \frac{2}{mr_b \left[ \left( \frac{r_h}{r_b} \right)^2 - 1 \right]} \frac{I_1(m r_h)K_1(m r_b) - I_1(m r_b)K_1(m r_h)}{I_o(m r_b)K_1(m r_h) + I_1(m r_h)K_o(m r_b)} \quad (3.47)$$

Computing this expression may prove rather cumbersome, thus tabulated Bessel functions must be used. Schmidt, 1950, gives for equation (3.47) the following approximation

$$\eta_F \approx \frac{\tanh(m r_b \varphi)}{mr_b \varphi} \quad (3.48)$$

with

$$\varphi = \left( \frac{r_K}{r_F} - 1 \right) \left( 1 + 0,35 \ln \frac{r_K}{r_F} \right)$$

The following figure shows the efficiency coefficient of the fin for various radius ratios  $\frac{r_h}{r_b}$  according to equation (3.47) and (3.48), respectively. Within the readability tolerance, the results of the two computations show no major deviation. For ratios

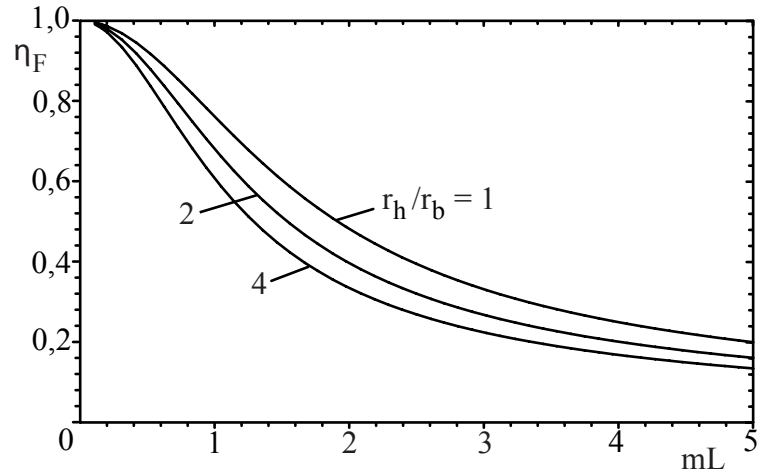


Figure 3.13: Efficiency coefficient of a circular fin

$\frac{r_h}{r_b} \rightarrow 1$  the values of the plane fin are obtained.

### 3.3 Steady state, one-dimensional heat conduction with heat sources

In many practical situations heat transfer processes for systems with inner heat production are to be estimated. Examples include fuel rods of nuclear plants, electric resistances or tanks in which chemical reactions take place, just to name a few. Often a one-dimensional analysis suffices as a first approximation.

As an example we use the cylindrical fuel rod to derive the differential equation of the temperature field.

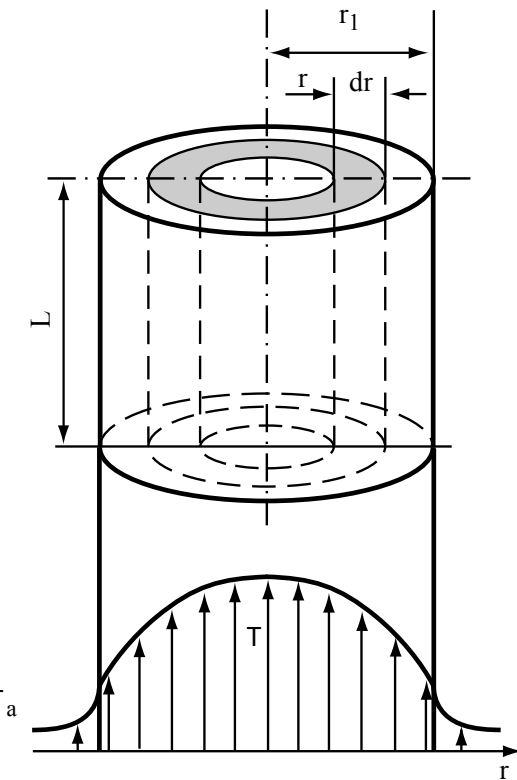


Figure 3.14: Heat conduction in a cylinder with heat sources

Energy balance at the volume element  $dV = 2\pi r dr L$  yields

$$+\dot{Q}_r - \dot{Q}_{r+dr} + \dot{\Phi}''' dV = 0$$

and thus

$$\frac{1}{r} \frac{d}{dr} \left( r \frac{dT}{dr} \right) + \frac{\dot{\Phi}'''}{\lambda} = 0 \quad (3.49)$$

or

$$\frac{d^2T}{dr^2} + \frac{1}{r} \frac{dT}{dr} + \frac{\dot{\Phi}'''}{\lambda} = 0 \quad (3.50)$$

This solution or the equivalent for the plane or spherical case can be taken from equation (3.8). The boundary conditions are

1.

$$r = 0 : \left( \frac{dT}{dr} \right)_{r=0} = 0 \quad (3.51)$$

2.

$$r = r_1 : \quad$$

As already mentioned in section 3.2, on the cylinder surface either a) the temperature or b) a heat transfer coefficient can be given

a)

$$T = T_1 \quad (3.52)$$

b)

$$\dot{Q} = 2\pi r_1 L \alpha (T_1 - T_a) \quad (3.53)$$

since the dissipated heat for steady state must be produced by the heat sources within the cylinder, we get

$$\dot{Q} = \pi r_1^2 L \dot{\Phi}'''$$

and hence

$$T_1 = T_a + \frac{r_1 \dot{\Phi}'''}{2\alpha}$$

Integrating the differential equation (3.49) using equation (3.51) and (3.53) gives the temperature shape in the cylinder

$$T = T_a + \frac{\dot{\Phi}''' r_1^2}{4\lambda} \left( 1 + \frac{2\lambda}{\alpha r_1} - \left( \frac{r}{r_1} \right)^2 \right) \quad (3.54)$$

This equation can be given in a general form valid both for the plane and spherical geometries

$$T = T_a + \frac{\dot{\Phi}''' s^2}{2(n+1)\lambda} \left( 1 + \frac{2\lambda}{\alpha s} - \left( \frac{\xi}{s} \right)^2 \right) \quad (3.55)$$

the parameter  $\xi$ , the characteristic length  $s$  and the control parameter  $n$  are to be included using the following rule:

Table 3.1: Definitions of the parameters in equation (3.55)

	Plate*)	Cylinder	Sphere
$\xi$	$x$	$r$	$r$
$s$	$\delta$	$r_1$	$r_1$
$n$	0	1	2

\*)For plates  $x$  should be with reference to the plane of symmetry and  $\delta$  is half the plate thickness

Using (3.55) the maximum temperature in the body ( $\xi = 0$ )

$$T_{\max} = T_a + \frac{\dot{\Phi}''' s^2}{2(n+1)\lambda} \left( 1 + \frac{2\lambda}{\alpha s} \right) \quad (3.56)$$

and the surface temperature ( $\xi = s$ ) can be calculated

$$T_s = T_a + \frac{\dot{\Phi}''' s}{(n+1)\alpha} \quad (3.57)$$

## 3.4 Steady state, multi-dimensional heat conduction without heat sources

A typical example of this group is the fin problem already mentioned in section 3.2.5. If the length of the fin is small compared to the diameter, or if the heat conduction resistances are higher than the heat transfer resistances, then a temperature profile exists not only over the length of the fin, but also over its radius, i.e. its thickness. The diagram shows the isotherms of such a fin, determined by a method of analogy, Schmidt 1966, and the corresponding heat flow lines.

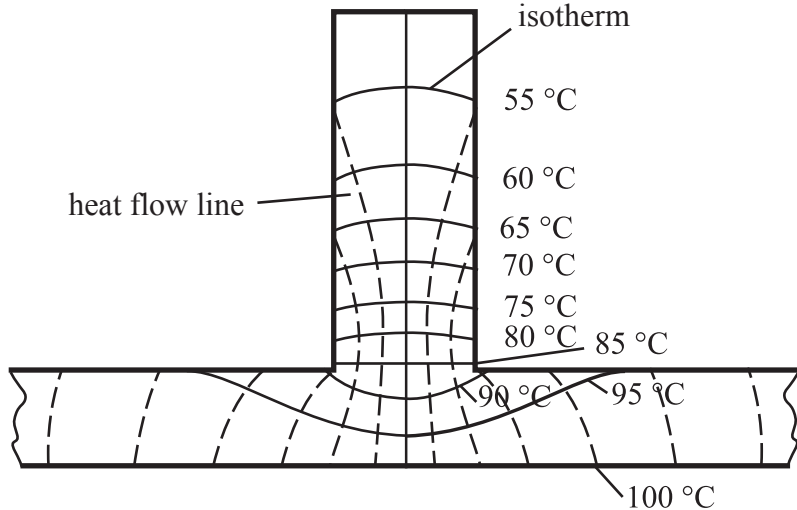


Figure 3.15: Isotherms and heat flow lines in a plane fin

This temperature field must be obtained from the energy balance derived in section 3.1 equation (3.8), for a planar body with constant thermal conductivity, i.e. from the Laplace equation.

$$\frac{\partial^2 T}{\partial x^2} + \frac{\partial^2 T}{\partial y^2} = 0$$

This equation can be solved either analytically, numerically, graphically or as in the case of the above shown fin, using methods of analogy. The analytical methods can be used for a limited number of geometries and boundary conditions, and even so, only after substantial effort has been invested. A detailed description can be found in books by Carslaw u. Jaeger (1948) or Schneider (1955). Graphical methods or analogy methods are usually used when only a qualitative estimate is required and especially when the consequences of parameter variations are of interest.

With the advance in computer technology, nowadays even complex problems can be solved numerically with high accuracy. To this purpose, Laplace's differential equation is approximated using the method of finite differences, i.e. the derivatives in the differential equation are substituted by algebraic approximations at discrete points of the body. The methods employed differ in the way these approximations are formulated as well as in the solution method of the respective system of equations.

As an example we will show this method employed on a plane fin. Detailed descriptions with the appropriate programming source code can be found in Croft u. Lilley (1977), or Bayley u. a. (1972).

For a better overview of the boundary conditions, we introduce the temperature difference  $\theta = T - T_a$  in the Laplace equation:

$$\frac{\partial^2 \theta}{\partial x^2} + \frac{\partial^2 \theta}{\partial y^2} = 0 \quad (3.58)$$

Dividing the body along the two coordinate axis in equal bands of width  $\Delta x$  and  $\Delta y$  (shown in Figure 3.16), then the temperature gradients can be approximated by the difference quotients as follows:

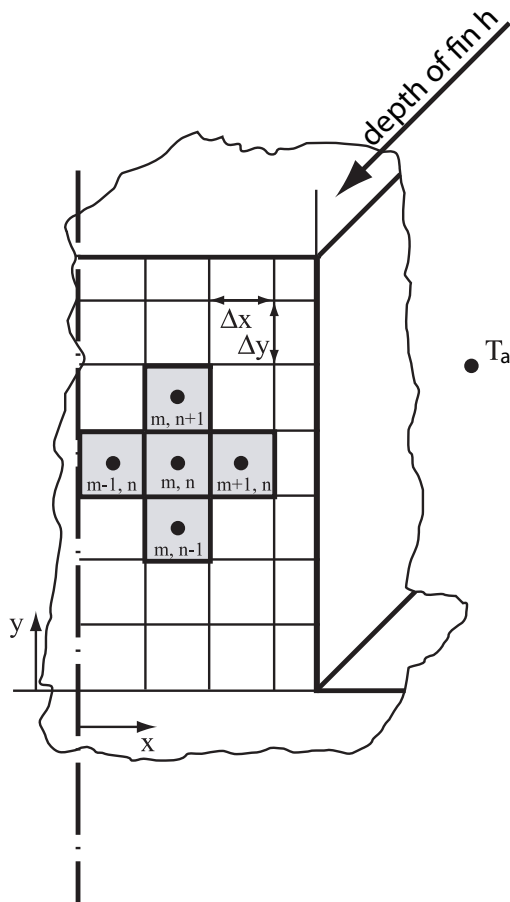


Figure 3.16: Description of the heat conduction in a fin using the method of finite differences

$$\begin{aligned}
 \frac{\partial \theta}{\partial x} \Big|_{m+\frac{1}{2},n} &\approx \frac{\theta_{m+1,n} - \theta_{m,n}}{\Delta x} \\
 \frac{\partial \theta}{\partial x} \Big|_{m-\frac{1}{2},n} &\approx \frac{\theta_{m,n} - \theta_{m-1,n}}{\Delta x} \\
 \frac{\partial \theta}{\partial y} \Big|_{m,n+\frac{1}{2}} &\approx \frac{\theta_{m,n+1} - \theta_{m,n}}{\Delta x} \\
 \frac{\partial \theta}{\partial y} \Big|_{m,n-\frac{1}{2}} &\approx \frac{\theta_{m,n} - \theta_{m,n-1}}{\Delta x}
 \end{aligned}$$

Which yields the finite differences for the second derivatives

$$\frac{\partial^2 \theta}{\partial x^2} \approx \frac{\frac{\partial \theta}{\partial x} \Big|_{m+\frac{1}{2},n} - \frac{\partial \theta}{\partial x} \Big|_{m-\frac{1}{2},n}}{\Delta x} = \frac{\theta_{m+1,n} + \theta_{m-1,n} - 2\theta_{m,n}}{(\Delta x)^2}$$

and

$$\frac{\partial^2 \theta}{\partial y^2} \approx \frac{\frac{\partial \theta}{\partial y} \Big|_{m,n+\frac{1}{2}} - \frac{\partial \theta}{\partial y} \Big|_{m,n-\frac{1}{2}}}{\Delta y} = \frac{\theta_{m,n+1} + \theta_{m,n-1} - 2\theta_{m,n}}{(\Delta y)^2}$$

and hence Laplace's equation in the form of finite differences

$$\frac{\theta_{m+1,n} + \theta_{m-1,n} - 2\theta_{m,n}}{(\Delta x)^2} + \frac{\theta_{m,n+1} + \theta_{m,n-1} - 2\theta_{m,n}}{(\Delta y)^2} = 0$$

which in turn, can be simplified by introducing a quadratic net  $\Delta x = \Delta y$

$$\theta_{m+1,n} + \theta_{m-1,n} + \theta_{m,n+1} + \theta_{m,n-1} - 4\theta_{m,n} = 0 \quad (3.59)$$

The Laplace differential equation has been already discussed in section 3.1 with the assumption that the thermal conductivity remains constant. Equation (3.59) is thus the energy balance in the form of the finite differences, which states that for the steady state case without heat sources, the sum of all inflowing and outflowing heat fluxes at net point m, n must be zero.

If inner heat sources exist, then equation (3.59) can be expanded to include the sources easily

$$\theta_{m+1,n} + \theta_{m-1,n} + \theta_{m,n+1} + \theta_{m,n-1} - 4\theta_{m,n} + \frac{\dot{\Phi}''' (\Delta x)^2}{\lambda} = 0 \quad (3.60)$$

For any other point of the mesh equations (3.59) and (3.60) can be employed, respectively, where on the surfaces of the body the boundary conditions must be obeyed.

If the temperatures on the surfaces are not given, then the appropriate heat transfer law and the surrounding temperature  $T_a$  must be known. Heat balance on the boundary net element  $(m,n)$  yields

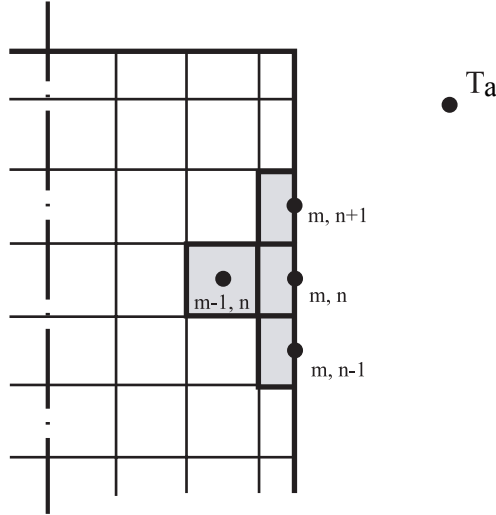


Figure 3.17: Formulation of the boundary conditions

$$-\lambda \frac{\Delta y}{\Delta x} (\theta_{m,n} - \theta_{m-1,n}) - \lambda \frac{\Delta x}{2\Delta y} (\theta_{m,n} - \theta_{m,n+1}) - \lambda \frac{\Delta x}{2\Delta y} (\theta_{m,n} - \theta_{m,n-1}) = \alpha \Delta y \theta_{m,n} \quad (3.61)$$

In the case of a quadratic mesh  $\Delta x = \Delta y$  we get for the temperature difference at the boundary point  $\theta_{m,n}$

$$\theta_{m,n} \left( \frac{\alpha}{\lambda} \Delta x + 2 \right) - \frac{1}{2} [2\theta_{m-1,n} + \theta_{m,n+1} + \theta_{m,n-1}] = 0 \quad (3.62)$$

Similar expressions can be obtained for edges or adiabatic surfaces, see e.g. Holman (1976).

The more detailed the mesh, the closer the finite differences are to the differential equations, yet the numerical complexity of the solution increases appropriately.

For a limited number of net points the solutions can be readily obtained using the method of relaxation, known from fluid dynamics.

The method of relaxation consists of the following steps:

1. A guessed value for the temperature is estimated for the mesh points. On the boundaries, the temperatures are already given by the boundary conditions, or can be obtained using an appropriate heat transfer law in case of convective heat transfer to the surrounding (see above).
2. Using the estimated temperatures and substituting the values in equation (3.59) or (3.62), respectively, we get a remainder, which can be considered as a “heat source” as was done in equation (3.60).
3. Changing the values for the estimated temperatures and starting from the element closest to the element with the greatest “heat source” is aimed at making the “heat source” disappear.
4. When the “heat source” are small enough, then the temperature field is obtained. The transferred heat can then be calculated according to

$$\dot{Q} = \sum \lambda h \Delta x \left. \frac{\Delta \theta}{\Delta y} \right|_{\text{Wall}} \quad \text{resp.} \quad \dot{Q} = \sum \lambda h \Delta y \left. \frac{\Delta \theta}{\Delta x} \right|_{\text{Wall}} \quad \text{where } h \text{ is the depth of the body.}$$

The iterative method of relaxation is modified for computer applications. For special problems though, direct methods, such as the Gauss method of elimination or the matrix inversion have proven their reliability.

## 3.5 Unsteady state heat conduction without heat sources

Previous chapters have dealt with conduction processes, for which a balance state has been reached. The obtained temperature field was not a function of time.

Here, the unsteady states of heating and cooling processes until an balance temperature is reached will be discussed. These processes are described by the differential equations (3.8), (3.9) or (3.10) from section 3.1 satisfying the initial and boundary conditions of the problem in question.

Since a general solution of these equations is not possible, we can only describe typical examples used in practice.

### 3.5.1 Bodies with high values of thermal conductivity

If a body has a high thermal conductivity, so that the thermal resistance of the body is small compared to the heat transfer resistance between the body and the surrounding fluid, then a nearly homogeneous temperature will be established at each point in time during heating or cooling.

Hence, it is not necessary to implement the differential equation for the temperature field, equation (3.8) - (3.10). It is much easier to formulate the energy balance for the entire body, which states that the inner energy of the body, which is a function of the time, will change due to heat transfer by convection from the surface to the surroundings.

Equating the energy:

$$\frac{dU}{dt} = -\alpha A (T - T_a)$$

or

$$\rho c V \frac{dT}{dt} + \alpha A (T - T_a) = 0 \quad (3.63)$$

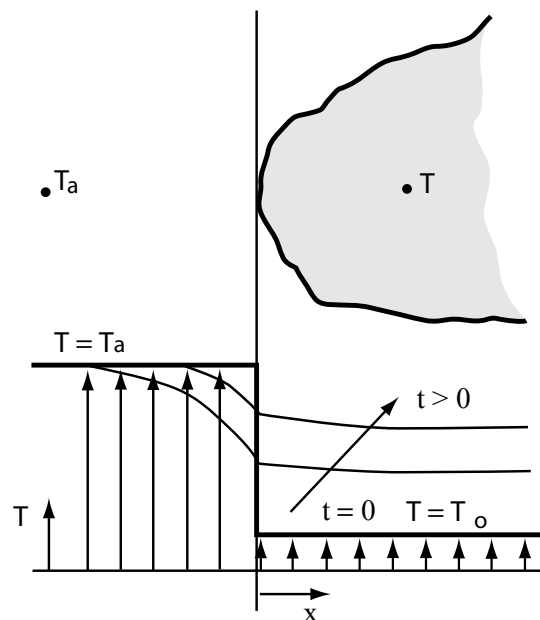


Figure 3.18: Heating of a body

Defining the dimensionless temperature  $\theta^* \equiv \frac{(T-T_0)}{(T_a-T_0)}$ , where  $T$  is the temperature as a function of the time and  $T_0$  is the initial temperature of the body, it is:

$$\frac{d\theta^*}{dt} + \frac{\alpha}{\rho c V} \frac{A}{V} (\theta^* - 1) = 0$$

and thus

$$\frac{d\theta^*}{(\theta^* - 1)} = -\frac{\alpha}{\rho c} \frac{A}{V} dt$$

This differential equation can be integrated using the boundary condition

$$t = 0: \quad T = T_0 \quad \text{i.e.} \quad \theta^* = 0$$

for  $0 \leq \theta^* \leq 1$  which finally yields

$$\frac{T - T_0}{T_a - T_0} = 1 - \exp \left[ -\frac{\alpha}{\rho c} \frac{A}{V} t \right] \quad (3.64)$$

Introducing two dimensionless numbers, namely, the Biot number

$$\text{Bi} \equiv \frac{\alpha L}{\lambda}, \quad (3.65)$$

and the Fourier number

$$\text{Fo} \equiv \frac{\lambda t}{\rho c L^2} = \frac{at}{L^2}, \quad (3.66)$$

where  $L$  is the characteristic length, resulting from the ratio  $\frac{V}{A}$ , equation (3.64) can be expressed in the following form:

$$\frac{T - T_0}{T_a - T_0} = 1 - \exp [-\text{Bi} \cdot \text{Fo}] \quad (3.67)$$

In other words, the dimensionless temporal progress of the temperature equilibrium between a body with high thermal conductivity and its surrounding (written in the form of equation (3.67)) is in general the same for all problems, where the boundary conditions are described by equal Biot numbers. Moreover, this is valid for all problems where the Biot number is very small,  $\text{Bi} \ll 1$ .

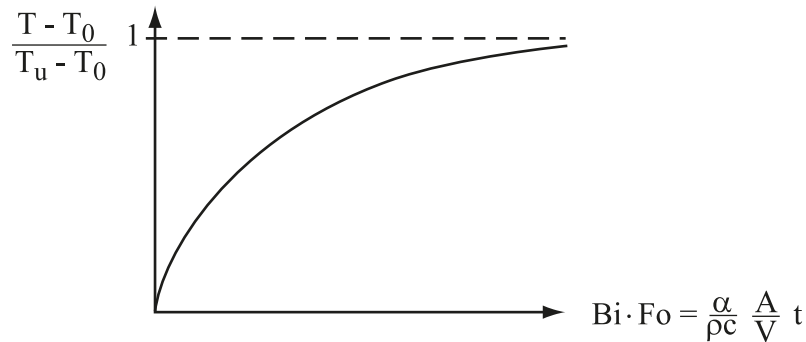


Figure 3.19: The temperature of a body as a function of the time

Equation (3.67) may still be used as a first approximation of the heat transfer behaviour of a body, in cases where the above conditions do not apply.

### 3.5.2 One-dimensional, unsteady state heat conduction examples

In cases where the thermal resistance within a body cannot be neglected, a general, analytical solution is possible only after complex calculations and only for a limited number of geometries and boundary conditions.

Since often in practice these solutions, usually shown in dimensionless diagrams, suffice for the preliminary approximation of the temperature/time behaviour, we will discuss next the basic mathematical procedures for selected examples.

#### Semi-infinite plate with given surface temperature

A very useful case for approximations of the temperature/time behaviour of bodies with high Biot numbers is the semi-infinite body, i.e. a model of a body for which the given temperature change has not yet penetrated deep under the surface and which can be analysed one-dimensionally.

Under these conditions, equation (3.8) simplifies to

$$\frac{\partial T}{\partial t} = \frac{\lambda}{\rho c} \frac{\partial^2 T}{\partial x^2} \quad (3.68)$$

with the initial and boundary conditions

IC 1:

$$\left. \begin{array}{l} t = 0 \\ 0 < x < \infty \end{array} \right\} T = T_0$$

BC 2: since  $\text{Bi} = \frac{\alpha L}{\lambda} \gg 1$

$$\left. \begin{array}{l} t > 0 \\ x = 0 \end{array} \right\} T = T_a$$

BC 3:

$$\left. \begin{array}{l} t > 0 \\ x \rightarrow \infty \end{array} \right\} T = T_0$$

Introducing the dimensionless temperature difference  $\theta^* \equiv \frac{T - T_o}{T_a - T_o}$  and the thermal

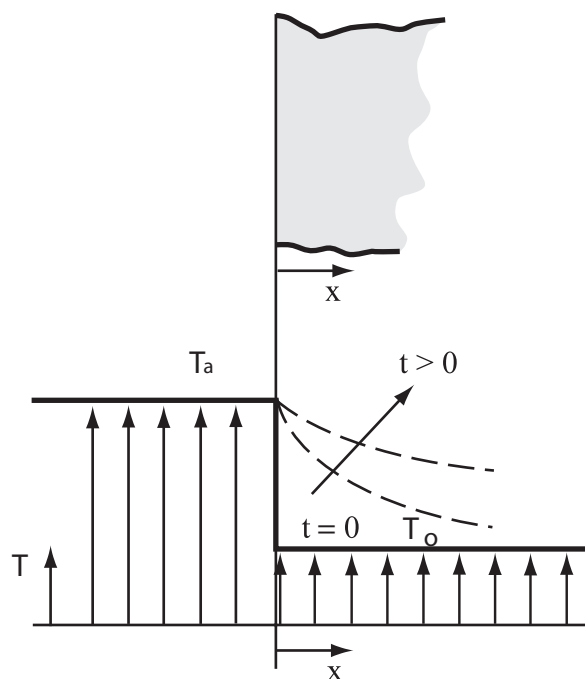


Figure 3.20: Initial and boundary conditions

diffusivity  $a \equiv \frac{\lambda}{\rho c}$ , it can also be written

$$\frac{\partial \theta^*}{\partial t} = a \left( \frac{\partial^2 \theta^*}{\partial x^2} \right) \quad (3.69)$$

and

IC 1:

$$\begin{cases} t = 0 \\ 0 < x < \infty \end{cases} \quad \left. \theta^* = 0 \right\}$$

BC 2:

$$\begin{cases} t > 0 \\ x = 0 \end{cases} \quad \left. \theta^* = 1 \right\}$$

BC 3:

$$\begin{cases} t > 0 \\ x \rightarrow \infty \end{cases} \quad \left. \theta^* = 0 \right\}$$

This differential equation can be solved using the method of variable separation.

However, the present case can be solved by an easier way. Instead of the two independent variables  $x$  and  $t$ , only one independent variable  $\eta(x,t)$  will be determined, for which the partial differential equation reduces to an ordinary differential equation, so that the following is valid

$$\theta^*(x,t) = \theta^*[\eta(x,t)]$$

For the independent variable,  $\eta$ , the following formulation will be used

$$\eta = b x^c t^d$$

Additionally the differentials of equation (3.69) will be rewritten, so that they depend on  $\eta$ .

$$\frac{\partial \theta^*}{\partial t} = \left( \frac{d\theta^*}{d\eta} \right) \left( \frac{\partial \eta}{\partial t} \right)$$

and

$$\frac{\partial^2 \theta^*}{\partial x^2} = \left( \frac{d^2 \theta^*}{d\eta^2} \right) \left( \frac{\partial \eta}{\partial x} \right)^2 + \left( \frac{d\theta^*}{d\eta} \right) \left( \frac{\partial^2 \eta}{\partial x^2} \right)$$

taking account of the mentioned formulation  $\eta = b x^c t^d$  the differential equation (3.69) is

$$\left( \frac{d\theta^*}{d\eta} \right) b x^c dt^{d-1} = a \left( \frac{d^2\theta^*}{d\eta^2} \right) (bc x^{c-1} t^d)^2 + a \left( \frac{d\theta^*}{d\eta} \right) (bc(c-1)x^{c-2}t^d)$$

and by rearranging it gives

$$\frac{d^2\theta^*}{d\eta^2} + \frac{\left( \frac{ac(c-1)t}{dx^2} - 1 \right)}{\left( \frac{abc^2t^{d+1}}{dx^{2-c}} \right)} \frac{d\theta^*}{d\eta} = 0$$

Thus, if this were to be an ordinary differential equation dependent only on  $\eta$  then the expressions in the brackets must also depend only on  $\eta$ .

Comparing the exponents of  $x$  and  $t$  we get

$$c = 1 \quad d = -\frac{1}{2} \quad \text{and } b = \frac{1}{\sqrt{4a}}$$

and thus the ordinary differential equation

$$\frac{d^2\theta^*}{d\eta^2} + 2\eta \frac{d\theta^*}{d\eta} = 0 \tag{3.70}$$

with  $\eta \equiv \frac{x}{\sqrt{4at}}$ . The new variable  $\eta$  can be rewritten using the Fourier number  $Fo$ , where the distance from the plate surface will be used as the characteristic length,

$$\eta \equiv \frac{x}{\sqrt{4at}} = \frac{1}{\sqrt{4Fo}}$$

The second-order differential equation (3.70) requires two boundary conditions in the new coordinates  $\eta$  and  $\theta^*$ . Transforming the boundary conditions yields

$$\begin{aligned} \text{BC1: } \eta &= \infty & : \theta^* &= 0 \\ \text{BC2: } \eta &\rightarrow 0 & : \theta^* &= 1 \\ \text{BC3: } \eta &\rightarrow \infty & : \theta^* &= 0 \end{aligned}$$

Since BC1 equals BC3 after transformation, and they do not contradict each other, a similar solution is possible using the variable  $\eta$ .

The solution of this second-order differential equation is carried out with the usual methods of substitution,

$$z \equiv \frac{d\theta^*}{d\eta}, \quad \frac{dz}{d\eta} = \frac{d^2\theta^*}{d\eta^2}$$

which yields

$$\frac{dz}{d\eta} + 2\eta z = 0$$

and integrating

$$\ln z = -\eta^2 + C_1 \quad \text{or} \quad \frac{d\theta^*}{d\eta} = C_2 e^{-\eta^2}$$

The second integration yields, using integration variable  $\xi$  and BC 2

$$\theta^*(\eta) - 1 = C_2 \int_{\xi=0}^{\xi=\eta} e^{-\xi^2} d\xi$$

$C_2$  can be determined from boundary condition

$$C_2 = \frac{-1}{\int_0^\infty e^{-\xi^2} d\xi} = -\frac{2}{\sqrt{\pi}}$$

Which yields the dimensionless temperature field

$$\theta^* = 1 - \frac{2}{\sqrt{\pi}} \int_{\xi=0}^{\xi=\eta} e^{-\xi^2} d\xi \quad (3.71)$$

The second term on the right side of equation (3.71) is called the error function  $\text{erf}(\eta)$  and can be found listed on the Appendix. So that,

$$\begin{aligned} \theta^* &= 1 - \text{erf} [\eta] & \text{or} \\ \theta^* &= 1 - \text{erf} \left[ \frac{1}{\sqrt{4F_0}} \right] \end{aligned} \quad (3.72)$$

This function is shown in the following diagram 3.21. The diagram shows that the initial temperature difference is reduced by 1% at a value of  $\eta = 1,8$ . This value is

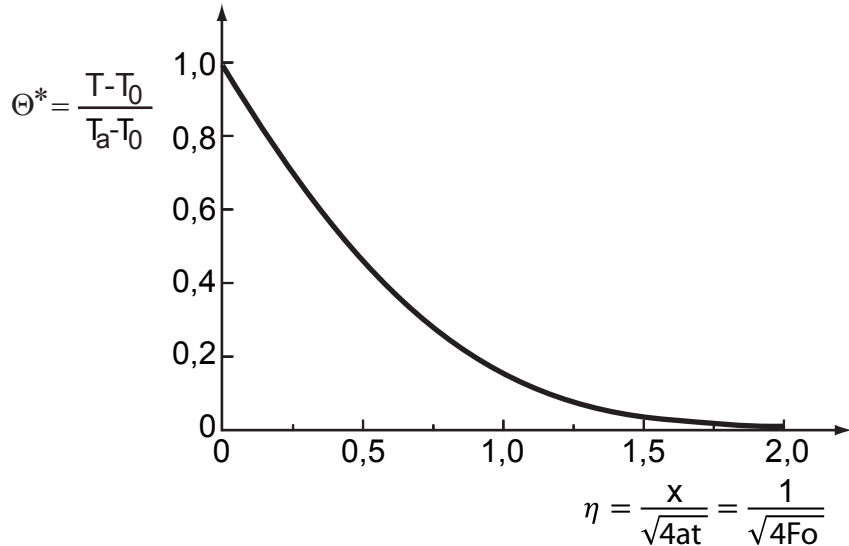


Figure 3.21: Temperature characteristics in a semi-infinite body - constant surface temperature

often used to define the penetration depth or thickness of the temperature boundary layer

$$\delta(t) = 3,6\sqrt{at} \quad (3.73)$$

From the temperature field (equation (3.71)) the heat transfer rate at the surface can be determined

$$\dot{q}'' \Big|_{x=0} = -\lambda \frac{\partial T}{\partial x} \Big|_{x=0}$$

Differentiation yields:

$$\begin{aligned} \dot{q}'' \Big|_{x=0} &= \frac{\lambda}{\sqrt{\pi at}} (T_a - T_o) \\ &= \sqrt{\frac{\lambda c \rho}{\pi t}} (T_a - T_o) \end{aligned} \quad (3.74)$$

In other words, the heat drops steadily with time, so that at time  $t$  the heat is reduced to

$$\int_{t=0}^t \dot{q}'' \Big|_{x=0} dt = 2\sqrt{\frac{\lambda c \rho}{\pi}} t (T_a - T_o) \quad (3.75)$$

Semi-infinite plate with non negligible heat transfer resistance

In the previous section it is assumed that the temperature at the body surface equals the surrounding temperature for all  $t > 0$ . This is valid only if the heat transfer resistance is small compared to the thermal resistance within the body, or if  $\text{Bi} = \frac{\alpha L}{\lambda} \gg 1$ .

If the heat transfer resistance cannot be neglected, then a surface temperature will be observed which is between the surrounding temperature and the initial temperature of the body. Instead of BC2, a new boundary condition is introduced

BC 2a:

$$\alpha (T_a - T_{x=0}) = -\lambda \left( \frac{\partial T}{\partial x} \right)_{x=0}$$

or

$$\left( \frac{\partial T}{\partial x} \right)_{x=0} = \frac{\alpha}{\lambda} (T_{x=0} - T_a) \quad (3.76)$$

This relationship can be presented illustratively, as shown in the following diagram. The extrapolations of all gradient lines intersect at point P, which is given by the coordinates  $T_a$  and  $-\frac{\lambda}{\alpha}$ .

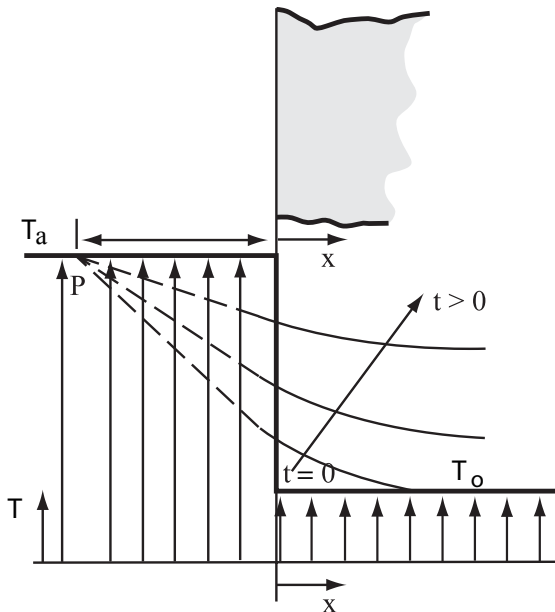


Figure 3.22: Boundary conditions

With these boundary conditions the computation load for solving equation (3.68) is much greater than before. Detailed discussion can be found in Schneider (1955). The following equation describes the temperature field

$$\theta^* = \frac{T - T_0}{T_a - T_0} = 1 - \operatorname{erf} \left( \frac{1}{\sqrt{4Fo}} \right) - \left[ \exp \left( Bi + Fo \cdot Bi^2 \right) \right] \left[ 1 - \operatorname{erf} \left( \frac{1}{\sqrt{4Fo}} + \sqrt{Fo} \cdot Bi \right) \right] \quad (3.77)$$

with  $Fo = at/x^2$  and  $Bi = \alpha x/\lambda$ .

The solution of this equation is shown in figure 3.23. The previously discussed case of negligible heat transfer resistances is thus a special case,  $\sqrt{Fo}Bi \rightarrow \infty$ , as shown in the diagram.

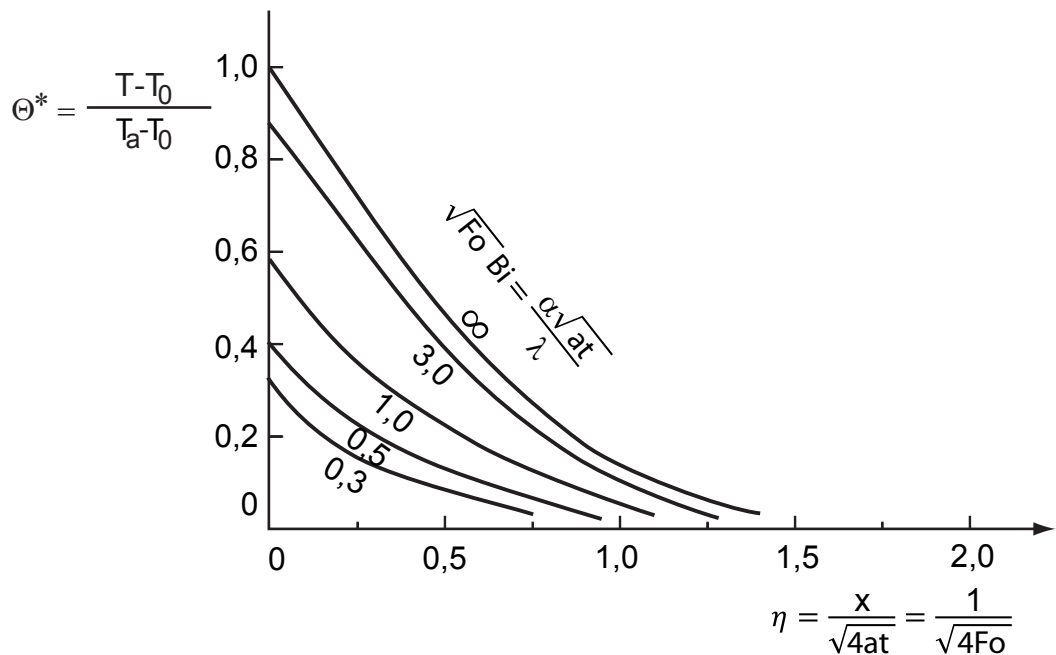


Figure 3.23: The temperature as a function of time of a semi-infinite body with finite convective heat transfer resistance.

### Semi-infinite plate with time dependent surface temperatures

Many temperature processes have boundary conditions that change periodically, e.g. the daily or annual temperature variations, which have consequences on the temperature distribution in the walls of buildings or floors, or the cyclic heat load of the cylinder wall of a combustion engine.

In general, such processes with boundary conditions that change periodically cannot be described by analytical solutions of the differential equation for the temperature field (eq.(3.8)).

Yet, the basic relationships can still be discussed using the model of the semi-infinite body. Equation (3.8) thus simplifies to

$$\frac{\partial T}{\partial t} = a \frac{\partial^2 T}{\partial x^2} \quad (3.78)$$

$$\text{BC1: } t = 0 : \quad T = T_o(x)$$

$$\text{BC1: } x = 0 : \quad T_{x=0} = f(t)$$

$$\text{BC2: } x \rightarrow \infty : \quad T_{x \rightarrow \infty} = T_m$$

If, for the simplest case, we assume that the surface temperature changes periodically according to a step function between  $T_{\max}$  and  $T_{\min}$ , then we can get results for the temperature profile within the body as shown in the diagram below.

At time  $t_1$  shortly before the temperature  $T_{\max}$  changes to  $T_{\min}$  we would expect a temperature distribution according to curve 1. Only in the deeper layers this curve differs from the symptotic case of long-period oscillations. Shortly after the change  $\Delta t$  to temperature  $T_{\min}$  a new temperature profile, curve 2, exists for which, although the temperature maximum in the deep layers flattens through heat conduction. In the areas close to the surface the reduced surface temperature is noticeable. The process of heat conduction e balance leads shortly before changing again from  $T_{\min}$  to  $T_{\max}$  at  $t_2$  to a new temperature profile, curve 4, which is the mirror image of curve 1. After the shift, the same process begins again. From these profiles on the right side, which are qualitatively derived, we can get the temperature profiles as a function of the time e.g. for a layer at depth  $x = x_1$  sketched on the left side. How this is done is shown in the diagram.

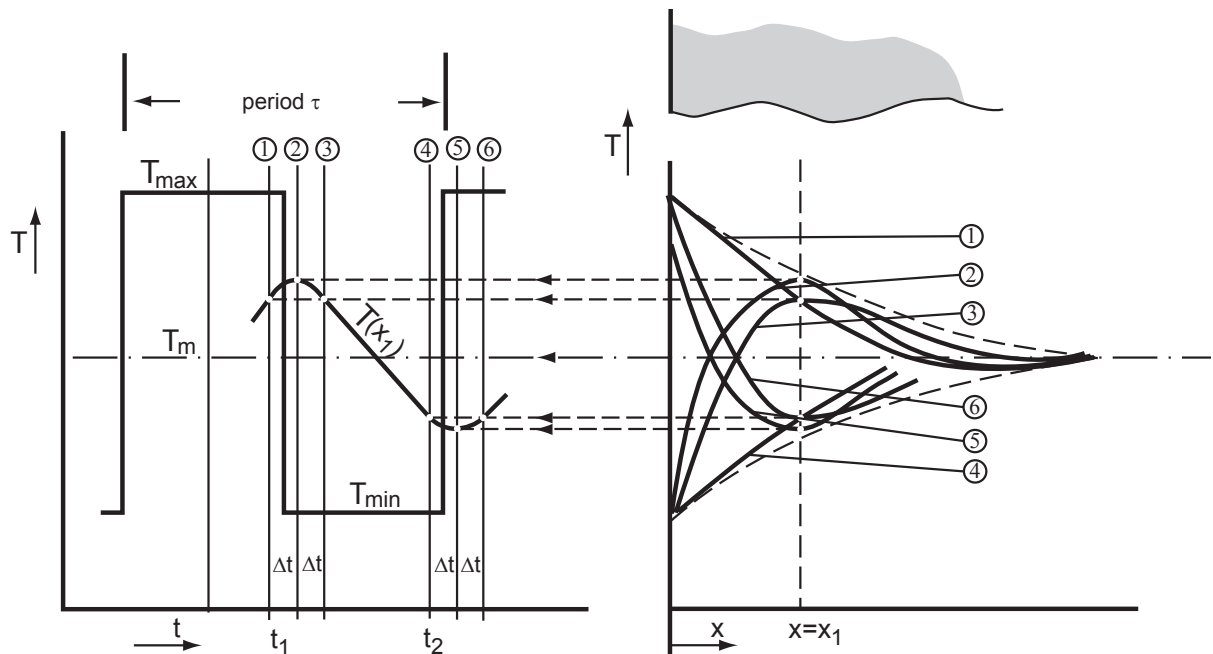


Figure 3.24: Penetration of a periodically changing surrounding temperature in a semi-infinite body

It can be concluded that

- the amplitude of the temperature oscillation diminishes at greater depths,
- the temperature maximum in the inner part of the body are phase shifted

If the surface temperature is described by a harmonic oscillation,

$$T_{x=0} - T_m = (T_{\max} - T_m) \cos \left( \frac{2\pi}{\tau} t \right)$$

and

$$\theta_{x=0} = \frac{T_{x=0} - T_m}{T_{\max} - T_m} \cos \left( \frac{2\pi}{\tau} t \right)$$

with the period  $\tau$ , then we get an analytical solution for the temperature field in the form of

$$\theta = \frac{T - T_m}{T_{\max} - T_m} = \underbrace{\exp\left(-\sqrt{\frac{\pi x^2}{a\tau}}\right)}_1 \cos\left(\underbrace{2\pi\frac{t}{\tau}}_2 - \underbrace{\sqrt{\frac{\pi x^2}{a\tau}}}_3\right) \quad (3.79)$$

with the amplitude (1):

$$\exp\left(-\sqrt{\frac{\pi x^2}{a\tau}}\right)$$

angular frequency (2):

$$\frac{2\pi}{\tau} \quad (3.80)$$

and phase shift (3):

$$\sqrt{\frac{\pi x^2}{a\tau}}$$

The above presented qualitative results of how the amplitudes of the temperature oscillations and phase shifts subside can be evaluated quantitatively using equation (3.79).

### 3.5.3 Dimensionless numbers and diagrams

In the previous layers, a number of examples were given, which had simple, analytical solutions of the Fourier equation (3.8),

$$\frac{\partial T}{\partial t} = \frac{\lambda}{\rho c} \left( \frac{\partial^2 T}{\partial x^2} + \frac{\partial^2 T}{\partial y^2} + \frac{\partial^2 T}{\partial z^2} \right)$$

However, if in cases of systems with complicated geometries or boundary and initial conditions, analytical solutions do not suffice, then numerical solutions using the method of finite differences are nowadays available.

One of the major disadvantages of such methods is the fact that, in general, the derived temperature field is dependent on a large number of parameters

$$T = T(x, y, z, t, \rho, c, \lambda, \text{initial and boundary conditions})$$

and that if one of the parameters changes, then the entire calculation has to be redone.

Next, using a simple example of unsteady state heat conduction in a plate, it will be shown that the number of dependent parameters can be considerably reduced by introducing dimensionless numbers, some of which have already been discussed in previous examples.

First two plates will be considered, with lengths much greater than their thickness and which are brought at a given time in another environment with different temperature. The thickness of the plate, its initial temperature, the new temperature of the surroundings, the material properties and the boundary conditions are labeled A for the first and B for the second plate.

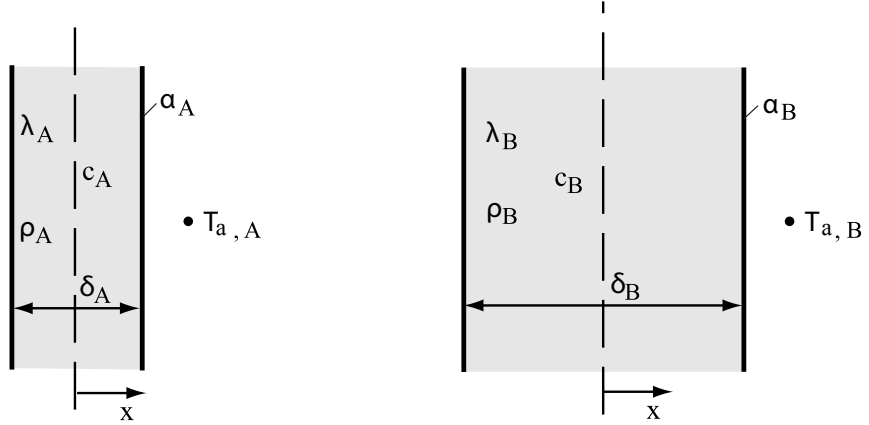


Figure 3.25: Unsteady heat transfer for a two different plate configurations

The temperatures in the plates are distributed according to the differential equations

System A

$$\frac{\partial T_A}{\partial t} = \left( \frac{\lambda}{\rho c} \right)_A \frac{\partial^2 T_A}{\partial x^2}$$

System B

$$\frac{\partial T_B}{\partial t} = \left( \frac{\lambda}{\rho c} \right)_B \frac{\partial^2 T_B}{\partial x^2}$$

with the initial and boundary conditions

$$\begin{aligned} t = 0 \quad & -\frac{\delta}{2} < x < +\frac{\delta}{2} & T = T_0 \\ t \rightarrow \infty \quad & -\frac{\delta}{2} < x < +\frac{\delta}{2} & T = T_a \\ t > 0 \quad & x = -\frac{\delta}{2} \text{ and } x = +\frac{\delta}{2} & \dot{q}_{\text{conduction}}'' = \dot{q}_{\text{convection}}'' \end{aligned}$$

The differential equations can be written in a dimensionless form. To this purpose, reference values will be selected that characterize the system. The geometry of both plates is described by the plate thickness  $\delta$ . If the heat conduction process is periodic in time the process is similar if only the period of oscillations  $\tau$  is different for both plates. The temperature, or the temperature difference  $\theta \equiv T - T_a$ , is referenced to the characteristic temperature difference  $\theta_0 \equiv T_0 - T_a$  of the system.

Hence, the dimensionless variables are

$$\begin{aligned} x^* &\equiv \frac{x_A}{\delta_A} = \frac{x_B}{\delta_B}, \\ t^* &\equiv \frac{t_A}{\tau_A} = \frac{t_B}{\tau_B} \\ \text{and } \theta^* &\equiv \frac{\theta_A}{\theta_{A0}} = \frac{\theta_B}{\theta_{B0}} \end{aligned} \tag{3.81}$$

by substituting them into the differential equations for the temperature field they read as follows

System A

$$\frac{\partial \theta^*}{\partial t^*} = \left( \frac{a_A \tau_A}{\delta_A^2} \right) \frac{\partial^2 \theta^*}{\partial x^{*2}}$$

System B

$$\frac{\partial \theta^*}{\partial t^*} = \left( \frac{a_B \tau_B}{\delta_B^2} \right) \frac{\partial^2 \theta^*}{\partial x^{*2}}$$

Thus, the differential equations are identical, if the Fourier numbers

$$Fo \equiv \frac{a\tau}{\delta^2} = \frac{\lambda}{\rho c} \frac{\tau}{\delta^2}$$

of both systems are equal. The equivalence of the parameters which are included in the Fourier number is not necessary. The dimensionless temperature fields are only then equal, if the boundary conditions of both systems are equal, too. At all times  $t$ , the energy balance at the wall must be obeyed. In other words, the conductive heat flow rate to the surface of the body must equal the convective heat flow from surface to the surroundings.

$$\dot{q}_{\text{wall}}'' = - \left( \lambda \frac{\partial T}{\partial x} \right)_{\text{wall}} = \alpha (T_{\text{wall}} - T_a) \quad (3.82)$$

and hence

$$\left( \frac{\partial T}{\partial x} \right)_{\text{wall}} = - \frac{\alpha}{\lambda} (T_{\text{wall}} - T_a)$$

In the dimensionless form, the boundary conditions are

System A

System B

$$\left( \frac{\partial \theta^*}{\partial x^*} \right)_{\text{Wand}} = - \left( \frac{\alpha_A \delta_A}{\lambda_A} \right) \theta_{\text{Wand}}^* \quad \left( \frac{\partial \theta^*}{\partial x^*} \right)_{\text{Wand}} = - \left( \frac{\alpha_B \delta_B}{\lambda_B} \right) \theta_{\text{Wand}}^*$$

Hence, it follows that the boundary conditions are identical, if the Biot numbers

$$Bi \equiv \frac{\alpha \delta}{\lambda}$$

of both systems are equal. If the system had to be extended to consider three-dimensional bodies, the dimensionless temperature field has to be described by dimensionless parameters

$$\begin{aligned} \frac{T - T_a}{T_0 - T_a} &= \frac{T - T_a}{T_0 - T_a} \left( \frac{x}{\delta_1}, \frac{y}{\delta_2}, \frac{z}{\delta_3}, \frac{t}{\tau}, \left( \frac{a\tau}{\delta^2} \right)_{1,2,3}, \left( \frac{\alpha \delta}{\lambda} \right)_{1,2,3} \right) \\ &= \frac{T - T_a}{T_0 - T_a} (x^*, y^*, z^*, t^*, Fo_{1,2,3}, Bi_{1,2,3}) \end{aligned} \quad (3.83)$$

The previously mentioned examples can be derived using these parameters, respectively. The analytical or numerical solutions of the differential equations are

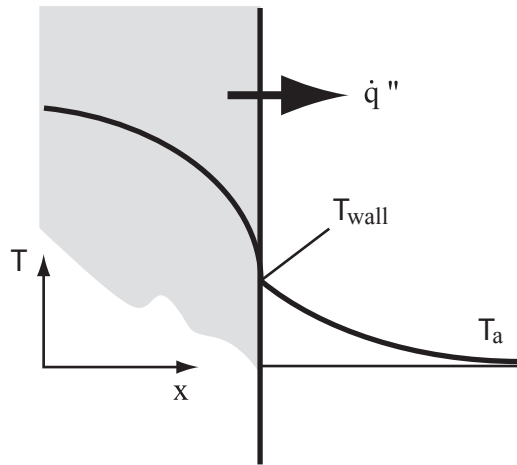


Figure 3.26: Boundary conditions at the surface

often presented in diagrams using these dimensionless parameters. In the following three examples will be shown which are useful to approximate many practical problems. These examples will show the temperature profile and the transferred heat during cooling (or heating) of extended plates, long cylinders and spheres, whose surrounding temperatures have been abruptly changed at a given time. Although these one-dimensional problems can be solved analytically, because of their complicated computations it is recommended to use the diagrams given by Heisler (1947). The following diagrams show the mid-plane temperature as a function of the time for a plate, cylinder and sphere, together with additional diagrams used for the determination of the temperatures at other points of the body. The diagrams will be interpolated appropriately in order to get the heat as a function of the time at the surface of the body.

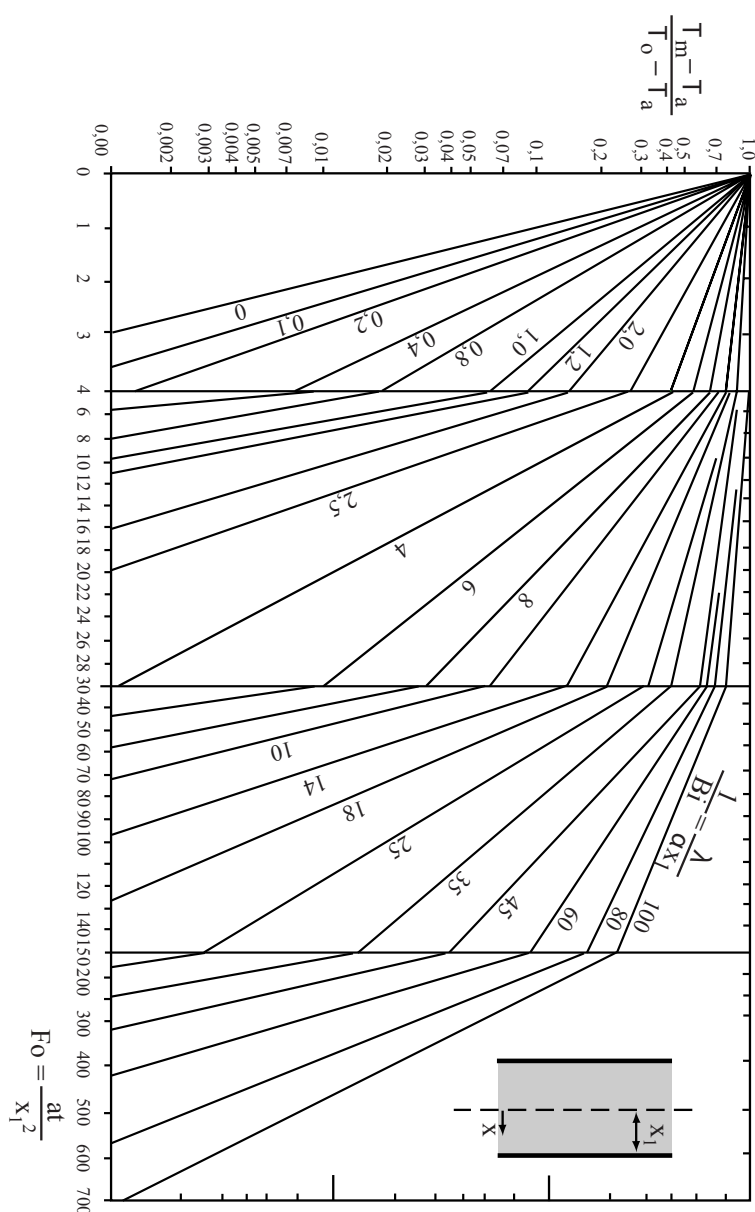


Figure 3.27: Mid-plane temperature of a plate with thickness  $2x_1$

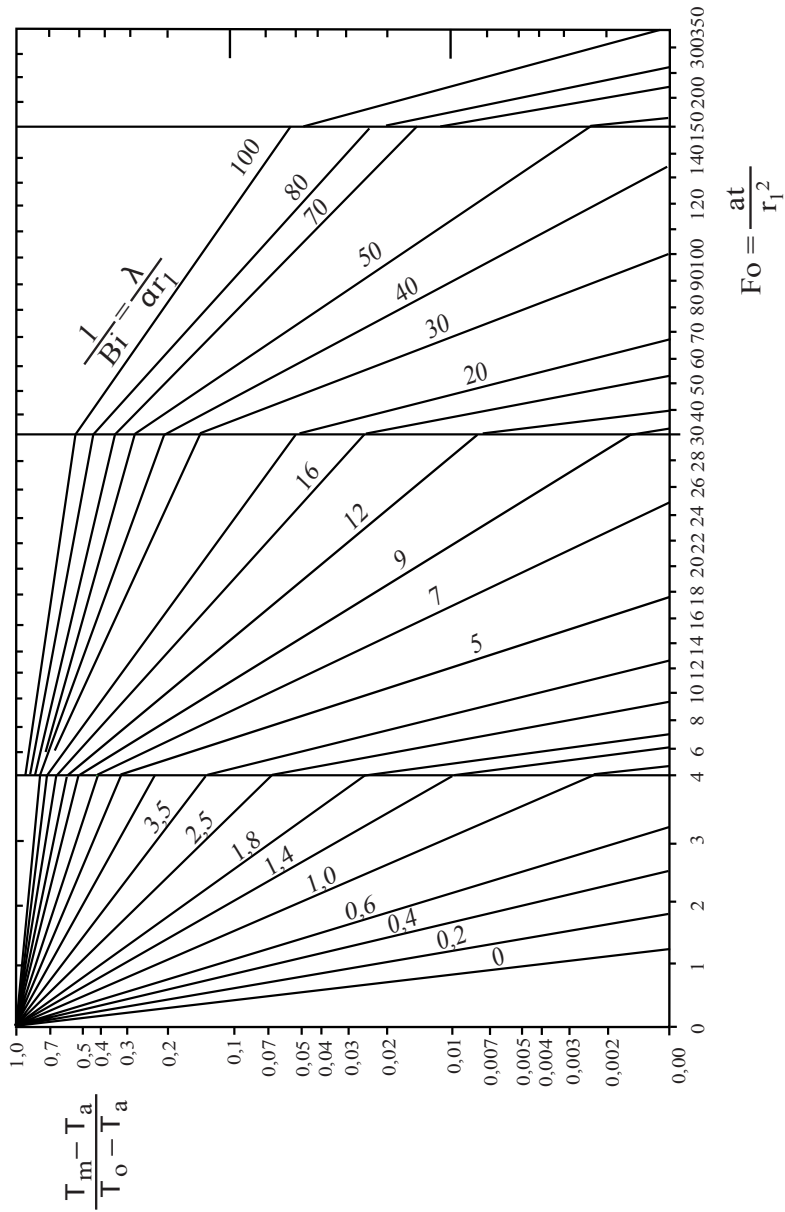


Figure 3.28: Temperature along the axis of a cylinder with radius  $r_1$

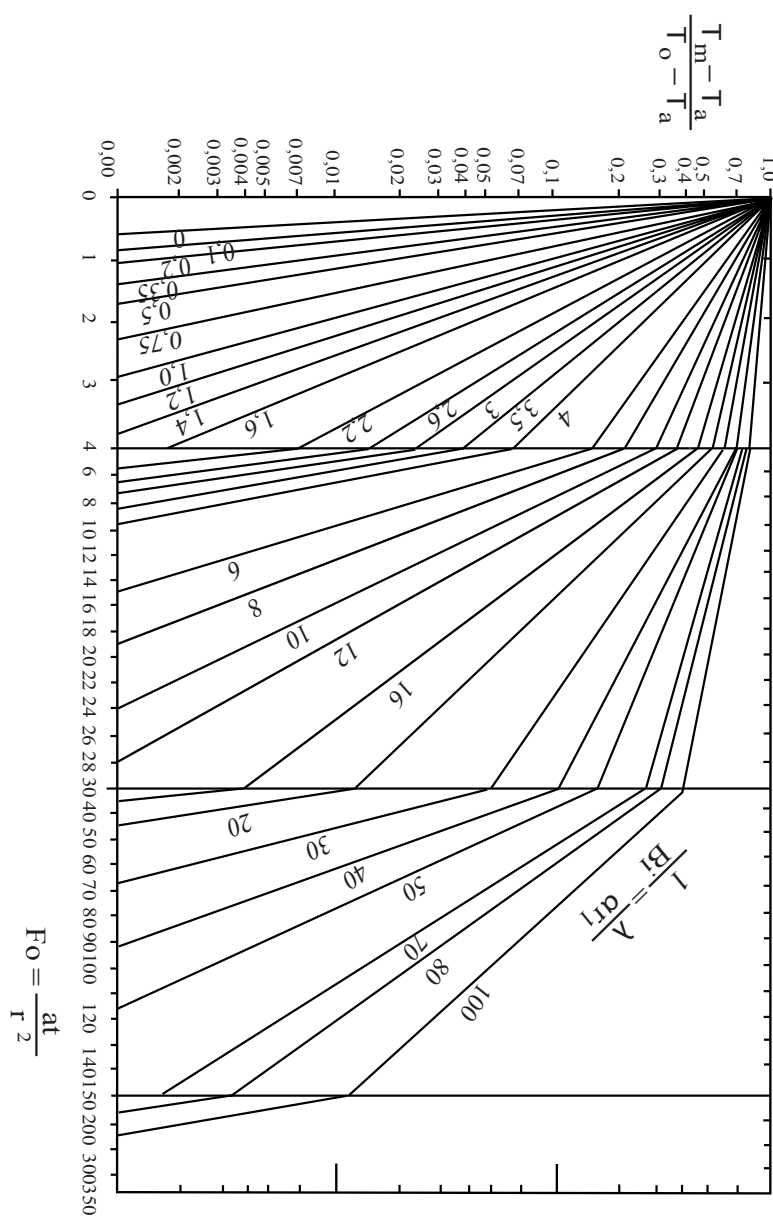


Figure 3.29: Temperature in the centre of a sphere with radius  $r_1$

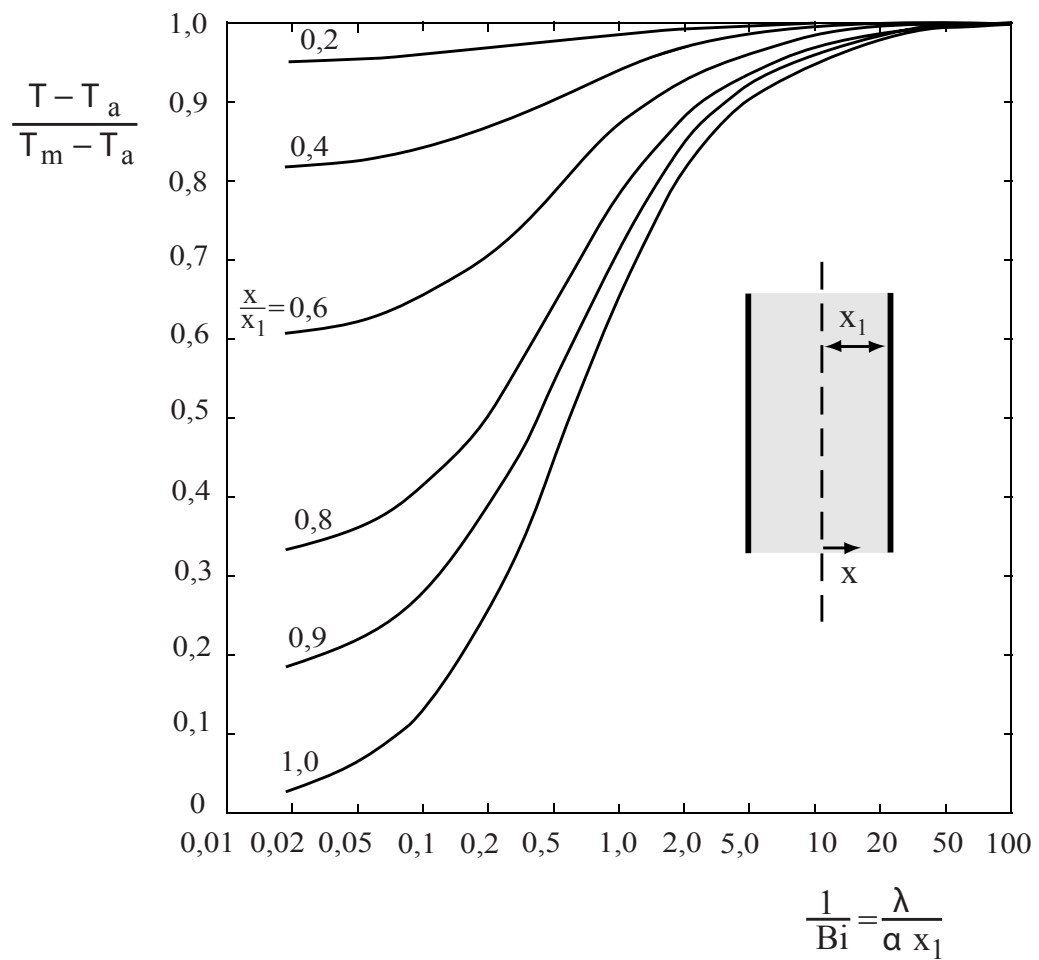


Figure 3.30: Temperature distribution in a plate (valid for  $Fo > 0,2$ )

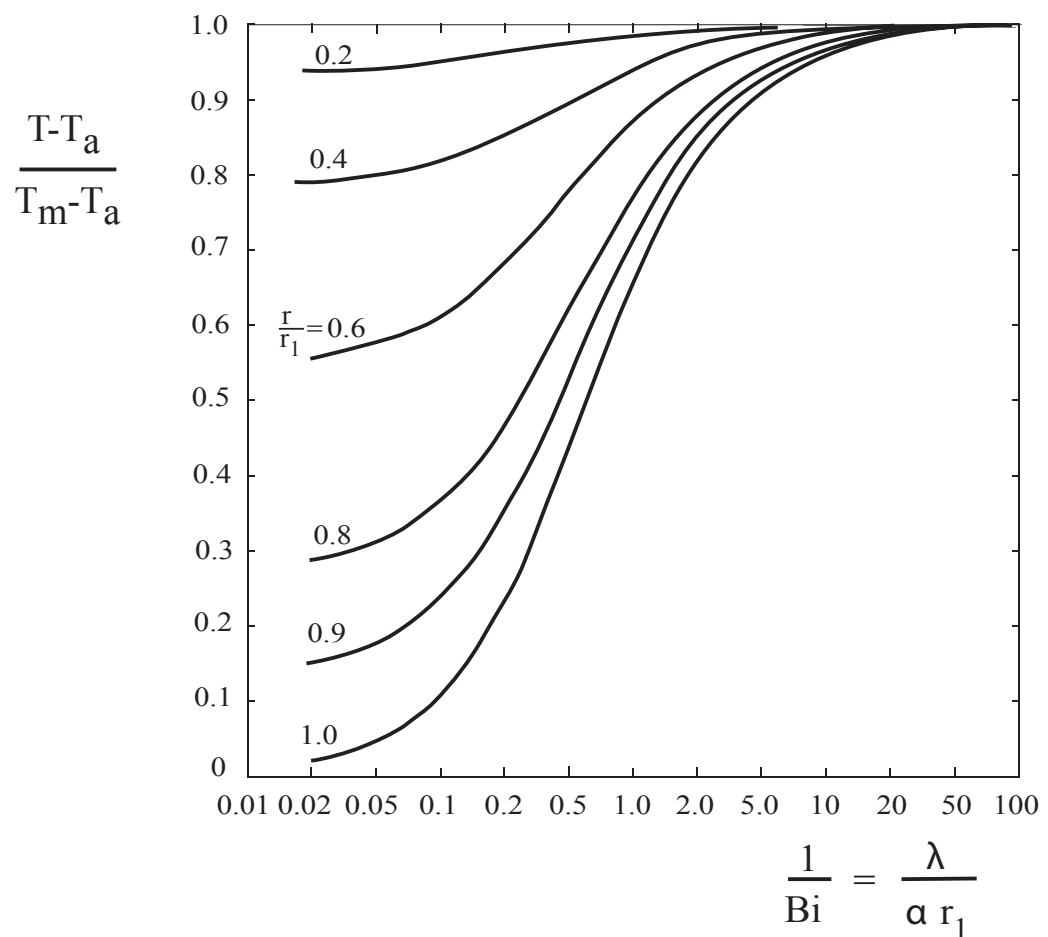
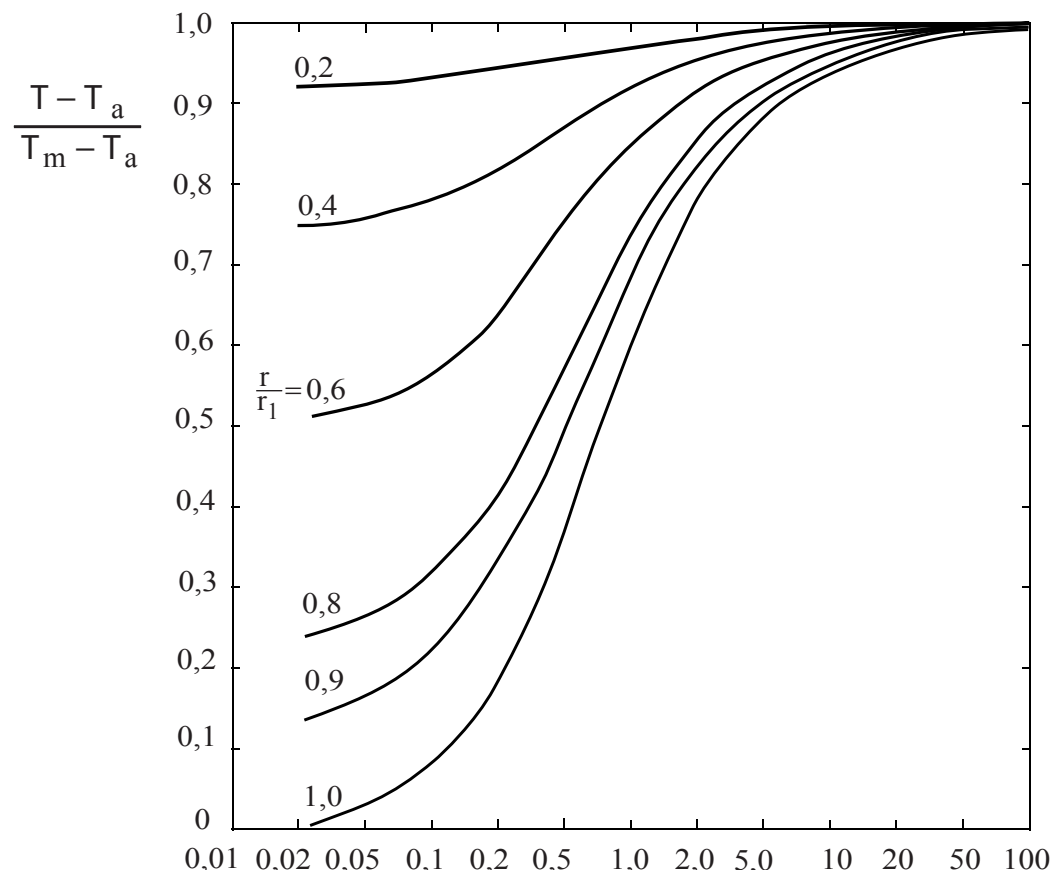


Figure 3.31: Temperature distribution in a cylinder (valid for  $\text{Fo} > 0,2$ )



$$\frac{1}{Bi} = \frac{\lambda}{\alpha r_1}$$

Figure 3.32: Temperature distribution in a sphere (valid for  $Fo > 0,2$ )

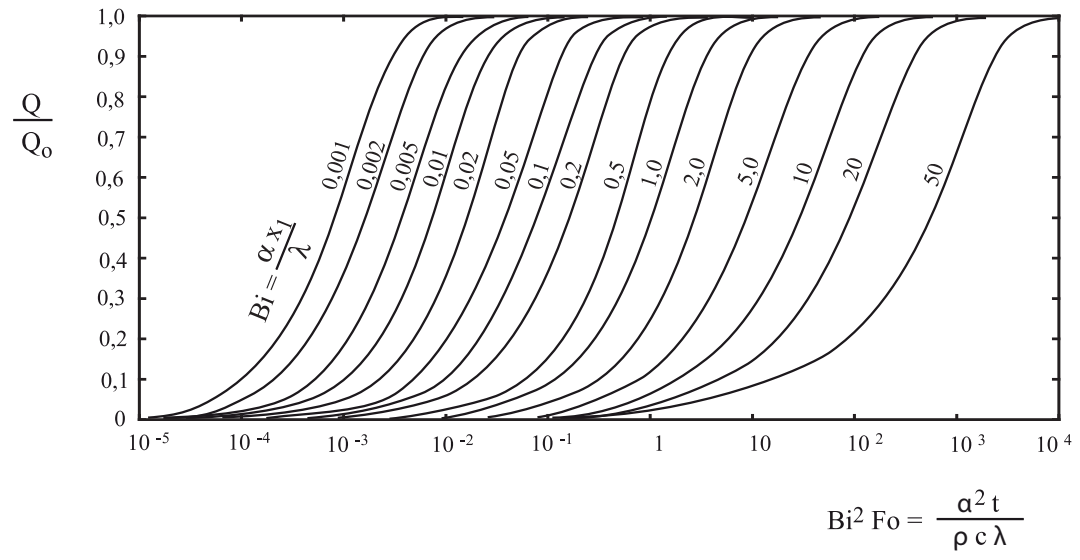


Figure 3.33: Heat loss of a plate

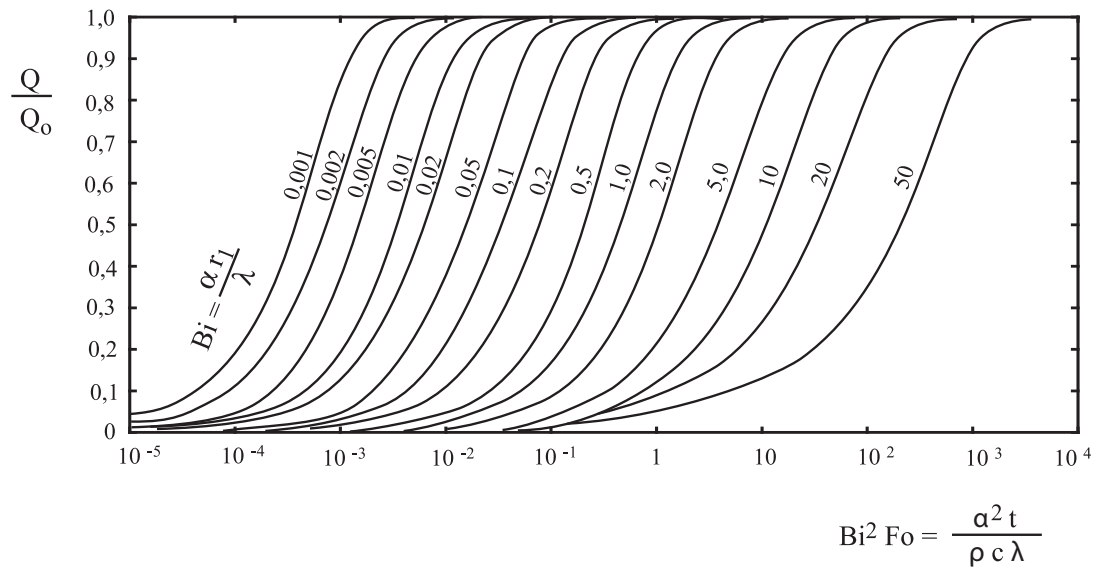


Figure 3.34: Heat loss of a cylinder

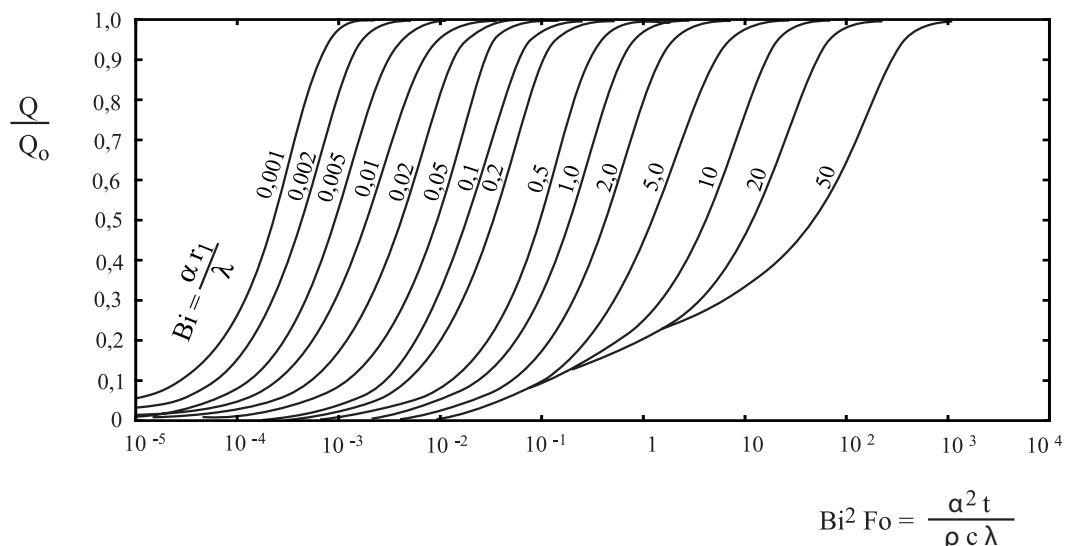


Figure 3.35: Heat loss of a sphere



---

# Chapter 4

## Convection

We discussed the energy transport by heat conduction in chapter 3. Molecular properties, described by the thermal conductivity of the material play a key role in heat transport.

In some of the energy transport examples discussed previously, we had to formulate the boundary conditions for heat transfer from the body to the flowing fluid along the body. Without detailed analysis of the physical relationships, we assumed that

$$\frac{\dot{Q}_w}{A} \equiv \dot{q}_w'' = \alpha(T_w - T_a) \quad (4.1)$$

whereat the heat transfer coefficient  $\alpha$  was assumed to be known. In this section, we will discuss the basic principles of this transport mechanism.

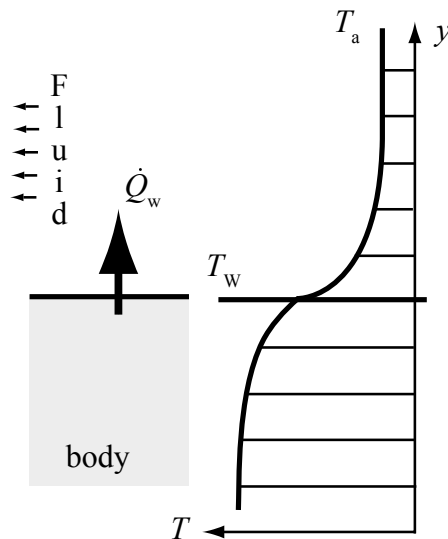


Figure 4.1: Heat transfer at a surface

The major difference between the transport mechanisms of heat conduction and heat convection can be demonstrated by a simple experiment, where a hot, horizontal wall is let to cool down.

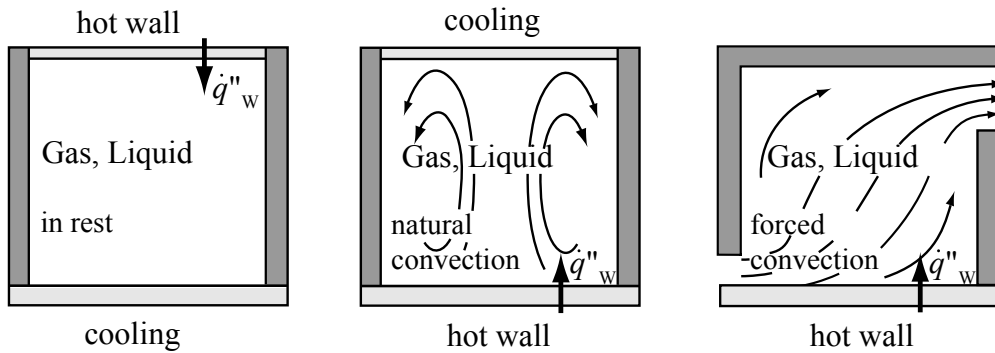


Figure 4.2: Cooling of a hot surface by conduction and convection

In the first experiment, the wall is cooled from below by a cold fluid, liquid or gas. For this arrangement we have a stagnant fluid, and the heat is transported solely by conduction to the area of lower heat. If the hot wall is placed at the bottom, the fluid will become unstable, and the warmer areas (in the lower part) will rise up due to their lower density and hence flow in the fluid will be initiated. This so-called *natural convection* amplifies the heat transfer. In the third case shown (rightmost diagram), the hot wall is cooled by a medium, which is pumped through the system. As was the case of natural convection, so again, in this case of *forced convection*, it is not only the thermal conductivity of the fluid that determines the characteristics of the heat transfer. An important, additional parameter that dictates the heat transfer is obviously the velocity of the fluid, which depends on the density differences as well as the electrical power of the pump.

Only in areas directly adjacent to the wall, where because of the boundary layer condition which states that the velocity drops to zero (non-slip condition), the Fourier equation for the heat transfer in the fluid still applies

$$\dot{q}_w'' = - \left( \lambda_{\text{fluid}} \frac{dT_{\text{fluid}}}{dy} \right)_w \quad (\text{regarding the fluid}) \quad (4.2)$$

as well as for the heat transfer in the body

$$\dot{q}_w'' = - \left( \lambda_{\text{body}} \frac{dT_{\text{body}}}{dy} \right)_w \quad (\text{regarding the solid body}) \quad (4.3)$$

The heat transfer coefficient defined by equation (4.1) can be determined from the temperature gradient at the fluid side of the wall by comparison with equation (4.2).

$$\alpha = \frac{-\left(\lambda_{\text{fluid}} \frac{dT_{\text{fluid}}}{dy}\right)_W}{T_W - T_a} \quad (4.4)$$

The temperature field in the fluid and hence the temperature gradient at the wall surface is described by the equation of energy conservation (1st Law of thermodynamics). In this section, we will have to expand the energy balance from chapter 3 by including the enthalpy flowing in and out of the volume element. To describe these flows, the velocities, in addition to the temperatures, have to be known. Thus, in addition to the energy equation, the momentum equation and the continuity equation will have to be formulated and solved. The necessary basic principles have been discussed in introductory lectures on fluid mechanics and will only be briefly presented here.

## 4.1 Conservation laws for laminar, steady state, two-dimensional flow

The general solution of a three-dimensional flow, for which the flow field and the temperature field are interdependent can only be determined by determining the three velocity components  $u$ ,  $v$  and  $w$ , the temperature  $T$  and pressure  $p$ , as well as the material properties of the fluid, the density  $\rho$ , the dynamic viscosity  $\eta$  and the thermal conductivity  $\lambda$ . Since these parameters are not independent of each other, a simultaneous solution of the conservation equations of mass, momentum and energy is required. To avoid too much writing, we will focus on the two-dimensional, steady state case.

The flow can be either laminar or turbulent, i.e. the streamlines are either parallel or superimposed to the mean, steady state fluctuating flow. These three-dimensional fluctuating velocities and their impact on the momentum and heat exchange will be discussed in section 4.4.

The following derivations are limited to laminar flow.

### 4.1.1 Equation of continuity

For steady state flow, the difference between mass flowing in and out must vanish.

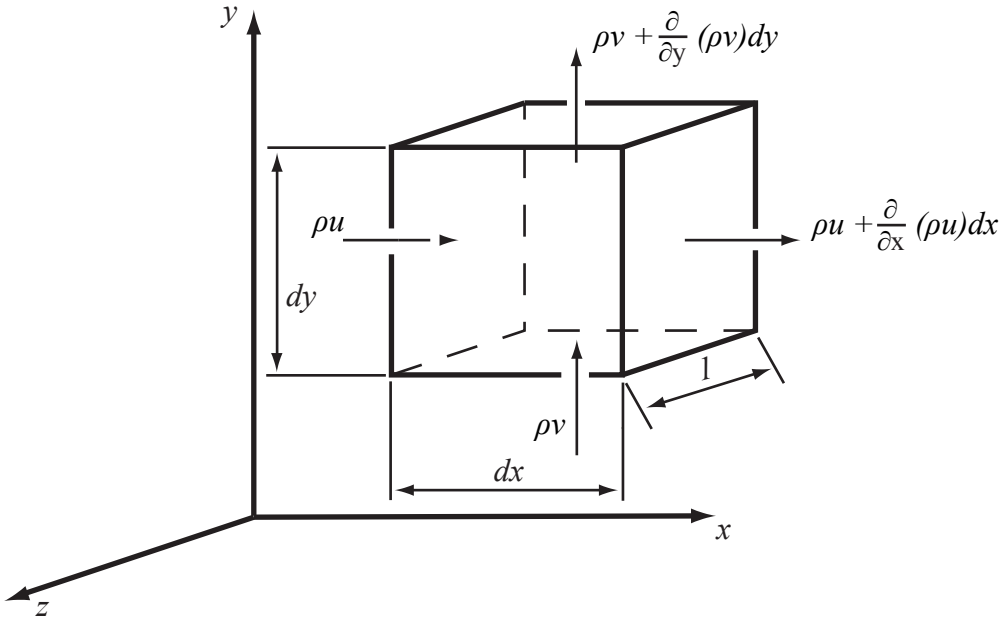


Figure 4.3: Mass balance at the control volume

Mass flowing in

$$\begin{aligned} \rho u dy l \\ \rho v dx l \end{aligned}$$

Mass flowing out

$$\begin{aligned} \rho u dy l + \frac{\partial}{\partial x} \rho u dx dy l \\ \rho v dx l + \frac{\partial}{\partial y} \rho v dy dx l \end{aligned}$$

Difference

$$\frac{\partial}{\partial x} \rho u dx dy l + \frac{\partial}{\partial y} \rho v dx dy l$$

This yields the equation of continuity

$$\frac{\partial \rho u}{\partial x} + \frac{\partial \rho v}{\partial y} = 0 \quad (\text{equation of continuity}) \quad (4.5)$$

or vectorically

$$\operatorname{div}(\rho \vec{w}) = 0$$

For incompressible fluids ( $\rho = \text{constant}$ ), this equation simplifies to

$$\frac{\partial u}{\partial x} + \frac{\partial v}{\partial y} = 0 \quad (4.6)$$

### 4.1.2 Equations of momentum

The momentum equation states that the difference between the momentum in and out flow of the volume element is equal to the external forces acting on the volume element, whereat inertial forces and surface forces can be relevant.

#### 4.1.2.1 Equation of momentum in x-direction

The difference between momentum flowing in and out is

$$\left( \frac{\partial(\rho uu)}{\partial x} + \frac{\partial(\rho vu)}{\partial y} \right) dx dy l = \left( \rho u \frac{\partial u}{\partial x} + \rho v \frac{\partial u}{\partial y} + u \left( \underbrace{\frac{\partial \rho u}{\partial x} + \frac{\partial \rho v}{\partial y}}_{=0 \text{ (eq.4.5)}} \right) \right) dx dy l \quad (4.7)$$

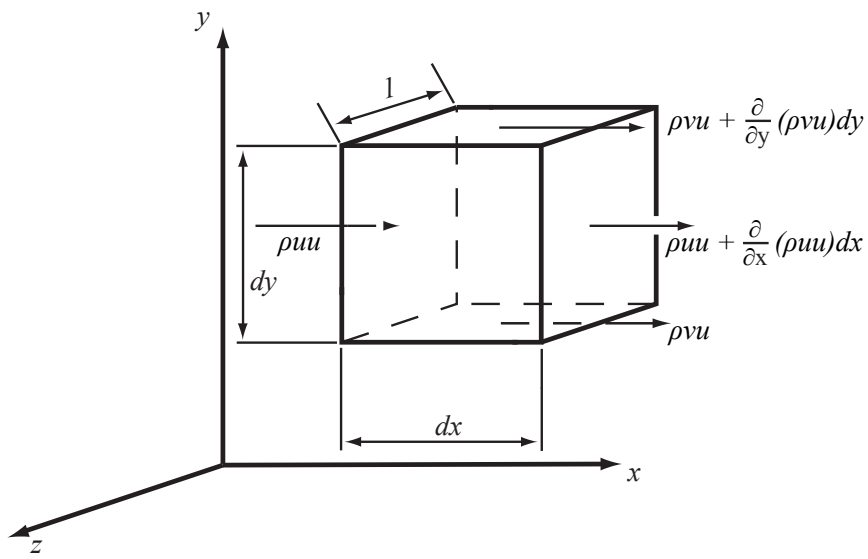


Figure 4.4: x-momentum balance at the control volume

The surface forces, i.e. pressure, shear and normal forces can be expressed by  $p_{xy}$ , where the first index indicates the orientation of the surface at which the force is applied (e.g. here perpendicular to the x-direction) and the second index shows the direction of the force (e.g. here in the y-direction).

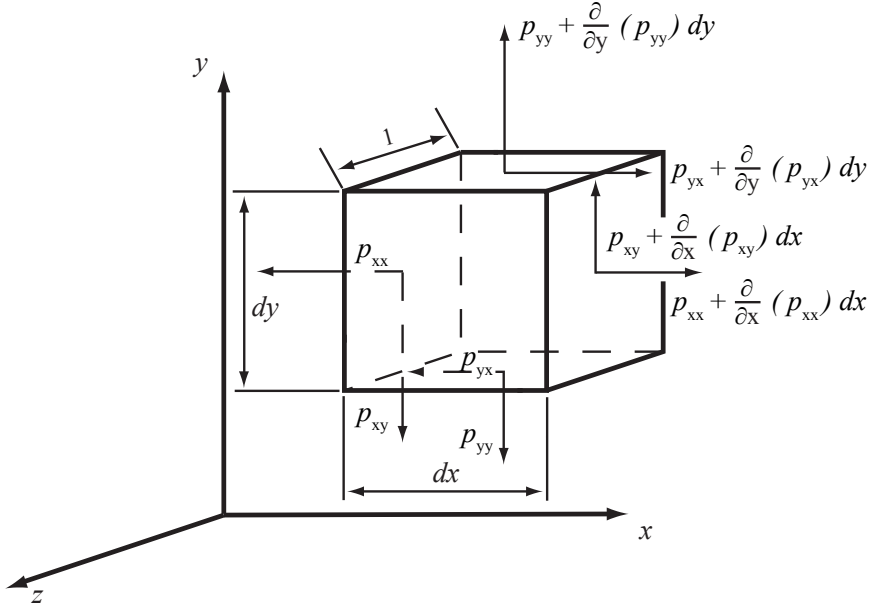


Figure 4.5: Forces at the control volume

In the equation of momentum for the x-direction, only the forces acting in x-direction are considered.

Hence, the balance of surface forces applied at the volume element is

$$\frac{\partial p_{xx}}{\partial x} dx dy l + \frac{\partial p_{yx}}{\partial y} dy dx l$$

with the normal stress  $p_{xx}$  and the shear stress  $p_{yx}$ , related to the pressure  $u$  and  $v$  and the dynamic viscosity  $\eta$  [kg/ms] given by Navier (1827) and Stokes (1845), see Schlichting u. Gersten (2006).

$$p_{xx} = -p + \sigma_x = -p - \frac{2}{3}\eta \left( \frac{\partial u}{\partial x} + \frac{\partial v}{\partial y} \right) + 2\eta \frac{\partial u}{\partial x}$$

and

$$p_{yx} = \tau_{yx} = \tau_{xy} = \eta \left( \frac{\partial v}{\partial x} + \frac{\partial u}{\partial y} \right)$$

This yields

$$\left[ -\frac{\partial p}{\partial x} + \frac{\partial}{\partial x} \left( 2\eta \frac{\partial u}{\partial x} - \frac{2}{3}\eta \left( \frac{\partial u}{\partial x} + \frac{\partial v}{\partial y} \right) \right) + \frac{\partial}{\partial y} \left( \eta \left( \frac{\partial v}{\partial x} + \frac{\partial u}{\partial y} \right) \right) \right] dx dy l$$

At the volume element, inertial forces are also applied, of which we will discuss only the force of gravity

$$\rho g_x dx dy l$$

Summarizing the momentum, surface and inertial forces, we get the momentum equation, the so-called Navier-Stokes equation

$$\begin{aligned} & \rho u \frac{\partial u}{\partial x} + \rho v \frac{\partial u}{\partial y} \\ &= -\frac{\partial p}{\partial x} + \frac{\partial}{\partial x} \left( 2\eta \frac{\partial u}{\partial x} - \frac{2}{3}\eta \left( \frac{\partial u}{\partial x} + \frac{\partial v}{\partial y} \right) \right) + \frac{\partial}{\partial y} \left( \eta \left( \frac{\partial v}{\partial x} + \frac{\partial u}{\partial y} \right) \right) + \rho g_x \end{aligned} \quad (4.8)$$

(equation of momentum, x-direction)

#### 4.1.2.2 Equation of momentum in y-direction

$$\begin{aligned} & \rho u \frac{\partial v}{\partial x} + \rho v \frac{\partial v}{\partial y} \\ &= -\frac{\partial p}{\partial y} + \frac{\partial}{\partial y} \left( 2\eta \frac{\partial v}{\partial y} - \frac{2}{3}\eta \left( \frac{\partial u}{\partial x} + \frac{\partial v}{\partial y} \right) \right) + \frac{\partial}{\partial x} \left( \eta \left( \frac{\partial v}{\partial x} + \frac{\partial u}{\partial y} \right) \right) + \rho g_y \end{aligned} \quad (4.9)$$

(equation of momentum, y-direction)

Assuming constant material properties (density, viscosity), the equations of momentum are further simplified to

$$\rho u \frac{\partial u}{\partial x} + \rho v \frac{\partial u}{\partial y} = -\frac{\partial p}{\partial x} + \eta \left( \frac{\partial^2 u}{\partial x^2} + \frac{\partial^2 u}{\partial y^2} \right) + \rho g_x \quad (4.10)$$

(equation of momentum, x-direction, ( $\rho, \eta$  constant))

$$\rho u \frac{\partial v}{\partial x} + \rho v \frac{\partial v}{\partial y} = -\frac{\partial p}{\partial y} + \eta \left( \frac{\partial^2 v}{\partial x^2} + \frac{\partial^2 v}{\partial y^2} \right) + \rho g_y \quad (4.11)$$

(equation of momentum, y-direction, ( $\rho, \eta$  constant))

or as vector equation

$$\rho (\vec{w} \times \text{grad } ) \vec{w} = -\text{grad } p + \eta \nabla^2 \vec{w} + \rho \vec{g} \quad (4.12)$$

(equation of momentum, ( $\rho, \eta$  constant))

### 4.1.3 Equation of energy conservation

The first law of thermodynamics

$$d\dot{Q} + dP = d\dot{U} + d\dot{E}_a \quad (4.13)$$

applied to a volume element of a flowing medium states that any heat or work added to the system will result in change of inner, potential or kinetic energy.

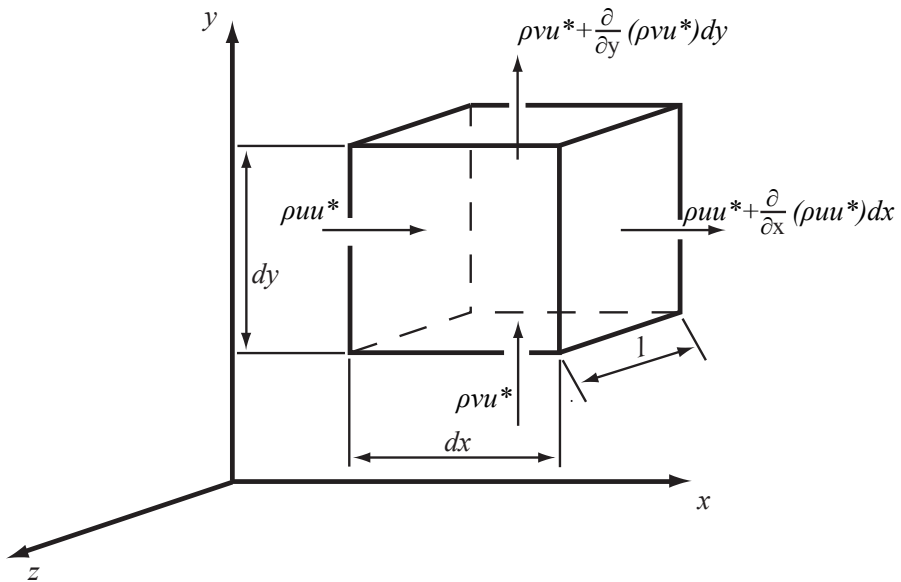


Figure 4.6: Energy flows at the control volume

The kinetic energy is to be considered for the net energy only for flow velocities in

the order of the speed of sound, and thus will be neglected here. The difference of inner energy flowing in and out is

$$\frac{\partial}{\partial x} (\rho u u^*) dx dy l + \frac{\partial}{\partial y} (\rho v u^*) dx dy l$$

where the specific inner energy is named  $u^* [\frac{J}{kg}]$ . If we introduce the specific enthalpy  $h \equiv u^* + \frac{p}{\rho}$  instead of the specific inner energy we get

$$\begin{aligned} & \left( \frac{\partial}{\partial x} (\rho u h) + \frac{\partial}{\partial y} (\rho v h) - \frac{\partial}{\partial x} (u p) - \frac{\partial}{\partial y} (v p) \right) dx dy l \\ &= \left( \rho u \frac{\partial h}{\partial x} + \rho v \frac{\partial h}{\partial y} + h \left( \underbrace{\frac{\partial \rho u}{\partial x} + \frac{\partial \rho v}{\partial y}}_{=0 \text{ (eq.4.5)}} \right) - \frac{\partial}{\partial x} (u p) - \frac{\partial}{\partial y} (v p) \right) dx dy l \end{aligned}$$

Resulting from Fourier's equation, the total *added heat* is

$$\left( \frac{\partial}{\partial x} \left( \lambda \frac{\partial T}{\partial x} \right) + \frac{\partial}{\partial y} \left( \lambda \frac{\partial T}{\partial y} \right) \right) dx dy l.$$

The volume element receives work from the surface (friction) forces as well as from the inertial forces.

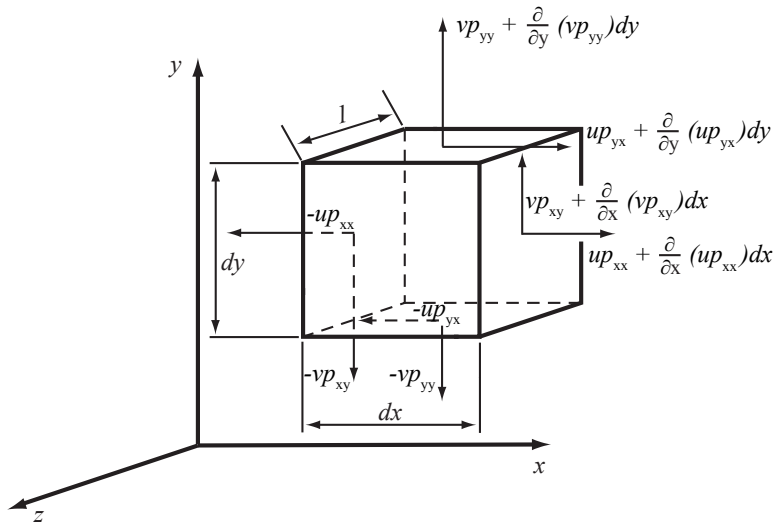


Figure 4.7: Contribution of the forces to the energy balance of the volume element

$$\left( \frac{\partial}{\partial x} (u\sigma_x) - \frac{\partial}{\partial x} (up) + \frac{\partial}{\partial y} (u\tau_{xy}) + \rho ug_x + \frac{\partial}{\partial y} (v\sigma_y) - \frac{\partial}{\partial y} (vp) + \frac{\partial}{\partial x} (v\tau_{xy}) + \rho vg_y \right) dx dy l$$

Hence, the energy equation is

$$\begin{aligned} \rho u \frac{\partial h}{\partial x} + \rho v \frac{\partial h}{\partial y} &= \frac{\partial}{\partial x} \left( \lambda \frac{\partial T}{\partial x} \right) + \frac{\partial}{\partial y} \left( \lambda \frac{\partial T}{\partial y} \right) \\ &\quad + \frac{\partial}{\partial x} (u\sigma_x + v\tau_{xy}) + \frac{\partial}{\partial y} (u\tau_{xy} + v\sigma_y) + \rho ug_x + \rho vg_y \end{aligned} \quad (4.14)$$

The stress contributions of the normal, shear and inertial forces will be omitted since their values are, in most cases, negligibly small and do not contribute significantly to the net energy balance.

The specific enthalpy may be substituted by the temperatures for systems without phase changes, no chemical reactions and, if the fluid can be considered an ideal gas ( $dh = c_p dT$ ) or an incompressible liquid ( $dh = c dT$ )

Hence,

$$\rho u c_p \frac{\partial T}{\partial x} + \rho v c_p \frac{\partial T}{\partial y} = \frac{\partial}{\partial x} \left( \lambda \frac{\partial T}{\partial x} \right) + \frac{\partial}{\partial y} \left( \lambda \frac{\partial T}{\partial y} \right) \quad (4.15)$$

Comparing this equation with the Fourier equation for heat conduction, equation 3.2, for steady state problems without heat sources, it can be shown that under the assumptions above the energy transport by heat conduction is extended by convective energy transport through enthalpy flow. For unsteady state processes, the left-hand side of equation 4.15 is to be supplemented by a term characteristic for the energy storage  $\rho c_p \frac{\partial T}{\partial t}$ .

If, in addition, the thermal conductivity is independent of location, following from equation (4.15)

$$\rho u \frac{\partial T}{\partial x} + \rho v \frac{\partial T}{\partial y} = \frac{\lambda}{c_p} \left( \frac{\partial^2 T}{\partial x^2} + \frac{\partial^2 T}{\partial y^2} \right) \quad (4.16)$$

or

$$\rho u \frac{\partial T}{\partial x} + \rho v \frac{\partial T}{\partial y} = \frac{\eta}{\text{Pr}} \left( \frac{\partial^2 T}{\partial x^2} + \frac{\partial^2 T}{\partial y^2} \right) \quad (4.17)$$

with the Prandtl number

$$\text{Pr} \equiv \frac{\eta}{\lambda/c_p} \quad (4.18)$$

or in vector form

$$\rho \vec{w} \times \text{grad } T = \frac{\eta}{\text{Pr}} \nabla^2 T \quad (4.19)$$

The temperature field of a flowing medium and hence the temperature gradient at its boundary, from which the heat transfer can be calculated, equation (4.2), is sufficiently described by the energy equation, (4.17), momentum equation, (4.10), the equation of continuity, (4.6), and appropriate estimates of the material properties as well as the boundary conditions of the system itself.

This system of interdependent partial differential equations can only be solved numerically using methods of finite differences or finite volumes, which nowadays can be obtained commercially and which will be discussed in depth at other lectures. Such computational fluid dynamic (CFD) methods reach the ultimate limits of modern high performance computers in cases of geometries or boundary conditions with a high degree of complexity, so that often it is more cost-efficient to carry out experiments to obtain heat transfer coefficients.

A major group of technologically important flows, *boundary layer flows*, uses a simplified form of the derived conservation equations. This leads to parabolic instead of elliptical partial differential equations, which in turn are much easier to handle numerically, and in some cases can be transformed into ordinary differential equations.

These solution methods will be briefly discussed further on, a detailed investigation of these problems can be found for example in Bayley u. a. (1972).

## 4.2 Forced convection - boundary layer equations for laminar, steady state flow

For flow along solid walls the influence of the viscous forces is limited to an area in the vicinity of the wall, called *velocity boundary layer*, with thickness  $\delta_u$ . The viscosity is of no influence outside of this boundary layer the flow behaves as a potential flow. The same applies for the area, where heat conduction dominates. The *thermal boundary layer* with thickness  $\delta_T$  outlines the area of heat conduction from the area of undisturbed flow.

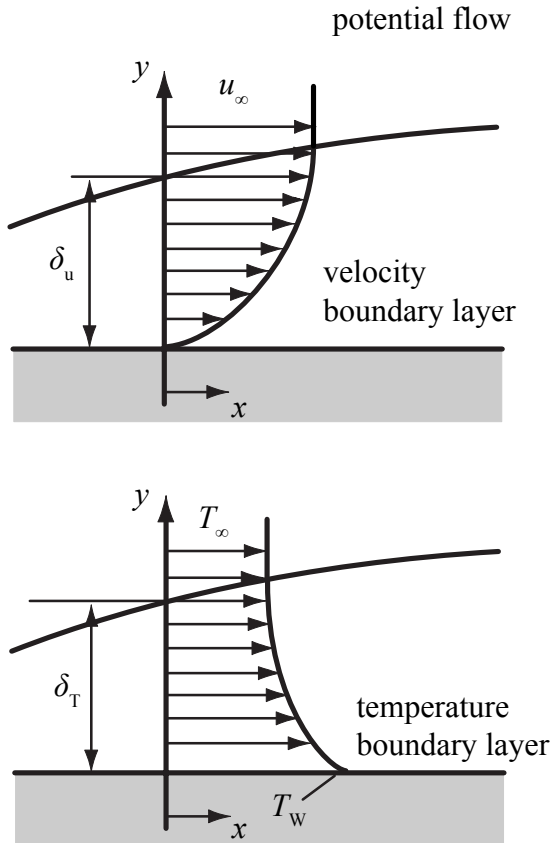


Figure 4.8: Velocity and thermal boundary layers of a surface in a stream flow

Prandtl (1904) derived the equations valid for boundary layers from the conservation laws through appropriate assumptions for the individual terms. These assumptions, which can also be found at Schlichting and Gersten (2006), state that for flow of the boundary layer type, i.e.  $\frac{\delta}{L} \ll 1$ , the following assumptions are valid

$$\frac{\partial^2 u}{\partial x^2} \ll \frac{\partial^2 u}{\partial y^2} \quad \text{and} \quad \frac{\partial^2 T}{\partial x^2} \ll \frac{\partial^2 T}{\partial y^2} \quad (4.20)$$

Thus, the parabolic differential equations for boundary layers with constant material properties are

$$\frac{\partial u}{\partial x} + \frac{\partial v}{\partial y} = 0 \quad (4.21)$$

(equation of continuity)

$$\rho u \frac{\partial u}{\partial x} + \rho v \frac{\partial u}{\partial y} = -\frac{\partial p}{\partial x} + \eta \frac{\partial^2 u}{\partial y^2} + \rho g_x \quad (4.22)$$

(momentum equation, x-direction)

$$\rho u \frac{\partial T}{\partial x} + \rho v \frac{\partial T}{\partial y} = \frac{\eta}{\text{Pr}} \frac{\partial^2 T}{\partial y^2} \quad (4.23)$$

(equation of energy conservation)

In general, the thicknesses of the velocity and thermal boundary layers are not equal. Yet, as a consequence of the approximations for the boundary layers, with  $\delta_u \approx \eta^{\frac{1}{2}}$  yields:

$$\frac{\delta_u}{\delta_T} \approx \text{Pr}^{\frac{1}{2}} \quad (4.24)$$

The Prandtl number for gases is approximately 1, so that the velocity and thermal boundary layer almost coincide in thickness.

#### 4.2.1 Exact solutions for the equations of boundary layers

Transformation of coordinates is possible for a flat plate ( $dp/dx = 0$ ), without inertial forces ( $\rho g_x = 0$ ) which leads to an ordinary differential equation with an exact solution, see Schlichting u. Gersten (2006).

The solution of the momentum equation, the velocity profile in the boundary layer, was firstly published by Blasius (1908) and is shown in 4.9 as a function of the dimensionless wall distance. The dimensionless wall shear stress, the friction coefficient  $\frac{c_f}{2}$ , derives from the velocity gradients at the wall.

$$\frac{c_f}{2} \equiv \frac{\tau_w}{\rho u_\infty^2} = \frac{\left(\eta \frac{du}{dy}\right)_w}{\rho u_\infty^2} \quad (4.25)$$

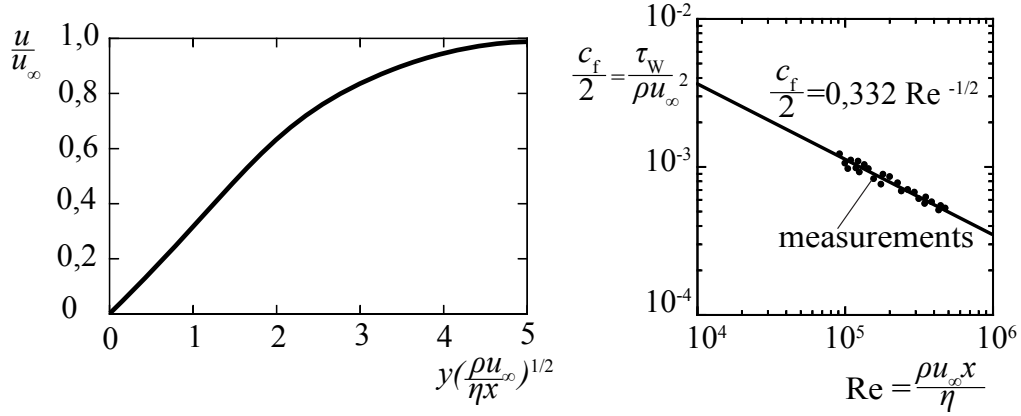


Figure 4.9: Laminar flow over a flat plate - velocity profile and friction coefficient, according to Blasius (1908)

The corresponding equation of energy conservation (equation 4.23) for the flat plate with constant wall temperature was solved by Pohlhausen (1921) and leads to the temperature profiles, which are additionally dependent on the Prandtl number. The temperature gradients at the wall and hence the local heat transfer coefficient  $\alpha$  derive from these temperature profiles, see equation (4.4), or its mean value  $\bar{\alpha}$ :

$$\alpha = \frac{-\left(\lambda \frac{dT}{dy}\right)_W}{(T_W - T_\infty)} \text{ and } \bar{\alpha} = \frac{1}{L} \int_0^L \alpha(x) dx \quad (4.26)$$

The dimensionless temperature profile and the dimensionless heat transfer coefficient, the Nusselt number

$$Nu \equiv \frac{\alpha x}{\lambda} \text{ and } \overline{Nu} \equiv \frac{\bar{\alpha} L}{\lambda} \quad (4.27)$$

are shown in Fig. 4.10.

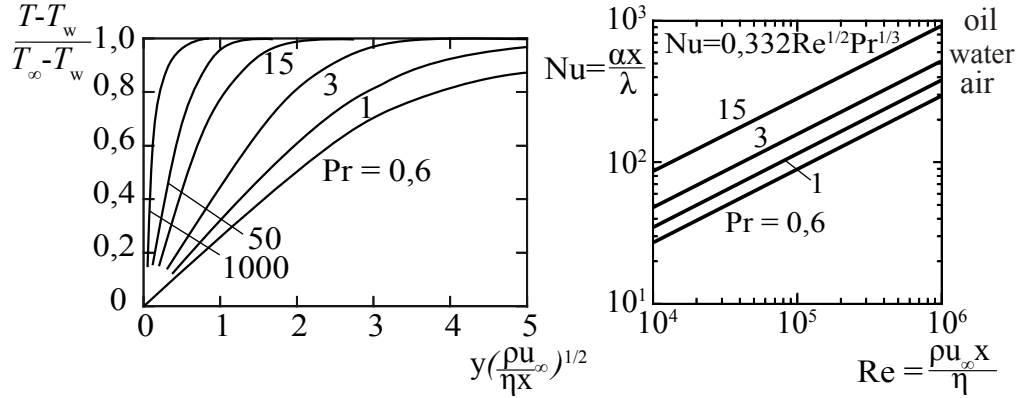


Figure 4.10: Laminar flow over a flat plate - temperature profile and Nusselt number according to Pohlhausen (1921)

For  $Pr = 1$  the momentum equation, equation (4.22), and the energy, equation (4.23), are identical if the pressure gradients and inertial forces are neglected. Hence, the dimensionless velocity and temperature profile must also be identical and thus

$$\left( \frac{d \left( \frac{u}{u_\infty} \right)}{dy} \right)_W = \left( \frac{d \left( \frac{T-T_W}{T_\infty - T_W} \right)}{dy} \right)_W$$

From equation (4.4) and (4.27) follows

$$Nu = \frac{x}{\lambda} \left( \lambda \frac{d \left( \frac{T-T_W}{T_\infty - T_W} \right)}{dy} \right)_W$$

and with equation (4.25)

$$\frac{c_f}{2} = \frac{\eta}{\rho u_\infty} \left( \frac{d \frac{u}{u_\infty}}{dy} \right)_W, \text{ (for } Pr = 1\text{)} \quad (4.28)$$

With the equality of the dimensionless temperature and velocity profiles, the ratio between the Nusselt number, the friction coefficient and Reynolds number,  $Re = \frac{\rho u_\infty x}{\eta}$  is:

$$Nu = \frac{c_f}{2} Re, \text{ (for } Pr = 1\text{)} \quad (4.29)$$

Taking the approximate influence of the Prantl number into account, the enhanced relation is:

$$Nu = \frac{c_f}{2} Re Pr^{\frac{1}{3}} \quad (4.30)$$

### 4.2.2 A simple approximation for the boundary layer equations

In the previous section the results of the exact solutions of the laminar, steady state boundary layer equations for plane flows were shown. The necessary mathematical methods are so complex that they cannot be included in the scope of this introductory course.

However, a very simple approximation for the boundary layer equations, which yields results comparable to those of the exact solutions and above all, shows the physical principles, will be discussed next.

We examine again the boundary layer flow over a flat plate. A control volume, bound by the planes  $\overline{11}$ ,  $\overline{12}$ ,  $\overline{22}$  and the wall will be used to formulate the conservation equations. Plane  $\overline{12}$  is located within the potential flow, outside of the boundary layer.

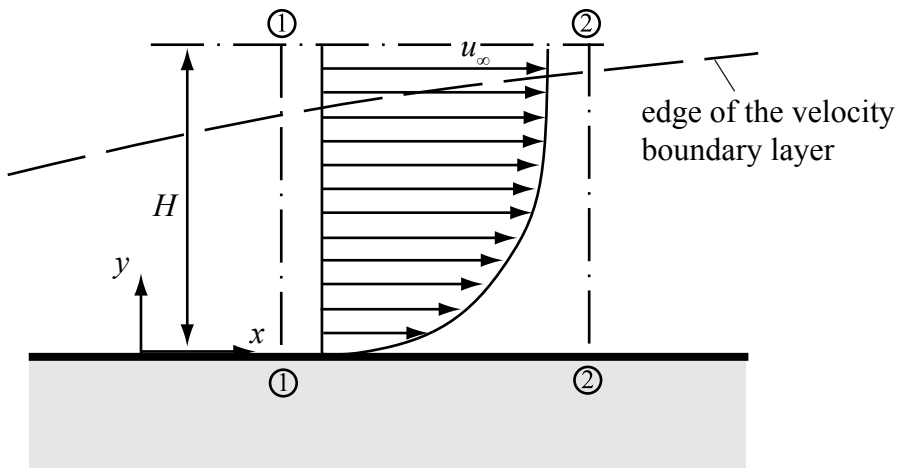


Figure 4.11: Integral momentum balance of a boundary layer flow

For the control volume described above, follows the integral *equation of continuity*

$$\frac{d}{dx} \int_0^H \rho u dy dx l + \rho v_\infty dx l = 0 \quad (4.31)$$

(equation of continuity)

and the integral momentum equation in x-direction

$$\frac{d}{dx} \int_0^H \rho u^2 dy dx l + \rho u_\infty v_\infty dx l = -\tau_w dx l$$

At the upper boundary plane, which is located in the potential flow, no shear forces are present. Normal forces in the planes  $\overline{11}$  and  $\overline{22}$  are to be neglected following the boundary layer approximation. At the wall, only the shear stress  $\tau_{yx} = (\eta \frac{du}{dy})_w$  should be considered. Considering the equation of continuity, equation (4.31), yields:

$$\frac{d}{dx} \int_0^H \rho u^2 dy - \frac{d}{dx} \int_0^H \rho u u_\infty dy = - \left( \eta \frac{du}{dy} \right)_w$$

or

$$\frac{d}{dx} \int_0^H \rho u (u_\infty - u) dy = \left( \eta \frac{du}{dy} \right)_w \quad (4.32)$$

(momentum equation, x-direction)

The integration is possible if the velocity profile in the boundary layer is known.

If, a *linear velocity profile* is assumed, as a crude approximation

$$\frac{u}{u_\infty} = \frac{y}{\delta_u} \quad (4.33)$$

and density is constant within the boundary layer, equation (4.32) yields

$$\rho u_\infty \frac{d}{dx} \int_0^{\delta_u} \frac{y}{\delta_u} \left( 1 - \frac{y}{\delta_u} \right) dy = \frac{\eta}{\delta_u}$$

Eventually a relationship for the thickness of the velocity boundary layer is found by integration

$$\delta_u = \sqrt{\frac{12\eta}{\rho u_\infty} x} \quad (4.34)$$

or dimensionless

$$\frac{\delta_u}{x} = \sqrt{\frac{12\eta}{\rho u_\infty x}} = \sqrt{\frac{12}{\text{Re}_x}} \quad (4.35)$$

with the Reynolds number,  $\text{Re} \equiv \frac{\rho u_\infty x}{\eta}$ , based on the length  $x$ .

If the thickness of the boundary layer is known, the *shear stress at the wall* can be determined

$$\tau_w = \left( \eta \frac{du}{dy} \right)_w = \eta \frac{u_\infty}{\delta_u} = \frac{1}{\sqrt{12\sqrt{\text{Re}}}} \rho u_\infty^2 \quad (4.36)$$

and in its dimensionless form, the friction coefficient  $\frac{c_f}{2}$

$$\frac{c_f}{2} = \frac{\tau_w}{\rho u_\infty^2} = \frac{1}{\sqrt{12\sqrt{\text{Re}}}} = 0,289 \text{ Re}^{-\frac{1}{2}} \quad (4.37)$$

This relationship shows the same dependence of the friction coefficient on the Reynolds number as the previously given exact solution of the momentum equation

$$\frac{c_f}{2} = 0,332 \text{ Re}^{-\frac{1}{2}} \quad (4.38)$$

merely the constant is 15% too low.

The *integral energy equation* can be derived using a similar control volume that includes the thermal boundary layer.

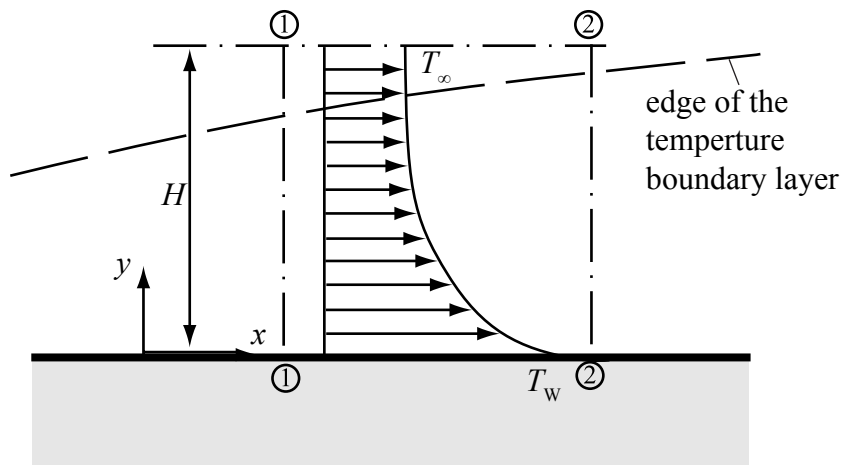


Figure 4.12: Integral energy balance at a boundary layer

Neglecting the dissipated heat of the forces acting on the volume and the heat conduction in direction of the flow, which is negligible compared to the convective energy transport in this direction, results in

$$\frac{d}{dx} \int_0^H \rho u c_p (T - T_0) dx dy l + \rho v_\infty c_p (T_\infty - T_0) dx l = - \left( \lambda \frac{dT}{dy} \right)_W dx l$$

where  $T_0$  is the reference temperature used to determine the enthalpy reference value.

Implementing the equation of continuity, equation (4.31), again results in

$$\frac{d}{dx} \int_0^H \rho u c_p (T - T_0) dy - \frac{d}{dx} \int_0^H \rho u c_p (T_\infty - T_0) dy = - \left( \lambda \frac{dT}{dy} \right)_W$$

or

$$\frac{d}{dx} \int_0^H \rho u c_p (T - T_\infty) dy = - \left( \lambda \frac{dT}{dy} \right)_W \quad (\text{energy equation}) \quad (4.39)$$

Assuming constant properties ( $\rho, \lambda, c_p$ ) the energy equation can be integrated assuming a linear temperature profile in the boundary layer

$$\frac{T - T_W}{T_\infty - T_W} \equiv \frac{\theta}{\theta_\infty} = \frac{y}{\delta_T} \quad (4.40)$$

Thus,

$$\rho c_p \frac{d}{dx} \int_0^H u_\infty \frac{y}{\delta_u} \left( \frac{y}{\delta_T} \theta_\infty - \theta_\infty \right) dy = - \lambda \frac{\theta_\infty}{\delta_T}$$

Assuming that the thermal boundary layer is as thick or thinner than the velocity boundary layer, yields  $H = \delta_T$ . After integration:

$$\delta_T d \left( \frac{\delta_T^2}{\delta_u} \right) = \frac{6\lambda}{\rho c_p u_\infty} dx \quad (4.41)$$

In case the ratio of the two boundary layer thicknesses remains constant:

$$\left( \frac{\delta_T}{\delta_u} \right)^3 \delta_u d \delta_u = \frac{6\lambda}{\rho c_p u_\infty} dx \quad (4.42)$$

Applying equation (4.34) leads to a relationship for the thickness of the thermal boundary layer

$$\frac{\delta_T}{\delta_u} = \left( \frac{\lambda}{\eta c_p} \right)^{\frac{1}{3}} = \frac{1}{Pr^{\frac{1}{3}}} \quad (4.43)$$

Gases have Prandtl numbers  $\text{Pr} \approx 1$ , so the assumption  $\delta_u = \delta_T$  was legitimate. If the thickness  $\delta_T$  of the thermal boundary layer is known, the heat flux at the wall can be calculated

$$\dot{q}_W'' = -\lambda \left( \frac{dT}{dy} \right)_W = -\lambda \frac{\theta_\infty}{\delta_T} = -\frac{\lambda \theta_\infty \text{Pr}^{\frac{1}{3}}}{\delta_u} \quad (4.44)$$

applying equation (4.35) for the thickness of the velocity boundary layer

$$\dot{q}_W'' = \frac{\lambda}{x} 0,289 \text{Re}^{\frac{1}{2}} \text{Pr}^{\frac{1}{3}} (T_w - T_\infty) \quad (4.45)$$

Comparing these relationships with the often used empirical assumption for convective heat transfer

$$\dot{q}_W'' = \alpha (T_w - T_\infty)$$

leads to the following equation for the heat transfer coefficient  $\alpha$

$$\alpha = \frac{\lambda}{x} 0,289 \text{Re}^{\frac{1}{2}} \text{Pr}^{\frac{1}{3}} \quad (4.46)$$

or in dimensionless form using the Nusselt number,  $\text{Nu} \equiv \frac{\alpha x}{\lambda}$ ,

$$\text{Nu} = 0,289 \text{Re}^{\frac{1}{2}} \text{Pr}^{\frac{1}{3}}. \quad (4.47)$$

As comparison to the exact solution according to Pohlhausen (1921) shows,

$$\text{Nu} = 0,332 \text{Re}^{\frac{1}{2}} \text{Pr}^{\frac{1}{3}} \quad (4.48)$$

the heat transfer coefficients, calculated in this manner, have the same function profile with only minor deviation from the absolute value, in spite of the simplified assumptions. With only little additional effort, integrating these equations using polynomials of 3rd order to describe the profiles, the solution's conformity to the exact solution can be considerably improved.

### 4.3 Natural convection - boundary layer equations for laminar, steady state flow

In the previous section we discussed the heat transfer between a surface and a fluid, where the flow was initiated e.g. by a ventilator. Inertial forces were discarded in the energy balance because of their small contribution.

In other cases the flow along a surface is not forced, but induced by a mass force, usually gravity. This *natural convection* has velocity and thermal boundary layers as shown in the figure below. These profiles result from the solutions of the boundary layer equations, the equation of continuity, equation (4.21), the momentum equation in x-direction, equation (4.22), and the equation of energy conservation, equation (4.23).

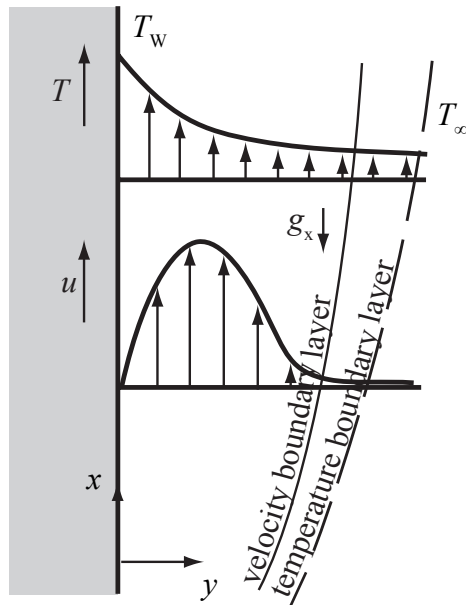


Figure 4.13: Natural convection at a vertical plate

In the momentum equation

$$\rho u \frac{\partial u}{\partial x} + \rho v \frac{\partial u}{\partial y} = - \frac{\partial p}{\partial x} + \eta \frac{\partial^2 u}{\partial y^2} + \rho g_x \quad (4.49)$$

the sign of the term that describes the impact of gravity force has been changed, since gravity acts against the positive x-direction in this example.

The pressure gradient  $\frac{dp}{dx}$  was zero for forced convection over a flat plate. For problems of natural convection, the pressure change over the height  $dx$  equals the weight of the liquid head over a unit area.

$$\frac{dp}{dx} = -\rho_\infty g \quad (4.50)$$

Hence, the momentum equation can be rewritten

$$\rho u \frac{\partial u}{\partial x} + \rho v \frac{\partial u}{\partial y} = g(\rho_\infty - \rho) + \eta \frac{\partial^2 u}{\partial y^2} \quad (4.51)$$

Usually, the difference in density in the buoyancy term is written in terms of the volumetric expansion coefficient  $\beta$  for homogeneous mediums

$$\beta \equiv \frac{1}{V} \left( \frac{\partial V}{\partial T} \right)_p = -\frac{1}{\rho} \left( \frac{\partial \rho}{\partial T} \right)_p = \frac{\rho_\infty - \rho}{\rho(T - T_\infty)}$$

hence,

$$\rho u \frac{\partial u}{\partial x} + \rho v \frac{\partial u}{\partial y} = g\rho\beta(T - T_\infty) + \eta \frac{\partial^2 u}{\partial y^2} \quad (4.52)$$

(momentum equation, x-direction)

The volumetric expansion coefficient is listed for many fluids, and for ideal gases it is valid that

$$\beta = \frac{1}{T}$$

Assuming constant properties is justified for many cases, except for the buoyancy term, although it is exactly the density deviations that causes the fluid to flow.

In order to determine the velocity and temperature fields and hence friction and heat transfer at a vertical surface, the following conservation equations must be solved:

$$\frac{\partial u}{\partial x} + \frac{\partial v}{\partial y} = 0 \quad (4.53)$$

(equation of continuity,  $\rho$  constant)

$$\rho u \frac{\partial u}{\partial x} + \rho v \frac{\partial u}{\partial y} = g\rho\beta(T - T_\infty) + \eta \frac{\partial^2 u}{\partial y^2} \quad (4.54)$$

(momentum equation, x-direction,  $\rho, \eta$  constant)

$$\rho u \frac{\partial T}{\partial x} + \rho v \frac{\partial T}{\partial y} = \frac{\eta}{\text{Pr}} \frac{\partial^2 T}{\partial y^2} \quad (4.55)$$

(energy equation,  $\lambda$  constant)

The solution renders more difficult than the one of the boundary layer equations for forced convection, since knowledge of the temperature field is necessary in order to solve the momentum equation.

Yet, for the simple geometry of the vertical flat plate with constant surface temperature, an exact solution by transformation of the partial differential equations into ordinary differential equations is possible again.

These ordinary differential equations have been solved by Ostrach (1953). The resulting velocity and temperature profiles are shown in a dimensionless form in the following diagrams.

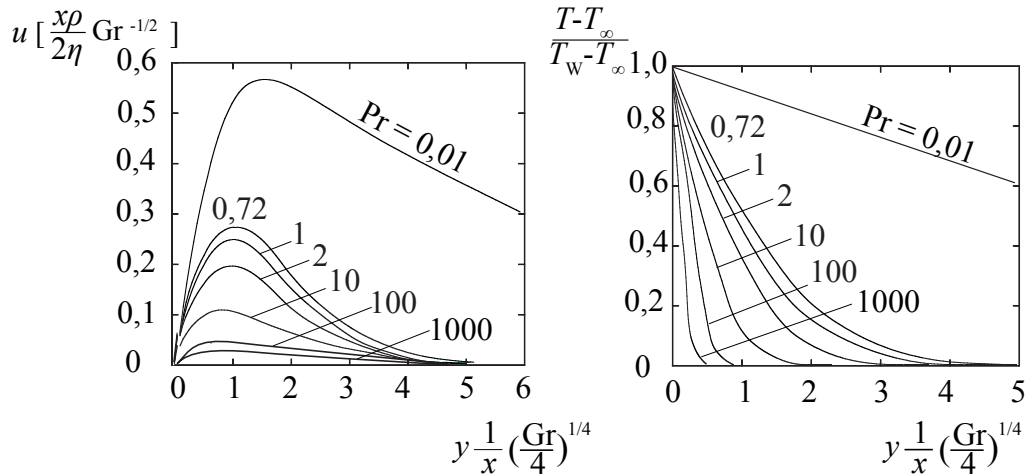


Figure 4.14: Velocity and temperature profiles at a vertical wall for natural convection according to Ostrach (1953)

Here, the new dimensionless number, the *Grashof number*

$$\text{Gr} \equiv \frac{\beta g \rho^2 (T_w - T_\infty) x^3}{\eta^2} \quad (4.56)$$

is the ratio of the buoyancy forces to the viscosity forces.

With the gradient of the temperature profile at the wall, the heat flux can be calculated according to the Fourier equation as well as the heat transfer coefficient using equation (4.25). Local mean Nusselt numbers can be written in the form

$$\overline{\text{Nu}} = C (\text{Gr} \text{ Pr})^{\frac{1}{4}} \quad (4.57)$$

where  $\overline{\text{Nu}}$  is the mean value of the Nusselt number over the height of the plate and  $C$  is a coefficient that depends on the Prandtl number, and is given in the following table

Pr	0,003	0,01	0,03	0,72	1	2	10	100	1000	$\infty$
C	0,182	0,242	0,305	0,516	0,535	0,568	0,620	0,653	0,665	0,670

Table 4.1: Values for the coefficient  $C$  of equation (4.57) according to Ostrach (1953)

A comparison between the theoretical results and measured values is shown in the following diagrams. In Fig. (4.15) the calculated values of the velocity and temperature fields at a vertical, heated plate in air are compared to experimental values. In (4.16) the mean Nusselt numbers are compared with measured values according to Whitaker (1974).

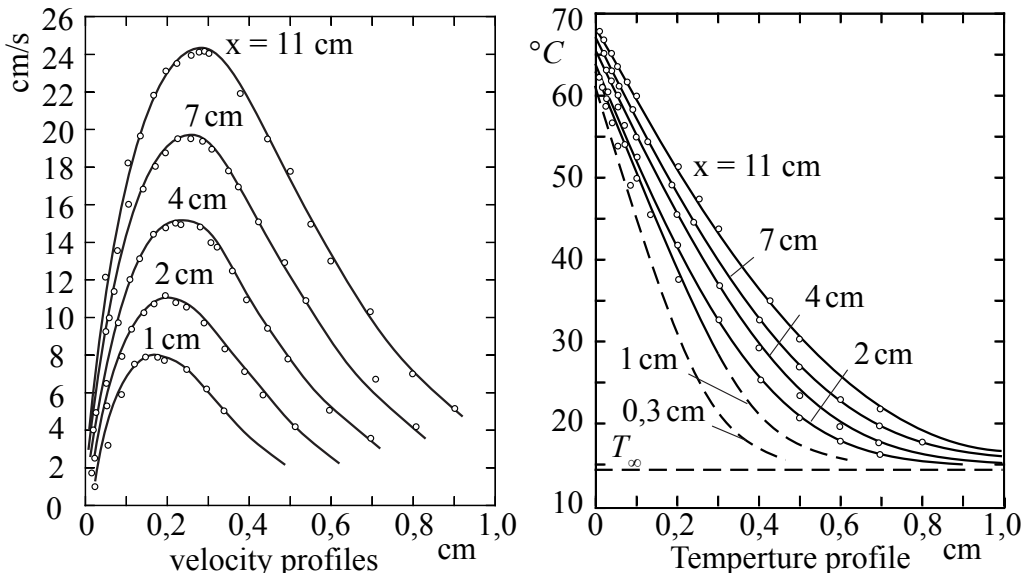


Figure 4.15: Calculated and measured velocity and temperature profiles at a vertical plate for natural convection in air, from Whitaker (1974)

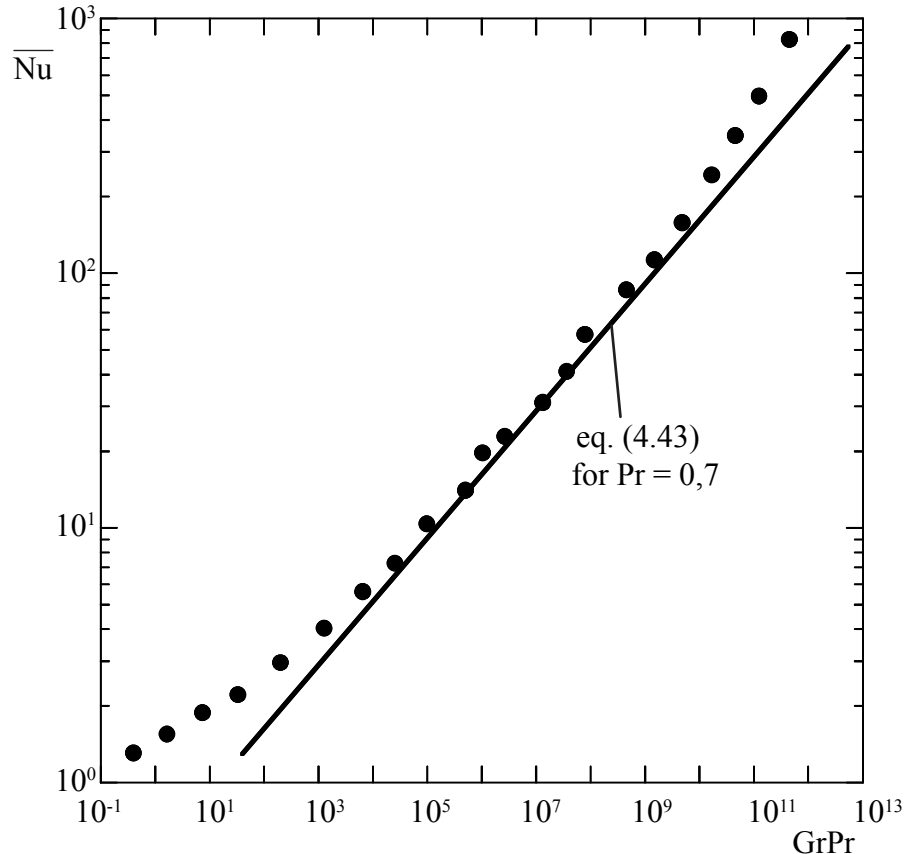


Figure 4.16: Calculated and measured mean values of the Nusselt number of a vertical plate for natural convection in air, from Whitaker (1974)

Comparing these profiles in air shows a very good accordance and proves the validity of the simplified assumptions used during the derivation of the conservation laws. For the local mean values of the Nusselt number, the theoretical values conform to the experimental values only in the middle range of  $(GrPr)$ -values. For  $GrPr < 10^3$  these boundary layer approximations are obviously no longer valid. In the range of  $GrPr > 10^9$  heat transfer is intensified by the shift from laminar to turbulent flow.

These two effects, which are also observed during forced convection, make the theoretical solution of the conservation equations significantly more difficult. If the boundary layer assumptions are dropped, instead of the parabolic differential equations elliptical differential equations have to be solved and numerical methods or eventually experiments will be necessary. In addition, when the flow shifts from laminar to turbulent, models have to be developed that include the impact of turbulence to the momentum and heat exchange.

The characteristics of turbulent flow will be discussed in the following section 4.4.

## 4.4 Heat transfer in turbulent flows

The previous sections described the heat transfer from a wall to a laminar flowing fluid. It was shown that adjacent to the wall, the dominating energy transport mechanisms is heat conduction, whereas in the layers further away, enthalpy transport by the flow dominates.

In many problems from practice though, the flow becomes turbulent, depending on a characteristic Reynolds number, so that additional exchange mechanisms have to be considered. In many cases on average the flow shows steady state characteristics yet. Measuring the instantaneous values of velocity or temperature by e.g. a hot wire anemometer, or a very thin thermocouple results in profiles as shown in the following diagrams.

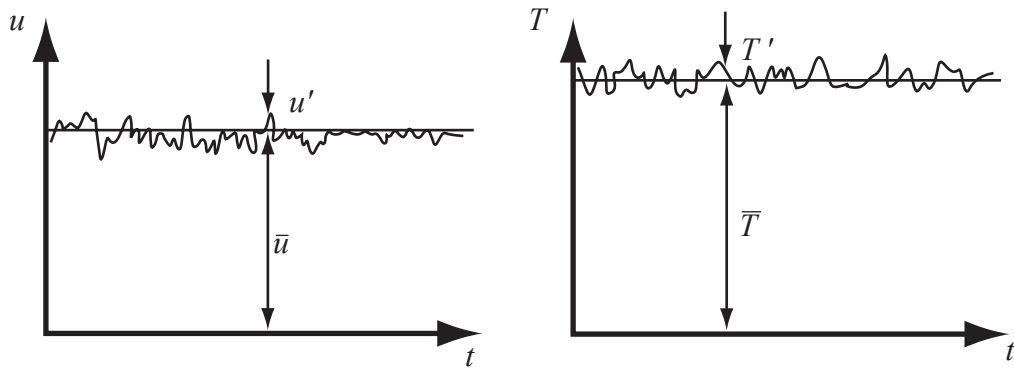


Figure 4.17: Velocity and temperature as a function of time for an - on the average - steady state, turbulent flow

For the instantaneous value of the velocity  $u$ , and the mean value  $\bar{u}$  with deviation  $u'$ , the following relationships are valid

$$u = \bar{u} + u'$$

and respectively,

$$v = \bar{v} + v' ; \quad T = \bar{T} + T' \quad \text{and} \quad p = \bar{p} + p'$$

Putting these instantaneous values in the equations of continuity, momentum and energy, and then calculate the mean values it follows, e.g. for flow with boundary layer character and assuming constant properties, from equations (4.21) to (4.23) a new set of conservation equations

$$\frac{\partial \bar{u}}{\partial x} + \frac{\partial \bar{v}}{\partial y} = 0 \quad (\text{equation of continuity}) \quad (4.58)$$

$$\rho \bar{u} \frac{\partial \bar{u}}{\partial x} + \rho \bar{v} \frac{\partial \bar{u}}{\partial y} = -\frac{d\bar{p}}{dx} + \eta \frac{\partial^2 \bar{u}}{\partial y^2} - \rho \frac{\partial \bar{u}' v'}{\partial y} \quad (\text{momentum equation}) \quad (4.59)$$

$$\rho \bar{u} c_p \frac{\partial \bar{T}}{\partial x} + \rho \bar{v} c_p \frac{\partial \bar{T}}{\partial y} = \lambda \frac{\partial^2 \bar{T}}{\partial y^2} - \rho c_p \frac{\partial \bar{v}' T'}{\partial y} \quad (\text{energy equation}) \quad (4.60)$$

The full derivation of these equations can be found for example in Schlichting u. Gersten (2006). The new equations valid for steady state turbulent flows differ from those for laminar flows by a newly introduced term on the right-hand side of the momentum and energy equation, which describes the additional transport of momentum and energy by the eddy movements of the flow.

Usually these additional terms are labeled "*turbulent shear stress*" or "*turbulent heat conduction*", respectively

$$\tau_t = -\rho \bar{u}' \bar{v}' \quad \text{and} \quad \dot{q}_t'' = \rho c_p \bar{v}' \bar{T}'.$$

If, in analogy to molecular transport of heat and momentum, a corresponding turbulent viscosity  $\eta_t$  and turbulent heat conductivity  $\lambda_t$  is defined:

$$\tau_t \equiv \eta_t \frac{\partial \bar{u}}{\partial y} \quad \text{and} \quad \dot{q}_t'' \equiv -\lambda_t \frac{\partial \bar{T}}{\partial y}.$$

then the molecular transport properties and the influence of the turbulence can be summarised in the *effective transport properties*, e.g.  $\eta_{\text{eff}} = \eta + \eta_t$ . This yields for example for a turbulent boundary layer flow to the following conservation equations

$$\frac{\partial \bar{u}}{\partial x} + \frac{\partial \bar{v}}{\partial y} = 0 \quad (\text{equation of continuity}) \quad (4.61)$$

$$\rho \bar{u} \frac{\partial \bar{u}}{\partial x} + \rho \bar{v} \frac{\partial \bar{u}}{\partial y} = -\frac{d\bar{p}}{dx} + \frac{\partial}{\partial y} \left( \eta_{\text{eff}} \frac{\partial \bar{u}}{\partial y} \right) \quad (\text{momentum equation}) \quad (4.62)$$

$$\rho \bar{u} c_p \frac{\partial \bar{T}}{\partial x} + \rho \bar{v} c_p \frac{\partial \bar{T}}{\partial y} = \frac{\partial}{\partial y} \left( \lambda_{\text{eff}} \frac{\partial \bar{T}}{\partial y} \right) \quad (\text{energy equation}) \quad (4.63)$$

Even though the equations are formally very similar to those for laminar boundary flows, it should not be forgotten that the turbulent properties describe the impact of turbulence and hence depend not only on the location in the flow, but also on the geometry and history of the flow. The turbulent transport properties are not material properties as is the case for their molecular counterparts. References for semi-empirical approaches used to describe them can be found under the keyword “turbulence models”, e.g. Jischa (1982).

These special properties render the exact solution of the conservation equations, in the way presented for laminar flow, impossible. Therefore complex numerical methods, like the method of finite differences or finite elements, are used. The way in which these methods are applied will be the topic of specialised courses on the subject. The application of advanced commercially available program codes for solving problems of energy engineering and combustion technology will be presented in the lecture “Design of Burners and Furnaces”.

## 4.5 Application of dimensional analysis for heat transfer

Although with the development in computer technology, major advances have been made in the numerical calculation of heat transfer, it is still necessary for most technical cases to use empirical heat transfer laws for design purposes.

These laws are a result of measurements, which are shown graphically or in a form of empirical formulas.

As will be shown in this section, it is not always necessary to repeat experiments if either fluid, geometry, or the flow conditions are changed.

The analytical solutions for heat transfer for forced and natural convection, dealt with previously, have shown that the results can be represented in an appropriate form by a few characteristic numbers

$$\text{Nu} = \text{Nu}(\text{Re}, \text{Pr}) \text{ for forced convection} \quad (4.64)$$

$$\text{Nu} = \text{Nu}(\text{Gr}, \text{Pr}) \text{ for natural convection} \quad (4.65)$$

The solutions rendered not only the characteristic numbers that describe the process, but also their functional relationship.

For cases in which a solution of the conservation laws is not known, it is often possible to reduce the number of parameters that influence the heat transfer by the method of the *dimensional analysis*. The functional relationships of these coefficients are obtained by specific measurements.

To determine the characteristic numbers, the conservation equations are rewritten in a dimensionless form. In order to reduce complexity, the two-dimensional, laminar boundary layer equations with constant properties in the form of equation (4.53) to (4.55), with an additional pressure gradient  $\left(\frac{dp}{dx}\right)_{\text{kin}}$  in the momentum equation will be regarded. It should be noted that while deriving the momentum equation (4.54) for the vertical flat plate only the pressure gradient, describing the fluid head  $\left(\frac{dp}{dx}\right)_{\text{pot}}$  was effective, and the pressure gradient caused by the acceleration of the fluid  $\left(\frac{dp}{dx}\right)_{\text{kin}}$ , as for example in a tube flow, was omitted. Hence the more general case is discussed here

$$\frac{\partial u}{\partial x} + \frac{\partial v}{\partial y} = 0 \quad (\text{equation of continuity}) \quad (4.66)$$

$$\rho u \frac{\partial u}{\partial x} + \rho v \frac{\partial u}{\partial y} = - \left( \frac{dp}{dx} \right)_{\text{kin}} + \eta \frac{\partial^2 u}{\partial y^2} - g_x \rho \beta (T - T_\infty) \quad (\text{momentum equation}) \quad (4.67)$$

$$\rho u c_p \frac{\partial T}{\partial x} + \rho v c_p \frac{\partial T}{\partial y} = \lambda \frac{\partial^2 T}{\partial y^2} \quad (\text{energy equation}) \quad (4.68)$$

All variables in these equations shall be made dimensionless by appropriate characteristic parameters, arising from the specific case. Hence, the coordinates  $x$  and  $y$  are referenced to a characteristic length  $L$ , which can be the diameter  $D$  for a sphere or tube, or the length of a plate for flow over a plate. The velocity components  $u$  and  $v$  are divided by the characteristic velocity  $u_\infty$ , for flow in tubes the mean velocity, and for flow over a plate the free stream velocity. The pressure is always rated over the double of the dynamic pressure and the temperature over a characteristic temperature difference, e.g. the temperature difference between the surface and the fluid at a greater distance from the body.

Labeling the dimensionless variables with  $*$

$$x^* \equiv \frac{x}{L}; \quad y^* \equiv \frac{y}{L}; \quad u^* \equiv \frac{u}{u_\infty}; \quad v^* \equiv \frac{v}{u_\infty}; \quad p^* \equiv \frac{p}{\rho u_\infty^2}; \quad \theta^* \equiv \frac{T - T_\infty}{T_w - T_\infty}$$

yields the dimensionless conservation equations

$$\frac{\partial u^*}{\partial x^*} + \frac{\partial v^*}{\partial y^*} = 0 \quad (\text{equation of continuity}) \quad (4.69)$$

$$u^* \frac{\partial u^*}{\partial x^*} + v^* \frac{\partial u^*}{\partial y^*} = - \left( \frac{dp^*}{dx^*} \right)_{\text{kin}} + \left( \frac{\eta}{\rho u_\infty L} \right) \frac{\partial^2 u^*}{\partial y^{*2}} + \left( \frac{g_x \beta L (T_w - T_\infty)}{u_\infty^2} \right) \theta^* \quad (4.70)$$

(momentum equation)

$$u^* \frac{\partial \theta^*}{\partial x^*} + v^* \frac{\partial \theta^*}{\partial y^*} = \left( \frac{\lambda}{\rho c_p u_\infty L} \right) \frac{\partial^2 \theta^*}{\partial y^{*2}} \quad (4.71)$$

(energy equation)

In addition to the dimensionless variables, these equations contain dimensionless quantities in the brackets. A closer look at these expressions, reveals that these are the dimensionless numbers from the previous sections.

The momentum equation, equation (4.70), contains two of these terms.

The expression for the friction term is the reciprocal of *the Reynolds number*

$$\text{Re} \equiv \frac{\rho u_\infty L}{\eta}$$

The expression for the buoyancy term is called *Archimedes number*

$$\text{Ar} \equiv \frac{g_x \beta L (T_w - T_\infty)}{u_\infty^2}$$

which in the literature is often expressed as a quotient of *the Grashof number* and the *Reynolds number* squared

$$\text{Ar} = \left( \frac{g_x \rho^2 \beta L^3 (T_w - T_\infty)}{\eta^2} \right) \left( \frac{\eta}{\rho u_\infty L} \right)^2 = \frac{\text{Gr}}{\text{Re}^2}$$

The dimensionless energy equation defines the *Péclet number*

$$\text{Pe} \equiv \frac{\rho c_p u_\infty L}{\lambda} = \frac{u_\infty L}{a}$$

which in turn, can be rewritten as a product of the *Reynolds* and *Prandtl number*

$$\text{Pe} = \left( \frac{\rho u_\infty L}{\eta} \right) \left( \frac{\eta c_p}{\lambda} \right) = \text{Re Pr}$$

If, for different applications, e.g. different fluids, different pipe diameters the coefficients or a combination of the same, given in the expressions in the brackets, are equal, then so are the solutions of the differential equations, i.e. the dimensionless fields of velocity, temperature and pressure. Yet, the boundary conditions must be equivalent, too, for the above statement to be valid. Hence, the velocity and temperature fields can be expressed as a function of these parameters

$$\vec{w} = \vec{w}(x^*, y^*, \text{Re}, \text{Gr}, \text{Pr}) \quad (4.72)$$

and

$$\theta^* = \theta^*(x^*, y^*, Re, Gr, Pr) \quad (4.73)$$

Velocity and temperature fields of the fluid are less interesting than the heat that is transferred between the fluid and the body and which can be derived from the gradient of the temperature profile in the fluid at the surface of the body.

$$\dot{q}'' = - \left( \lambda \frac{\partial T}{\partial y} \right)_W$$

A comparison with the equation that defined the heat transfer coefficient  $\alpha$

$$\dot{q}'' \equiv \alpha (T_W - T_\infty)$$

yields

$$\alpha = \frac{- \left( \lambda \frac{dT}{dy} \right)_W}{(T_W - T_\infty)}$$

or written in a dimensionless form, the *Nusselt number* :

$$Nu \equiv \frac{\alpha L}{\lambda} = - \left( \frac{d\theta^*}{dy^*} \right)_W$$

The Nusselt number, already introduced in previous sections as a dimensionless heat transfer coefficient, is thus equal to the dimensionless temperature gradient and hence, can be expressed as the temperature field

$$Nu = Nu(Re, Gr, Pr) \quad (4.74)$$

This shows that heat transfer for problems with similar geometries and boundary conditions can formally be expressed by 4 dimensionless numbers.

This statement is also valid for turbulent flow, as long as the levels of turbulence are comparable.

For many practical purposes, the relationship (4.74), can be further simplified.

For *forced convection* the inertial and friction forces are greater than the buoyant forces resulting from the changes in temperature. Neglecting the buoyant term in the equation of motion leads to

$$Nu = Nu(Re, Pr) \quad (4.75)$$

For *natural convection* the velocity field is caused by temperature differences, and a velocity  $u_\infty$  induced by external sources is not present. The inertial forces may be neglected, hence

$$\text{Nu} = \text{Nu}(\text{Gr}, \text{Pr}) \quad (4.76)$$

The dimensional analysis cannot state the form of the functional relationship between the Nu number and the Re, Gr, Pr numbers. This relationship can either be found from the analytical solutions, if these are expressed in characteristic numbers, or from experiments. Often, it is aimed at representing the experimental results as a power law, i.e. in the form

$$\text{Nu} = C \text{Re}^m \text{Pr}^n \text{Gr}^p$$

Important examples of such power laws will be shown in the next chapter.

---

# Chapter 5

## Heat transfer laws

The heat flux from a wall with the surface area  $A$  and temperature  $T_W$  to a fluid with the temperature  $T_{\text{fl}}$  is:

$$\dot{Q}_W = A\alpha (T_W - T_{\text{fl}}) \quad (5.1)$$

To determine the heat transfer coefficient  $\alpha$ , Nusselt number correlations for a number of important applications are given below.

These correlations have the general form

$$\begin{aligned} \text{Nu} &= \text{Nu}(\text{Re}, \text{Pr}) \text{ for forced convection} \\ \text{Nu} &= \text{Nu}(\text{Gr}, \text{Pr}) \text{ for natural convection} \end{aligned}$$

With the definitions for Nusselt number

$$\text{Nu} \equiv \frac{\alpha L}{\lambda} \quad (5.2)$$

Reynolds number

$$\text{Re} \equiv \frac{\rho u_\infty L}{\eta} \quad (5.3)$$

Grashof number

$$\text{Gr} \equiv \frac{\rho^2 g \beta (T_W - T_{\text{fl}}) L^3}{\eta^2} \quad (5.4)$$

Prandtl number

$$\text{Pr} \equiv \frac{\eta c_p}{\lambda} \quad (5.5)$$

The applicability of the given correlations should be checked for each case according to the following criteria:

The *geometry* of the given problem must be analogous to the geometry of the experiment from which the heat transfer law is estimated.

The flow profile must be checked by means of the critical Reynolds and Grashof numbers in the range describing the shift from laminar to turbulent flow. A law valid for laminar flow cannot be applied for turbulent flow.

The *thermal boundary conditions* of the investigated case should be compared to those under which the applied heat transfer law was derived. Laws that are valid for example for flow in tubes with constant wall temperature can be used only with restrictions for cases with a constant heat flux rate on the wall. For cases, where high temperature changes occur in the system, care should be taken to use the same reference temperature at which the properties were determined. In most of the heat transfer laws the properties are to be determined at a mean temperature. In special cases, where the variable properties are to be described, the correlations are extended to include additional terms, either those of temperature ratios or viscosity ratios.

An additional problem is the assumption for the fluid temperature  $T_{\text{fl}}$  for the *local heat flux* of an enclosed flow. In this case, normally a caloric mean value is used to determine the temperature:

$$T_{\text{fl}} = \frac{\int_{A_c} \rho u c_p T dA_c}{\int_{A_c} \rho u c_p dA_c} \quad (5.6)$$

Many heat transfer laws are a result of integral measurement on a system and thus yield only the *averaged heat transfer coefficients*  $\bar{\alpha}$  of a heat transporting medium. The same applies for the *average heat flux*

$$\dot{Q}_W = \bar{\alpha} A (T_W - T_{\text{fl}})_m = \bar{\alpha} A \Delta T_m \quad (5.7)$$

where both the wall temperature as well as the fluid temperature may depend on the location. It can be shown that for many practical purposes, for which the heat transfer coefficient is not dependent on the temperature, the so-called *logarithmic temperature difference*, made up of the temperature differences at the entrance and exit of the heat exchanger, may be used

$$(T_W - T_{\text{fl}})_m = \Delta T_{\ln} \equiv \frac{\Delta T_{\text{inlet}} - \Delta T_{\text{outlet}}}{\ln \left( \frac{\Delta T_{\text{inlet}}}{\Delta T_{\text{outlet}}} \right)}$$

This will be discussed in detail in the lecture “Heat Exchangers and Steam Generators”.

Eventually it must be verified, that the field of characteristic numbers in which the law was determined matches the one of the problem under investigation.

This is especially important for laws that have been determined experimentally, which describe the functional relationships only approximately.

Next, a selection of important heat transfer laws for forced and natural convection are presented. A detailed summary of the heat transfer laws can be found, for example in VDI Wärmeatlas, 1997.

## 5.1 Heat transfer laws for forced convection

### 5.1.1 Forced convection at flows along surfaces

The properties used in the characteristic numbers are to be determined, if not stated otherwise, at

$$T_{\text{prop.}} = \frac{T_w + T_\infty}{2}$$

#### 5.1.1.1 Flat plate - laminar boundary layer flow $\text{Re}_{x,\text{crit}} \approx 2 \cdot 10^5$

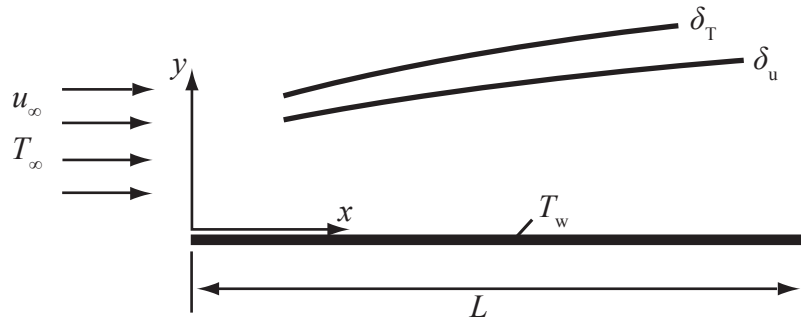


Figure 5.1: Laminar boundary layer of a plate with isothermal surface

(Note: The heat transfer laws for laminar boundary layers are ‘exact’ solutions of the conservation laws)

Simultaneous hydrodynamic and thermal inflow, isothermal surface

- Nusselt law for the local heat transfer:

$$\text{Nu}_x = 0,332 \text{Re}_x^{\frac{1}{2}} \text{Pr}^{\frac{1}{3}} \quad (\text{WÜK.1})$$

for  $0,6 < \text{Pr} < 10$   
and  $\text{Re}_x < \text{Re}_{x,\text{crit}} \approx 2 \cdot 10^5$

- Nusselt law for the mean heat transfer:

$$\overline{\text{Nu}_L} = \frac{\bar{\alpha}L}{\lambda} = \frac{1}{L} \int_0^L \alpha(x) dx = 2 \text{ Nu}_{x=L}$$

$$\overline{\text{Nu}_L} = 0,664 \text{ Re}_L^{1/2} \text{ Pr}^{1/3} \quad (\text{WÜK.2})$$

for  $0,6 < \text{Pr} < 10$   
and  $\text{Re}_L < \text{Re}_{L,\text{crit}} \approx 2 \cdot 10^5$

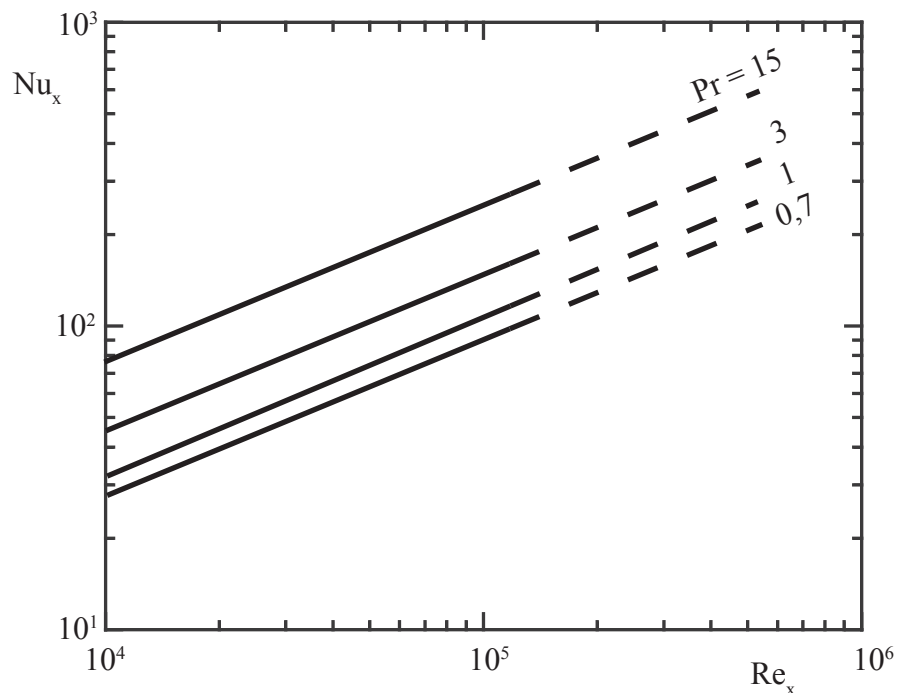


Figure 5.2: Local Nusselt number for the laminar boundary layer of a plate

Hydrodynamical inflow, heated or cooled from position  $x = x_0$ , isothermal surface

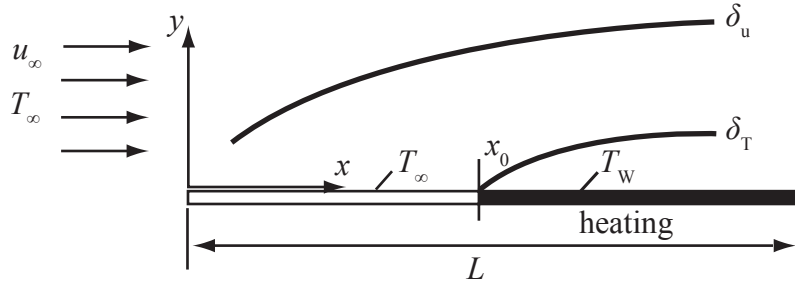


Figure 5.3: Laminar boundary layer of a plate, heated from  $x = x_0$  with isothermal surface

- Nusselt law for the local heat transfer:

$$Nu_x = 0,332 \operatorname{Re}_x^{\frac{1}{2}} \operatorname{Pr}^{\frac{1}{3}} \left[ 1 - \left( \frac{x_0}{x} \right)^{\frac{3}{4}} \right]^{-\frac{1}{3}} \quad (\text{WÜK.3})$$

for  $0,6 < \operatorname{Pr} < 10$   
and  $\operatorname{Re}_x < \operatorname{Re}_{x,\text{crit}} \approx 2 \cdot 10^5$

- Nusselt law for the mean heat transfer:

$$\begin{aligned} Nu_L &= \frac{L}{L - x_0} \frac{1}{\lambda} \int_{x_0}^L \alpha(x) dx \\ Nu_L &= 0,664 \operatorname{Re}_L^{\frac{1}{2}} \operatorname{Pr}^{\frac{1}{3}} \frac{\left[ 1 - \left( \frac{x_0}{L} \right)^{\frac{3}{4}} \right]^{\frac{2}{3}}}{\left[ 1 - \frac{x_0}{L} \right]} \end{aligned} \quad (\text{WÜK.4})$$

for  $0,6 < \operatorname{Pr} < 10$   
and  $\operatorname{Re}_x < \operatorname{Re}_{x,\text{crit}} \approx 2 \cdot 10^5$

### 5.1.1.2 Flat plate - turbulent boundary layer flow $\operatorname{Re}_{x,\text{crit}} \approx 2 \cdot 10^5$

(Note: The shift from laminar to turbulent flow depends on the degree of turbulence of the undisturbed flow, the surface roughness, etc, see below. For flow over flat surfaces the critical Reynolds number, i.e. the beginning of the eddy area is expected at 1 to  $2 \cdot 10^5$ . In extremely low turbulence wind tunnels, critical Reynolds numbers in the order of  $\operatorname{Re}_{x,\text{crit}} \approx 1 \cdot 10^6$  can be reached.)

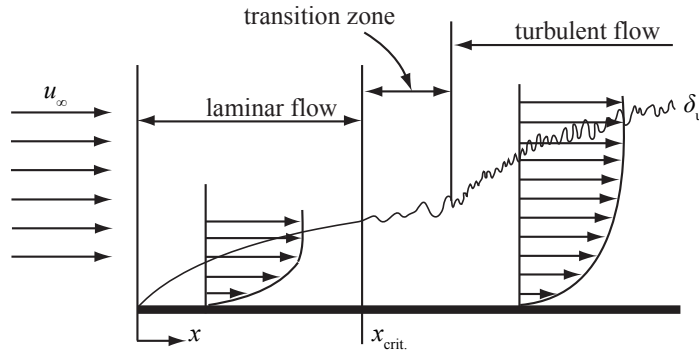


Figure 5.4: Laminar / turbulent boundary layer of a plate

The given relationships are derived from experimental data.

Isothermal surface, simultaneous hydrodynamic and thermal inflow

- Nusselt correlation for local heat transfer

$$Nu_x = 0,0296 \operatorname{Re}_x^{0,8} \operatorname{Pr}^{0,43} \quad \text{for } 5 \cdot 10^5 < \operatorname{Re}_x < 10^7 \quad (\text{WÜK.5})$$

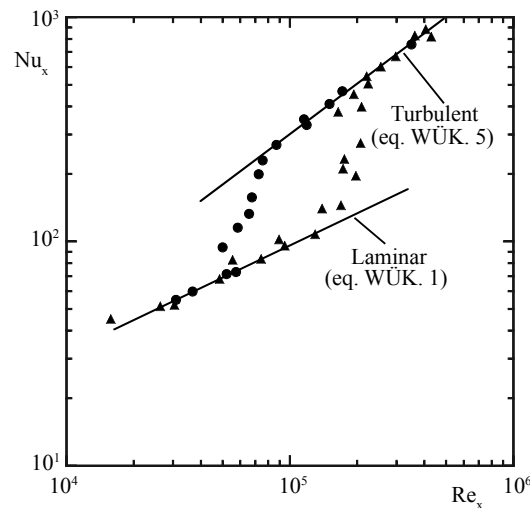


Figure 5.5: Local Nusselt number for a flat plate in air flow, Level of turbulence  $T_a = 0,7$  to  $1,6\%$ ; Level of turbulence  $T_a = 2,4$  to  $3,8\%$  according to Kestin u. a. (1961)

- Nusselt law for mean heat transfer:

(Note : The average heat transfer of a plate with length L can be calculated by integrating equations (WÜK.1) and (WÜK.5)

$$\overline{\text{Nu}_L} = \frac{\overline{\alpha}L}{\lambda} = \frac{1}{\lambda} \left( \int_0^{x_{\text{crit}}} \alpha(x)_{\text{eq. (WÜK.1)}} dx + \int_{x_{\text{crit}}}^L \alpha(x)_{\text{eq. (WÜK.5)}} dx \right) \quad (5.8)$$

Hence, the result depends on the actual critical Reynolds number).

- Nusselt law for mean heat transfer:

$$\overline{\text{Nu}_L} \approx 0,036 \text{ Pr}^{0,43} (\text{Re}_L^{0,8} - 9400) \quad (\text{WÜK.6})$$

$$\text{for } \text{Re}_{L,\text{crit}} \approx 2 \cdot 10^5$$

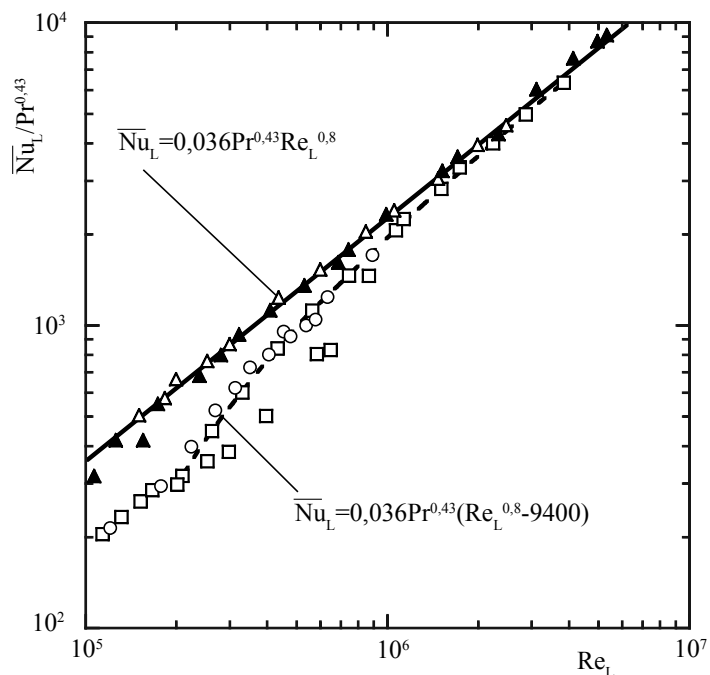


Figure 5.6: Mean Nusselt number for the turbulent boundary layer of a plate  
 (⊟ Air (heating) with low level of turbulence, △ Air (heating) with 5% level of turbulence, Air, water, oil (heating and cooling) with unknown level of turbulence, Whitaker (1976))

### 5.1.1.3 Cylinders in a flow parallel to their longitudinal axis

As long as the diameter of the body is much greater than the thickness of the boundary layer, cylinders in longitudinal flow can be regarded as flat plates.

### 5.1.1.4 Cylinders in a flow perpendicular to their longitudinal axis

- Local heat transfer

The local Nusselt number depicted in figure 5.7 shows a strong influence of the circumference angle, which is a result of the transition from laminar to turbulent flow and of the detachment of the flow.

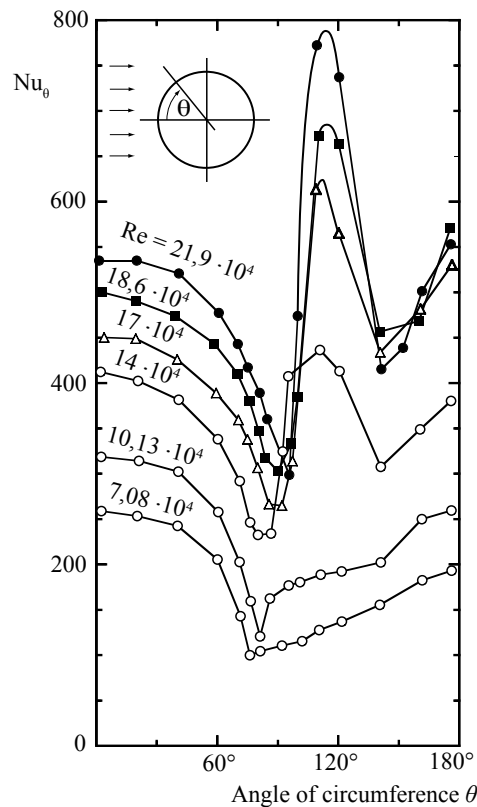


Figure 5.7: Local Nusselt number for cylinders in a flow perpendicular to their longitudinal axis, according to Holman (1976)

- Mean heat transfer:  
Nusselt law for the mean heat transfer

$$\overline{\text{Nu}_d} = C \text{ Re}_d^m \text{Pr}^{0,4} \quad (\text{WÜK.7})$$

With the constants C and m relevant for the given ranges of Reynolds numbers.

Table 5.1: Constants C and m for corresponding Reynolds numbers

$Re_d$	C	m
0,4 - 4	0,989	0,330
4 - 40	0,911	0,385
40 - 4000	0,683	0,466
4000 - 40000	0,193	0,618
40000 - 400000	0,0266	0,805

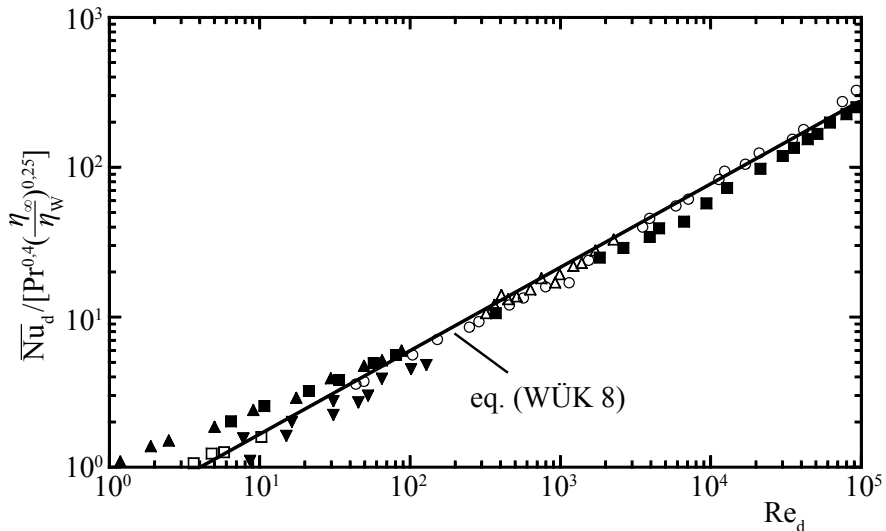


Figure 5.8: Mean Nusselt number for circular cylinders in a flow perpendicular to their longitudinal axis ( $\mp$  Water, glycol;  $\Delta$  nitrogen;  $\circ$  water;  $\blacktriangle$  air;  $\blacktriangledown$  water, paraffin, oil), Whitaker (1976)

For all Reynolds numbers, the following simple approximation is valid according to Whitaker (1976):

$$\overline{Nu}_d = \left[ 0,40 \, Re_d^{\frac{1}{2}} + 0,06 \, Re_d^{\frac{2}{3}} \right] Pr^{0,4} \left( \frac{\eta_\infty}{\eta_w} \right)^{\frac{1}{4}} \quad (WÜK.8)$$

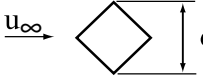
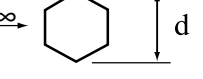
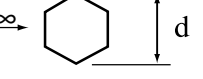
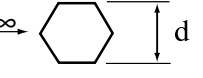
(Note: the properties used for the characteristic numbers in (WÜK.8) are to be determined at free-flow temperature. The last factor, the ratio between the viscosity at free-flow temperature and the viscosity at the temperature of the wall, approximates the dependence of the temperature on the properties.)

- Mean heat transfer for non circular cylinders

$$\overline{\text{Nu}_d} = C \text{ Re}_d^m \text{Pr}^{0,4} \quad (\text{WÜK.9})$$

Constants of equation (WÜK.9) according to Jakob (1949)

Table 5.2: Constants C and m of equation (WÜK.9)

Geometry	$\text{Re}_d$	C	m
	$5 \cdot 10^3 - 10^5$	0,246	0,588
	$5 \cdot 10^3 - 10^5$	0,102	0,675
	$5 \cdot 10^3 - 1,94 \cdot 10^4$	0,160	0,638
	$1,95 \cdot 10^4 - 10^5$	0,0385	0,782
	$5 \cdot 10^3 - 10^5$	0,153	0,638
	$5 \cdot 10^3 - 10^5$	0,228	0,731

### 5.1.1.5 Bundles of smooth tubes in an orthogonal flow

(Note: Since the temperature of the fluid in the tube bundle changes from row to row, a representative mean temperature difference must be used calculating the heat transfer.)

$$\dot{Q}_W = \bar{\alpha} A (T_W - T_{fl})_m = \bar{\alpha} A \Delta T_m \quad (5.9)$$

For many practical purposes, the logarithmic temperature difference is a good approximation

$$\Delta T_m = \Delta T_{ln} \equiv \frac{\Delta T_{inlet} - \Delta T_{outlet}}{\ln \frac{\Delta T_{inlet}}{\Delta T_{outlet}}}$$

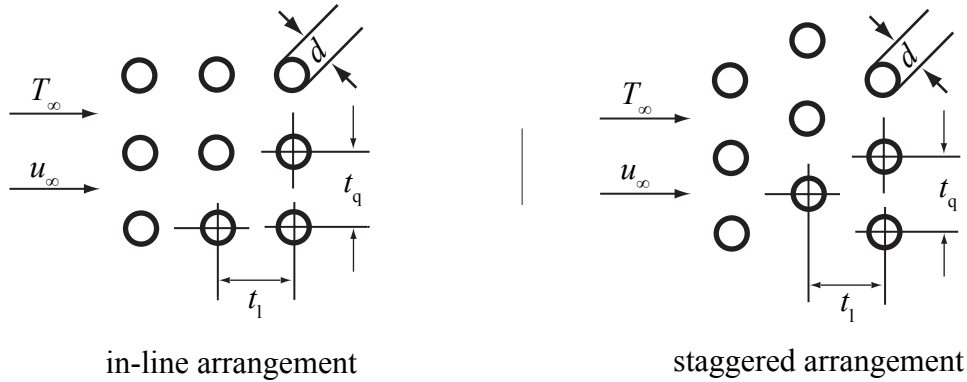


Figure 5.9: Arrangements of tubes for flow at right angles to tube bundles

In most industrial cases, where bundles of smooth tubes are used, the following equation for the heat exchange at the outer side of the tubes is valid according to Witte (1974)

$$\overline{Nu}_d = 0,287 \text{ } Re_d^{0,6} \text{ } Pr^{0,36} \cdot f_e \quad (\text{WÜK.10})$$

The Reynolds number is calculated using the free-flow velocity. The properties are to be determined at a mean temperature of the fluid inlet and outlet temperatures.

The tube arrangement factor  $f_e$  depends on the relative longitudinal distance/diameter ratio  $t_l/d$ , the relative transverse distance/diameter ratio  $t_q/d$  of the tubes, as well as the tube arrangement. This factor is shown in the following diagrams.

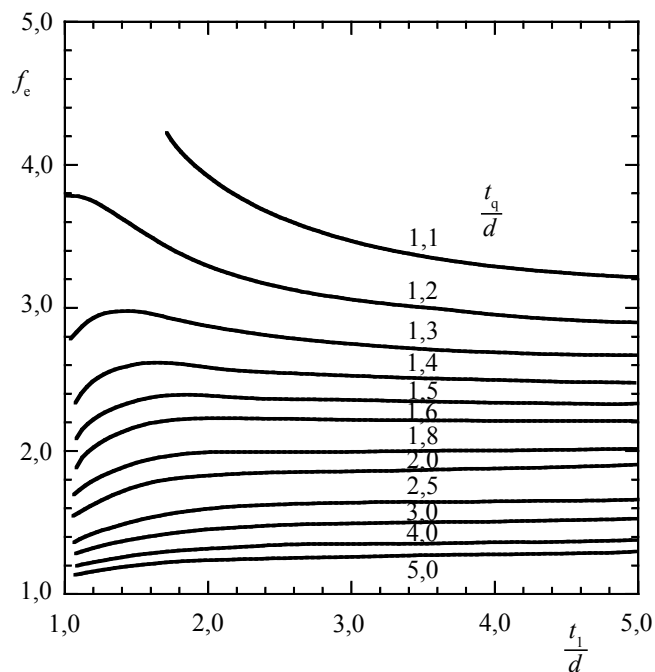


Figure 5.10: Arrangement factor, in-line arrangement, Witte (1974)

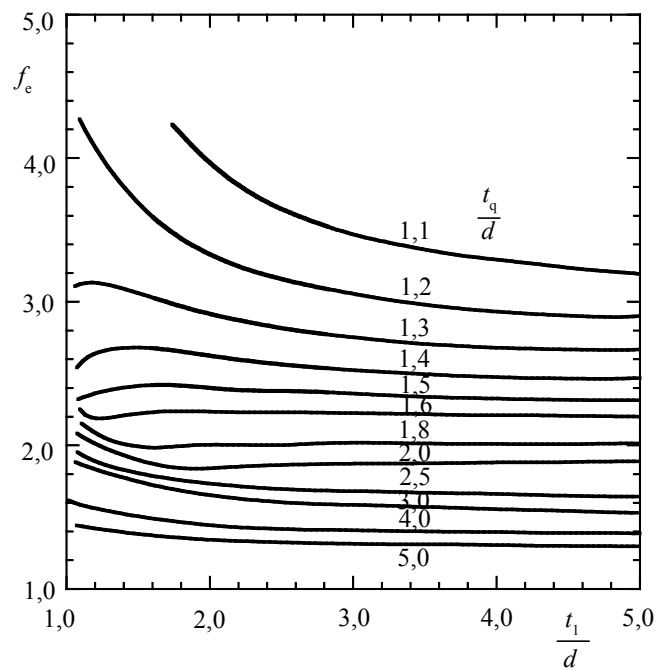


Figure 5.11: Arrangement factor, staggered arrangement, Witte (1974)

### 5.1.1.6 Flow around spheres

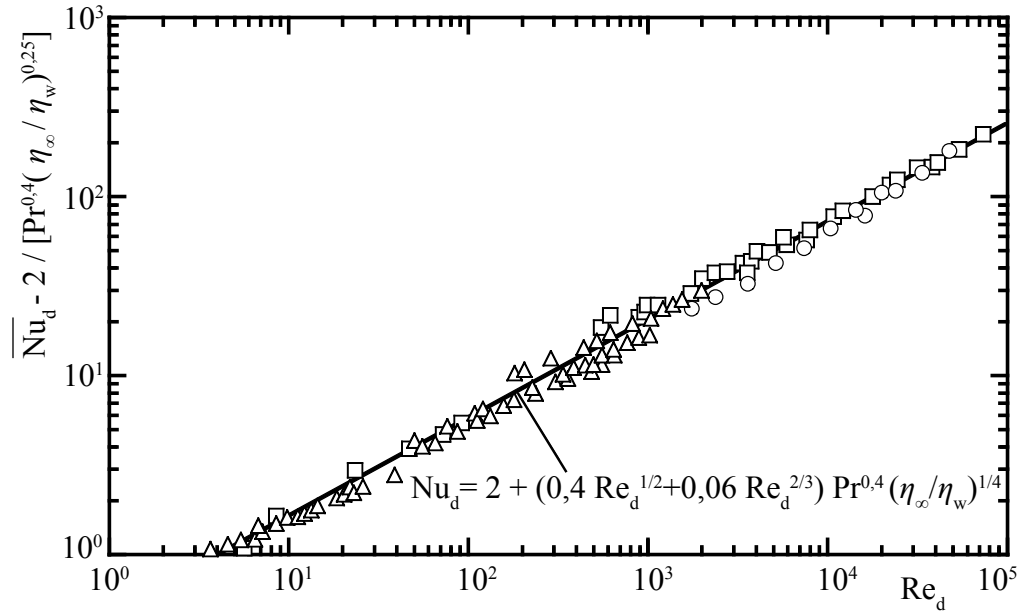


Figure 5.12: Mean Nusselt number for flow around spheres ( $\square$  water,  $\Delta$  ????,  $\circ$  air, according to Whitaker (1976))

In analogy to the example with the cylinders in flow perpendicular to their longitudinal axis, according to Whitaker (1976) the experimental results can be summarised in the following equation:

$$\overline{Nu}_d = 2 + \left(0.4 \text{ Re}_d^{\frac{1}{2}} + 0.06 \text{ Re}_d^{\frac{2}{3}}\right) \text{ Pr}^{0.4} \left(\frac{\eta_\infty}{\eta_w}\right)^{\frac{1}{4}} \quad (\text{WÜK.11})$$

$$\begin{aligned} \text{for } & 0,7 < \text{Pr} < 380 \\ \text{and } & 3,5 < \text{Re}_d < 8 \cdot 10^4 \end{aligned}$$

In this case too, the properties used for the characteristic numbers have to be determined at free-flow temperature.

### 5.1.2 Forced convection in tubes

For flow in tubes, channels or nozzles, the heat transfer coefficient is defined by

$$\dot{Q}_W = \bar{\alpha} A \Delta T_m$$

where  $\Delta T_m$  is a representative temperature difference between the temperature at the wall  $T_W$  and the energetically averaged mean temperature of the fluid  $T_{fl}$  (see introductory remarks). For greater changes of the fluid temperature along the flow path the logarithmic temperature difference should be used.

The properties used for the characteristic numbers are to be determined, if not stated otherwise, at a mean fluid temperature over the tube length

$$T_{mat} = \frac{T_{fl,outlet} + T_{fl,inlet}}{2}$$

The Reynolds number  $Re_d$  is determined using the mean fluid velocity and the diameter.

The relationships given for turbulent flow of tubes can also be used for channels with non circular cross section, if the diameter is replaced by the so-called hydraulic mean diameter  $d_h$ :

$$d_h = 4 \frac{\text{cross-section area}}{\text{wetted perimeter}} = 4 \frac{A_c}{U}$$

#### 5.1.2.1 Laminar flow in tubes, $Re_{d,crit} \approx 2300$

Isothermal surface, fully developed flow at the start of the heated (cooled) section of a tube

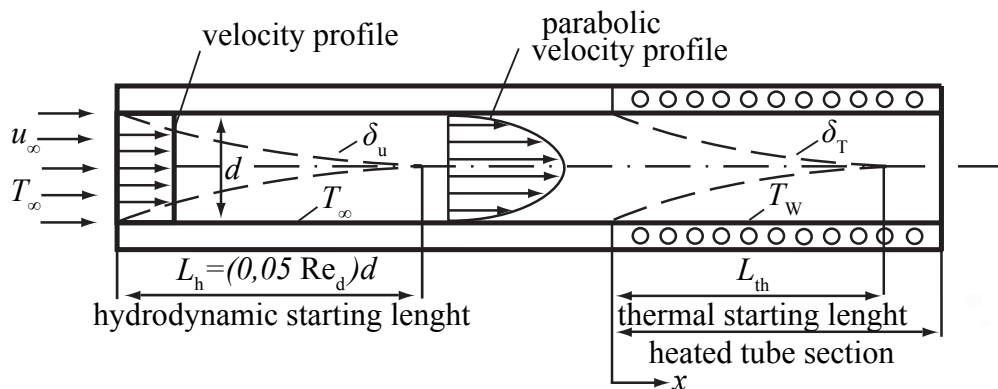


Figure 5.13: Heated tube with fully developed flow

There are theoretical solutions for the local and mean heat transfer in the form of Taylor series, shown in the following diagram. It can be seen from the diagram that

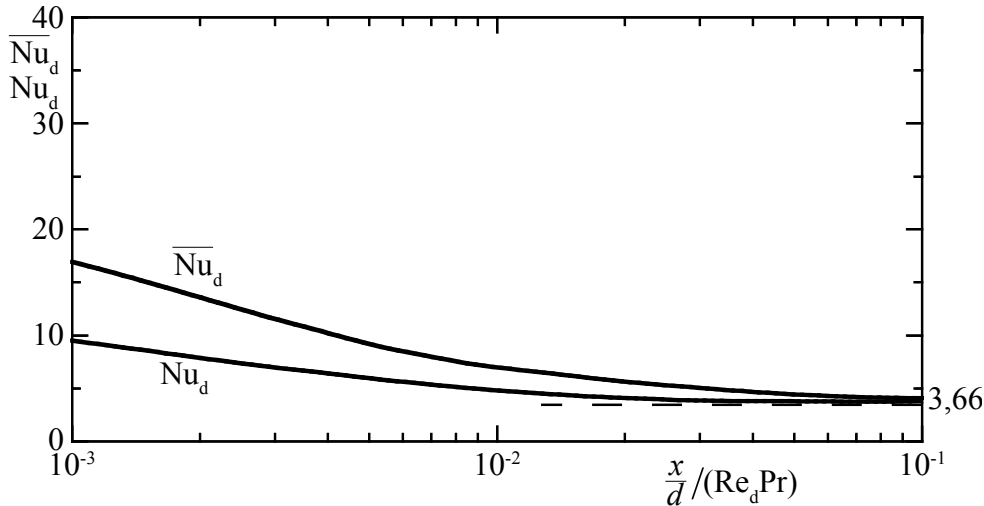


Figure 5.14: Local and mean Nusselt number for laminar fully developed tube flow, Rohsenow u. Harnett (1973)

after a thermal inflow of

$$\frac{L_{\text{th}}}{d} \approx 0,05 \text{ Re}_d \text{Pr}$$

is reached, the Nusselt number has a constant final value of  $\text{Nu}_{d,\infty} = 4,36 \left( \frac{\eta}{\eta_w} \right)^{0,14}$ .

The results for the mean Nusselt number  $\overline{\text{Nu}}_d$  can be approximated by

$$\overline{\text{Nu}}_d = \left( 3,66 + \frac{0,19 \left( \text{Re}_d \text{Pr} \frac{d}{L} \right)^{0,8}}{1 + 0,117 \left( \text{Re}_d \text{Pr} \frac{d}{L} \right)^{0,467}} \right) \left( \frac{\eta}{\eta_w} \right)^{0,14} \quad (\text{WÜK.12})$$

If instead of the wall temperature, the heat flux at the wall remains constant, the heat transfer coefficients increase by about 20%. The constant final value for long tubes is  $\text{Nu}_{d,\infty} = 4,36 \left( \frac{\eta}{\eta_w} \right)^{0,14}$  in this case.

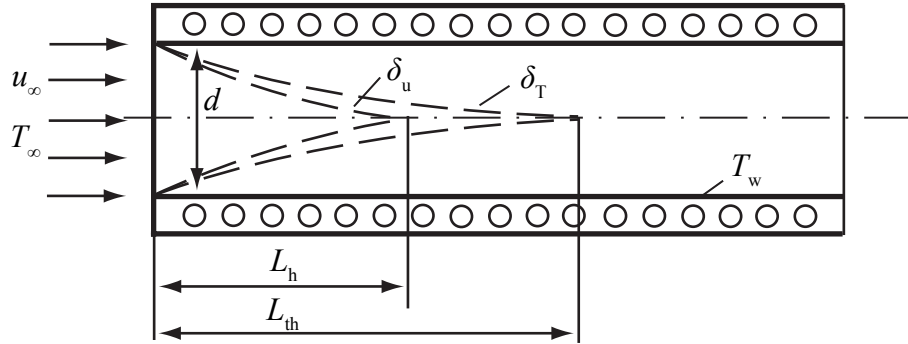
Isothermal surface, simultaneous hydrodynamic and thermal inflow


Figure 5.15: Heated tube with simultaneous hydrodynamic and thermal inflow

This problem can be solved theoretically as well. The results are additionally dependent on the Prandtl number of the fluid. The mean Nusselt number is shown in Fig. (5.16).

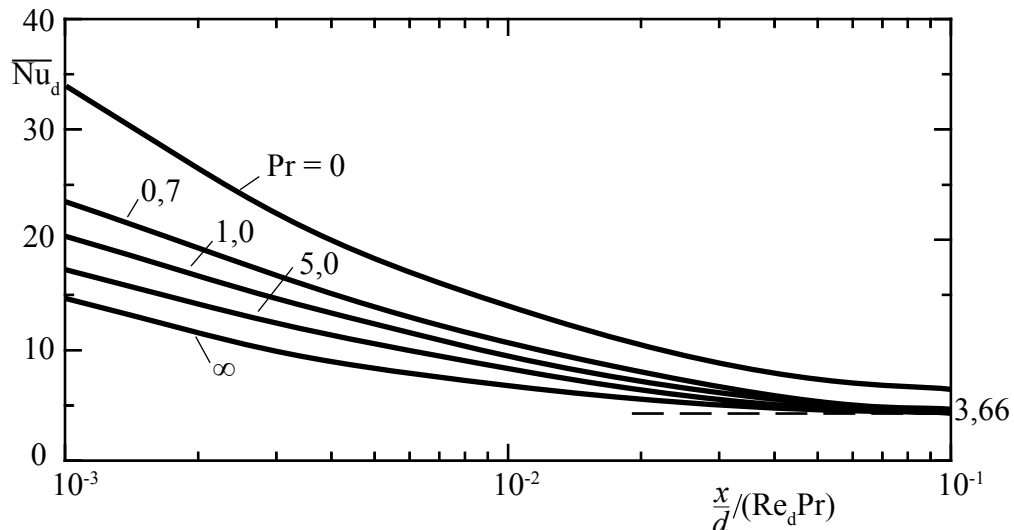


Figure 5.16: Mean Nusselt number for laminar flow in tubes and simultaneous hydrodynamic and thermal inflow

The solution can be approximated by

$$\overline{Nu}_d = \left( 3,66 + \frac{0,0677 \left( Re_d Pr \frac{d}{L} \right)^{1,33}}{1 + 0,1 Pr \left( Re_d \frac{d}{L} \right)^{0,83}} \right) \left( \frac{\eta}{\eta_w} \right)^{0,14} \quad (\text{WÜK.13})$$

### 5.1.2.2 Turbulent flow in tubes, $Re_{d,crit} \approx 2300$

Isothermal surface, simultaneous hydrodynamic and thermal inflow

An empirical relationship for the mean Nusselt number for turbulent pipe flows heated from the beginning based on a large number of experiments can be found in VDI Wärmeatlas, 1997.

$$\overline{Nu_d} = 0,0235 \left( Re_d^{0,8} - 230 \right) \left( 1,8 Pr^{0,3} - 0,8 \right) \left( 1 + \left( \frac{d}{L} \right)^{\frac{2}{3}} \right) \left( \frac{\eta}{\eta_w} \right)^{0,14} \quad (\text{WÜK.14})$$

$$\text{for } 0,6 < Pr < 500 \quad \frac{L}{d} > 1 \\ \text{and } Re_d > 2300$$

which also approximates part of the thermal inflow by the term  $\left( 1 + \left( \frac{d}{L} \right)^{\frac{2}{3}} \right)$ . The thermal inflow ends at a length of 10 to 40 times the tube diameter, for turbulent flow, depending on the value of the Reynolds number.

Heat transfer coefficients that have been measured in conditions of constant heat flux deviate by 5% from the values obtained at constant wall temperature, with exception of flow of liquid metals with very low Prandtl number.

In many cases the following relationship, instead of equation (WÜK.14) is a sufficient approximation:

$$\overline{Nu_d} = 0,027 Re_d^{0,8} Pr^{\frac{1}{3}} \left( \frac{\eta}{\eta_w} \right)^{0,14} \quad (\text{WÜK.15})$$

$$\text{for } 3000 < Re_d < 10^5 \quad \frac{L}{d} > 40$$

## 5.2 Heat transfer laws for natural convection

### 5.2.1 Natural convection at circumflowed bodies

#### 5.2.1.1 Vertical plate - laminar boundary layer flow, $\text{Gr}_{x,\text{crit}}\text{Pr} \approx 4 \cdot 10^9$

(Note: All properties, if not stated otherwise, are to be determined at a mean boundary layer temperature, excluding the isobaric expansion coefficient  $\beta$ , which for ideal gases is determined by  $\beta = \frac{1}{T_\infty}$ .)

##### Isothermal surface

- Local heat transfer

As already mentioned in section 4.3 a theoretical relationship for the Nusselt number can be derived from an approximation of the conservation equations.

$$\text{Nu}_x = 0,508 \left( \frac{\text{Pr}}{0,952 + \text{Pr}} \right)^{\frac{1}{4}} (\text{Gr}_x \text{Pr})^{\frac{1}{4}} \quad (\text{WÜK.16})$$

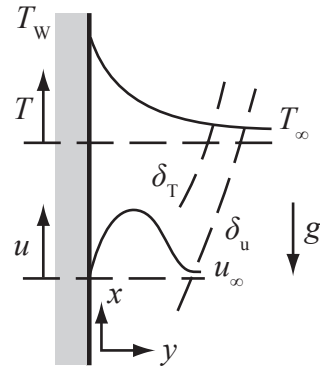


Figure 5.17: Heated plate, natural convection

- Mean heat transfer ( $\text{Gr}_{L,\text{crit}}\text{Pr} \approx 4 \cdot 10^9$ )

$$\overline{\text{Nu}_L} = \frac{\overline{\alpha} L}{\lambda} = \frac{1}{\lambda} \int_0^L \alpha(x) dx \quad (5.10)$$

$$\overline{\text{Nu}_L} = C (\text{Gr}_L \text{Pr})^{\frac{1}{4}} \quad (\text{WÜK.17})$$

for  $\text{GrPr} < \text{Gr}_{L,\text{crit}}\text{Pr}$

with the constant  $C$ , dependent on the Prandtl number

Table 5.3: Constant C of equation (WÜK.17)

Pr	0,003	0,01	0,03	0,72	1	2	10	100	1000	$\infty$
C	0,182	0,242	0,305	0,516	0,535	0,568	0,620	0,653	0,665	0,670

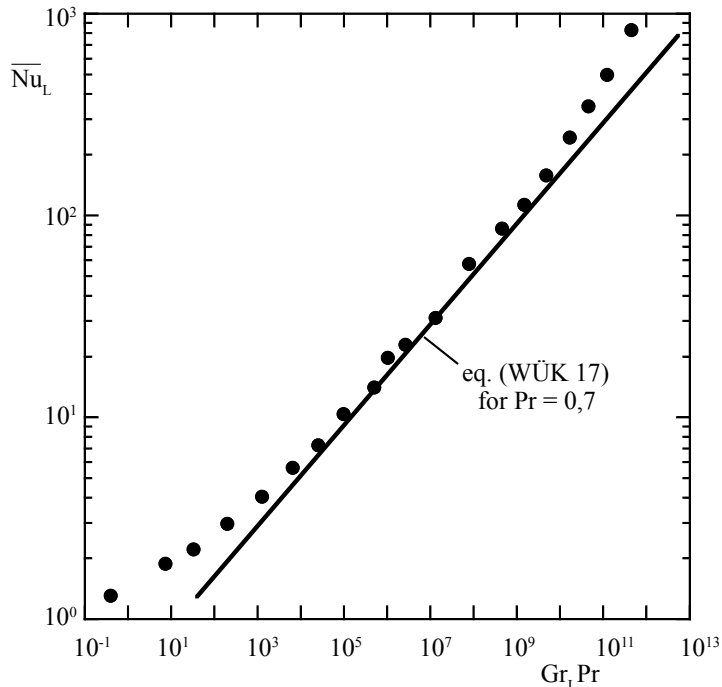


Figure 5.18: Mean Nusselt number for natural convection at a vertical plate, • air, according to Whitaker (1976)

(Note: This exact solution, already given in chapter 4 deviates insignificantly from the solution obtained by integration of equation (WÜK.16))

#### Constant heat flux

(Note: Since the heat flux is given as a boundary condition, for simplicity, a modified Grashof number  $Gr_x^*$  shall be defined  $Gr_x^* \equiv Gr_x Nu_x = \frac{\rho^2 g \beta \dot{q}_w'' x^4}{\lambda \eta^2}$  )

- local heat transfer

Derived from experiments the following equation is valid for local heat transfer, according to Holman (1976)

$$Nu_x = 0,60 (Gr_x^* Pr)^{\frac{1}{5}} \quad (WÜK.18)$$

$$\text{for } 10^5 < Gr_x^* < 10^{11}$$

### 5.2.1.2 Vertical plate, turbulent boundary layer flow, $\text{Gr}_{x,\text{crit}}\text{Pr} \approx 4 \cdot 10^9$

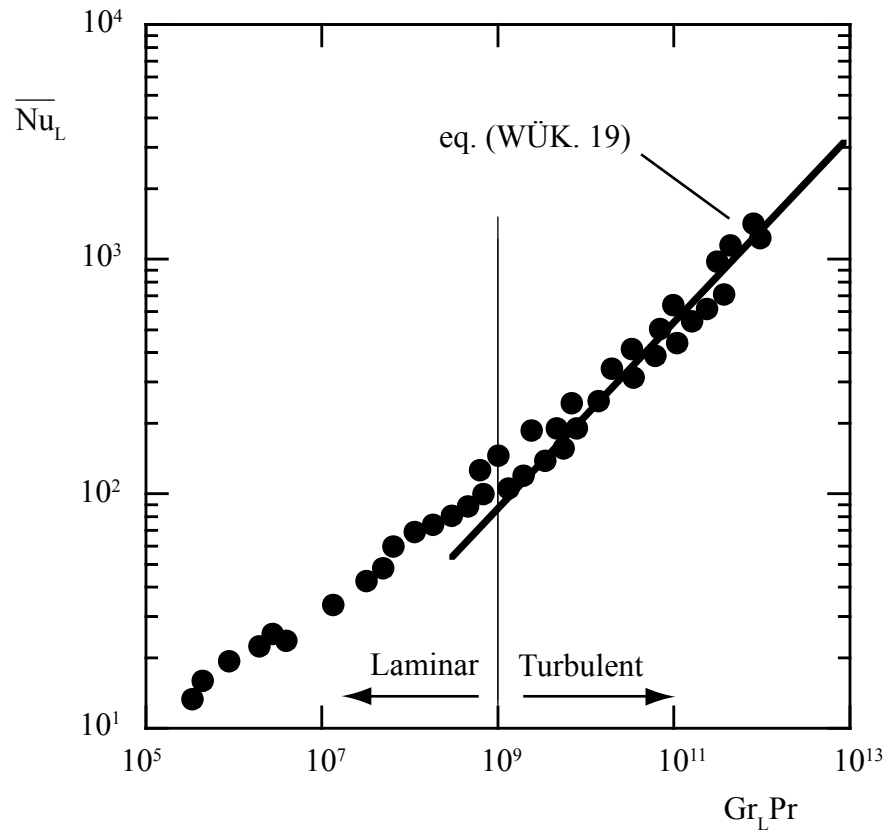


Figure 5.19: Mean Nusselt number for turbulent, natural convection at a vertical plate, • air, according to Whitaker (1976)

- Mean heat transfer

$$\overline{\text{Nu}}_L = 0,13 (\text{Gr}_L \text{Pr})^{\frac{1}{3}} \quad (\text{WÜK.19})$$

for  $10^9 < (\text{Gr}_L \text{Pr}) < 10^{12}$

(Note: For turbulent boundary layer flow the exponent  $\frac{1}{3}$  of the Grashof number makes the heat transfer coefficient independent of the height of the plate)

### 5.2.1.3 Vertical cylinder - laminar and turbulent boundary layer flow

As long as the diameter of the cylinder is significantly higher than the developed boundary layer thickness, the relationships valid for the vertical plate can be applied to this case. The limiting factor is approximately  $\frac{d}{L} > 35 \cdot Gr_L^{-\frac{1}{4}}$ . The characteristic geometrical length is the length of the cylinder.

### 5.2.1.4 Horizontal cylinder - laminar and turbulent boundary layer flow, isothermal surface

(Note: the characteristic length  $L$  is in this case the cylinder diameter  $d$ ).

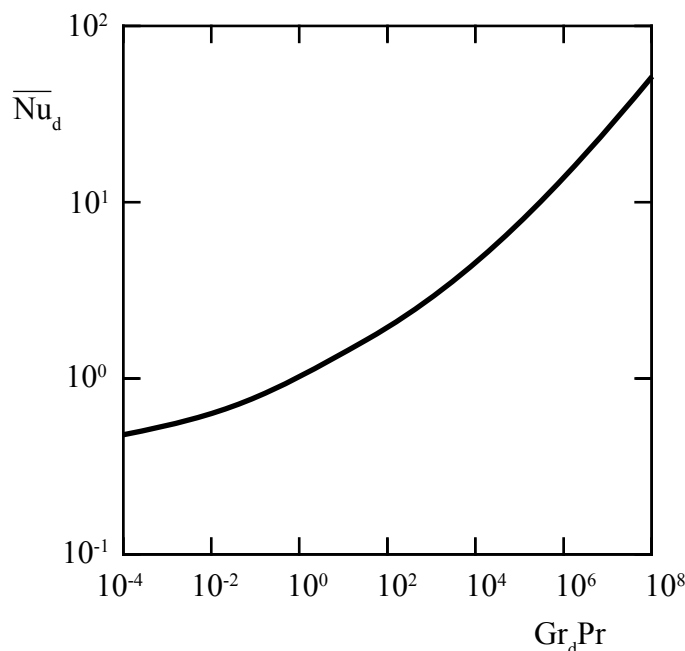


Figure 5.20: Mean Nusselt number for natural convection at a horizontal cylinder, McAdams (1954)

Using the approximations introduced by Bayley u. a. (1972)

- for the **laminar** range  $10^4 < Gr_d Pr < 10^9$

$$\overline{Nu}_d = 0,53 (Gr_d Pr)^{\frac{1}{4}} \quad (\text{WÜK.20})$$

- for the **turbulent** range  $10^9 < Gr_d Pr < 10^{12}$

$$\overline{Nu}_d = 0,13 (Gr_d Pr)^{\frac{1}{3}} \quad (\text{WÜK.21})$$

### 5.2.1.5 Horizontal plates - laminar and turbulent boundary layer flow, Holman (1976)

(Note: the relationships presented below are derived from measurements on square plates. They are approximately valid for rectangular and circular surfaces, as long as one mean side length or  $(0,9d)$ , respectively is taken as the characteristic length.)

Isothermal surface, heated upper plate side or cooled lower side

- **laminar** range  $2 \cdot 10^4 < Gr_L Pr < 8 \cdot 10^6$

$$\overline{Nu_L} = 0,54 (Gr_L Pr)^{\frac{1}{4}} \quad (\text{WÜK.22a})$$

- **turbulent** range  $8 \cdot 10^6 < Gr_L Pr < 10^{11}$

$$\overline{Nu_L} = 0,15 (Gr_L Pr)^{\frac{1}{3}} \quad (\text{WÜK.23a})$$

Isothermal surface, cooled upper plate side or heated lower side

- **laminar** range  $10^5 < Gr_L Pr < 10^{11}$

$$\overline{Nu_L} = 0,27 (Gr_L Pr)^{\frac{1}{4}} \quad (\text{WÜK.24a})$$

Constant heat flux, heated upper plate side or cooled lower side

- **laminar** range  $Gr_L Pr < 2 \cdot 10^8$

$$\overline{Nu_L} = 0,13 (Gr_L Pr)^{\frac{1}{3}} \quad (\text{WÜK.22b})$$

- **turbulent** range  $2 \cdot 10^8 < Gr_L Pr < 10^{11}$

$$\overline{Nu_L} = 0,16 (Gr_L Pr)^{\frac{1}{3}} \quad (\text{WÜK.23b})$$

Constant heat flux, cooled upper plate side or heated lower side

- **laminar** range  $10^6 < Gr_L Pr < 10^{11}$

$$\overline{Nu_L} = 0,58 (Gr_L Pr)^{\frac{1}{5}} \quad (\text{WÜK.24b})$$

## 5.2.2 Natural convection in enclosed volumes

(Note: The characteristic length  $L$  is the distance  $s$  between the heated and cooled surface, the effective temperatures are the heated and cooled wall temperatures.)

### 5.2.2.1 Fluid layers between isothermal, vertical walls with the height/distance ratio $3,1 < \frac{H}{s} < 42,2$ , Bayley u. a. (1972)

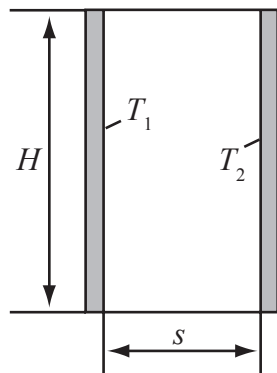


Figure 5.21: Vertical, enclosed fluid layers

For  $\text{Gr}_s < 2 \cdot 10^3$  (heat conduction only)  $\overline{\text{Nu}}_s = 1$

For the laminar range  $2 \cdot 10^3 < \text{Gr}_s < 2 \cdot 10^4$

$$\overline{\text{Nu}}_s = 0,20 \left( \frac{H}{s} \right)^{-\frac{1}{9}} (\text{Gr}_s \text{Pr})^{\frac{1}{4}} \quad (\text{WÜK.25})$$

For the turbulent range  $2 \cdot 10^5 < \text{Gr}_s < 10^7$

$$\overline{\text{Nu}}_s = 0,071 \left( \frac{H}{s} \right)^{-\frac{1}{9}} (\text{Gr}_s \text{Pr})^{\frac{1}{3}} \quad (\text{WÜK.26})$$

### 5.2.2.2 Fluid layers between isothermal, horizontal walls, lower wall is heated, Holman (1976)

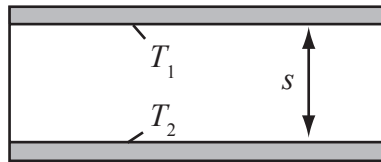


Figure 5.22: Horizontal, enclosed fluid layers

(Note: If heated from above, stable layers are formed. The heat is transferred by conduction).

For  $\text{Gr}_s < 2 \cdot 10^3$  (**heat conduction only**)  $\overline{\text{Nu}}_s = 1$

For the **laminar** range  $10^4 < \text{Gr}_s < 3,2 \cdot 10^5$

$$\overline{\text{Nu}}_s = 0,21 (\text{Gr}_s \text{Pr})^{\frac{1}{4}} \quad (\text{WÜK.27})$$

For the **turbulent** range  $3,2 \cdot 10^5 < \text{Gr}_s < 10^7$

$$\overline{\text{Nu}}_s = 0,075 (\text{Gr}_s \text{Pr})^{\frac{1}{3}} \quad (\text{WÜK.28})$$



---

# Chapter 6

## Mass transfer

As an introduction to mass transfer, the self-diffusion<sup>1</sup> mechanism on a molecular level is discussed.

### 6.1 Molecular concept of diffusion processes

#### 6.1.1 Diffusion in gases

A gaseous, diluted, binary mixture of substances (substance A, B), in which molecules behave very similarly, is considered. Figure 6.1 shows a one-dimensional example. On the left side the number of molecules A is higher than the number of molecules B. This relation is inverse on the right side. Temperature and pressure of the mixture are assumed constant and the velocity of the centre of mass, i.e. the velocity that describes the movement of all particles on a macroscopic level, is zero.

On a molecular level, each molecule moves with a velocity  $\vec{w}$ , which varies in absolute value and direction from one to another. This velocity is also called thermal velocity. The mean velocity at which the molecules A and B move is defined as  $\bar{w}$ . Hence the average frequency at which molecules pass the plane  $x = x_0$  is proportional to  $c \cdot \bar{w}$ , where  $c$  is the number of molecules per Volume [ $1/m^3$ ]. Before molecules pass the  $x_0$  plane they travel a mean free path length  $l$ . The mean free path length is the average path length that a particle or molecule travels without interacting with other particles or molecules. The right-hand particle flow of molecules A across  $x_0$  from their initial position  $x_0 - l$  is proportional to the number of molecules A, given as  $\frac{c_A}{c_{tot}}$  at position  $x_0 - l$ . The left-hand particle flow from  $x_0 + l$  to  $x_0$  is proportional to the amount content of molecules A  $\frac{c_A}{c_{tot}}$  at position  $x_0 + l$ . There is a higher chance of molecules A to flow across the plane  $x_0$  from left to right than the other way around, as the number of molecules A is higher on the left-hand side (assuming the particle distribution from fig 6.1). Hence the expected value of random molecule movement determines this kind of mass transfer.

---

<sup>1</sup>This process is called self-diffusion, because the driving potential is the concentration difference

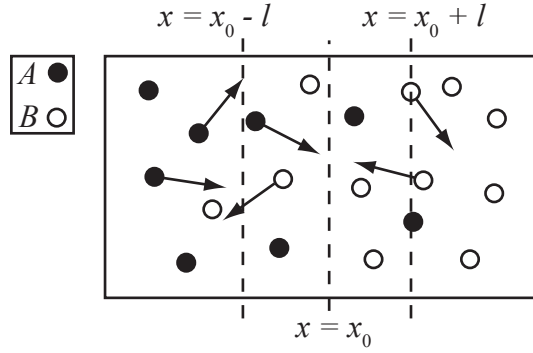


Figure 6.1: Diffusion regarded on molecular level

The mass of the molecules of A,  $m_A$ , is related to the molar concentration  $c_A$  by  $\frac{M_A}{N_A}$ , where  $N_A$  is the Avogadro constant and  $M_A$  the molecular mass of A. Hence the mass flow in x-direction is:

$$j_A''|_{x=x_0} \approx \eta(c_{\text{tot}} \bar{w}) \left( \frac{M_A}{N_A} \right) \left( \frac{c_A}{c_{\text{tot}}} \Big|_{x_0-l} - \frac{c_A}{c_{\text{tot}}} \Big|_{x_0+l} \right) \quad (6.1)$$

Where  $\eta$  is a proportional constant. Because the concentration doesn't change much in the range of twice the free path length  $2l$ , the difference can be approximated by a first order taylor series expansion about  $x_0$ .

$$j_A''|_{x=x_0} = \eta(c_{\text{tot}} \bar{w}) \left( \frac{M_A}{N_A} \right) \left( -2l \frac{d(c_A/c_{\text{tot}})}{dx} \Big|_{x_0} \right) = -2\eta(\bar{w}l)\rho \frac{d\xi_A}{dx} \Big|_{x_0} \quad (6.2)$$

With  $\xi_A = m_A/m_{\text{tot}}$  as mass concentration. While in the transformation  $c_A$ , as it is used in the unit of  $[1/\text{m}^3]$ , was substituted by:

$$c_A = \frac{m_{\text{ges}}}{V} \cdot \frac{\xi_A N_A}{M_A}$$

Hence the mass flow of component A is proportional to the gradient of the mass concentration of A. The constants that scale the gradient can be summarized in the diffusion coefficient  $D_{AB}$ . The indexation of this coefficient defines which component diffuses in which (e.g.  $D_{AB}$  stands for a diffusion from A to B).

$$D_{AB} = 2\eta(\bar{w}l) \quad (6.3)$$

This yields the following equation for the mass flow, which is also known as Fick's law:

$$j_A'' = -\rho D_{AB} \frac{d\xi}{dx} \quad (6.4)$$

Eventually the indication of this mass transfer as "self-diffusion" shall be explained. As equation (6.3) shows, the only driving potential is the gradient of mass- and molar concentration. The stochastic process of molecular movement is responsible for an even distribution of the components after all and hence for mass transfer. See Lienhard (2008).

### 6.1.2 Diffusion in liquids

The kinetic gas theory is not valid anymore, if diffusion occurs in liquids instead of gases, because every molecule has strong interactions with its surrounding molecules. For this case Einstein (1905) developed the theory of diffusion of small suspended spheres  $A$ , which is briefly explained here: A liquid layer in which suspended particles are randomly spread is assumed, as shown in figure 6.2. The number of particles

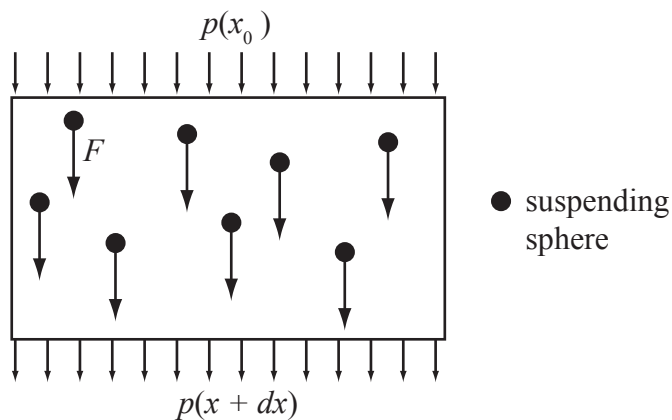


Figure 6.2: Model for diffusion in liquids

per volume unit is defined as  $n_V$ . A force  $F$  acts on each particle, which is position but not time-dependent. To simplify the example it is assumed that the force acts in x-direction only. This yields the following equation for the partial pressure:

$$-\frac{\partial p_i}{\partial x} = n_V F \quad (6.5)$$

Because of the force acting on the particle, it moves, assuming Stokes' hypothesis (creeping flow,  $Re < 1$ ) with the velocity

$$u = \frac{F}{6\pi\eta r}, \quad (6.6)$$

With  $\eta$  as the viscosity of the liquid and  $r$  the radius of the particle. The particle flow through a plane derives from  $u \cdot n_V$  and the mass flow:

$$\dot{m}'' = M_i \cdot u \cdot \frac{n_V}{N_A}. \quad (6.7)$$

With  $M_i$  as the molar mass of component  $i$  and  $N_A$ , the Avogadro constant. Inserting the force  $F$  (6.6) to the mass flow (6.7) yields:

$$\dot{m}'' = -\frac{M_i n_V}{6\pi\eta r N_A} \frac{\partial p_i}{\partial x} \quad (6.8)$$

Hereafter it is assumed, that partial pressure of the gas dissolved in the liquid can be described using the ideal gas law ( $pV = Nk_B T$ ), with  $N$  as the number of particles. This assumption is valid, if the individual dissolved gas molecules don't interact. With the Boltzmann constant<sup>2</sup>  $k_B$  follows:

$$\dot{m}'' = -\frac{M_i}{6\pi\eta r N_A} \frac{k_B T}{V} \frac{\partial N_i}{\partial x} \quad (6.9)$$

If the mass flow on the other side is described by Fick's law and a concentration gradient, the diffusion coefficient  $D$  can be determined.

$$\dot{m}'' = -\rho D \frac{\partial \xi_i}{\partial x} \quad (6.10)$$

With  $\xi_i = \rho_i / \rho$ , the density can be eliminated on the right side. Substituting  $\rho_i$  by  $N_i \cdot M_i / (N_A \cdot V)$  leads to

$$\dot{m}'' = -\frac{M_i}{6\pi\eta r N_A} \frac{k_B T}{V} \frac{\partial N_i}{\partial x} = -D \frac{M_i}{N_A V} \frac{\partial N_i}{\partial x} \quad (6.11)$$

which leads to the diffusion coefficient

$$D = \frac{k_B T}{6\pi\eta r} \quad (6.12)$$

Many empiric correlations are based on this equation.

---

<sup>2</sup>The Boltzmann-constant is named after the austrian physicist Ludwig Boltzmann (1844-1906), known as one of the founders of statistical mechanics. This constant is not to be mistaken for the Stefan-Boltzmann-constant from heat radiation.  $k_B = 1,3806504 \cdot 10^{-23} \text{ J/K}$

## 6.2 Fundamentals

In the previous introduction the diffusion process was described by the amount of substance and the mass concentration  $\xi$ . Hence the system describing variables are introduced again: The following relationship can be formed for the mole fraction  $\psi$  and the mass concentration  $\xi$ :

Table 6.1: Definition of variables in binary mixtures

(filling) mass	$m_1; m_2$	[kg]
molar mass of the gases	$M_1; M_2$	[kg/kmol]
partial density	$\rho_1 = \frac{m_1}{V}; \rho_2 = \frac{m_2}{V}$	[kg/m <sup>3</sup> ]
mixture density	$\rho = \frac{m_1+m_2}{V}$	[kg/m <sup>3</sup> ]
molar quantity	$n_1 = \frac{m_1}{M_1}; n_2 = \frac{m_2}{M_2}$	[kmol]
molar concentration	$C_1 = \frac{n_1}{V}; C_2 = \frac{n_2}{V}$	[kmol/m <sup>3</sup> ]
molar concentration of the mixture	$C = \frac{n_1+n_2}{V}$	[kmol/m <sup>3</sup> ]
mole fraction	$\psi_1 = \frac{n_1}{n_1+n_2} = \frac{C_1}{C}; \psi_2 = \frac{n_2}{n_1+n_2} = \frac{C_2}{C}$	[−]
mass concentration	$\xi_1 = \frac{\rho_1}{\rho} = \frac{m_1}{m_{\text{tot}}}; \xi_2 = \frac{\rho_2}{\rho} = \frac{m_2}{m_{\text{tot}}}$	[−]
partial pressure	$p_1 = \frac{R_m}{M_1} \rho_1 T = R_m C_1 T; p_2 = \frac{R_m}{M_2} \rho_2 T = R_m C_2 T$	[N/m <sup>2</sup> ]

$$\psi_1 = \frac{\frac{\rho_1}{M_1} \frac{1}{\rho}}{\left( \frac{\rho_1}{M_1} + \frac{\rho_2}{M_2} \right) \frac{1}{\rho}} = \frac{\frac{\xi_1}{M_1}}{\frac{\xi_1}{M_1} + \frac{\xi_2}{M_2}} \quad (6.13)$$

Furthermore the mean molar mass is defined as:

$$\overline{M} = \frac{m_1 + m_2}{n_1 + n_2} = \frac{\frac{1}{V}(m_1 + m_2)}{\frac{1}{V}(n_1 + n_2)} = \frac{\rho}{C} \quad (6.14)$$

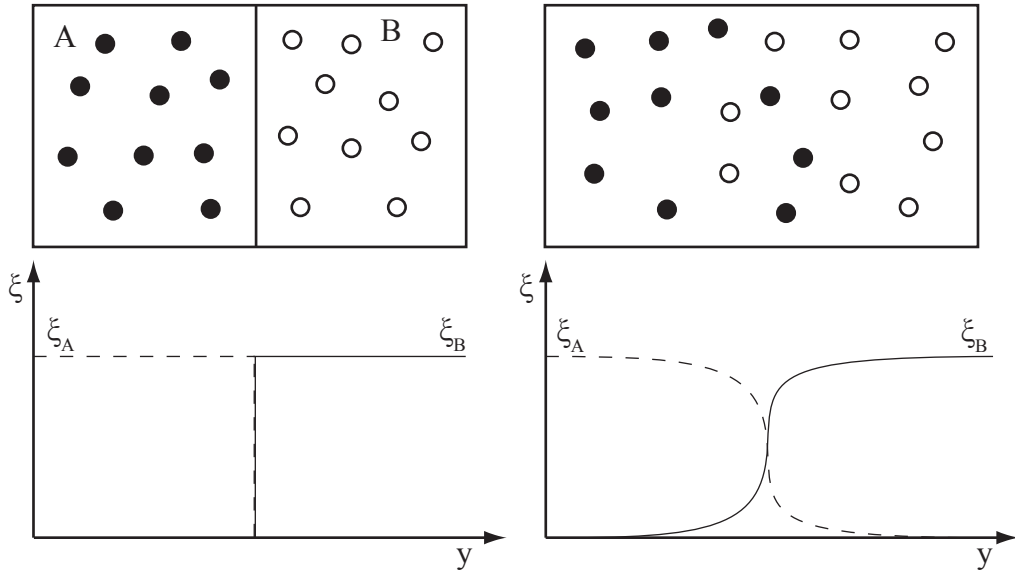


Figure 6.3: One-dimensional, equimolar diffusion in resting, binary mixtures

If the gaseous components and the mixture are assumed to behave like ideal gases

$$p = R_m c T = R_m(c_1 + c_2)T = p_1 + p_2 \quad (6.15)$$

is valid. Hence total pressure is the sum of partial pressures (Dalton's law, 1805). Because pressure is directly proportional to the amount of substance this yields:

$$\psi_1 = \frac{p_1}{p} \text{ and } \psi_2 = \frac{p_2}{p} \quad (6.16)$$

### **Example: One-dimensional, equimolar diffusion in resting binary gas mixtures**

The system shown in figure 6.3 is closed, hence the amount of substance of each component and consequently the overall amount of substance is constant. As a result, mixture concentration  $C$  and pressure are also constant. The particle flow, which is responsible for the mixing of the components, depends on the negative concentration gradient.

$$\text{Flow} = \text{diffusion coefficient} \cdot \text{neg. mass concentration gradient} \quad (6.17)$$

This yields

$$\dot{n}_1'' = D_{12} \cdot \left( -\frac{dC_1}{dy} \right) \quad (6.18)$$

and

$$\dot{n}_2'' = D_{21} \cdot \left( -\frac{dC_2}{dy} \right) \quad (6.19)$$

for the substance flow. The initial precondition, that the molar concentrations of the components and the overall molar concentration are constant within the regarded system

$$C_1 + C_2 = C = \text{const} \quad (6.20)$$

leads to the equality of both concentration gradients

$$\frac{dC_1}{dy} + \frac{dC_2}{dy} = 0 \quad (6.21)$$

With the additional precondition of constant amount of substance

$$n = n_1 + n_2 = \text{const} \quad (6.22)$$

the sum of substance flows has to be zero

$$\dot{n}_1'' + \dot{n}_2'' = 0 \rightarrow \dot{n}_1'' = -\dot{n}_2'' \quad (6.23)$$

Equations (6.18) and (6.19) yield

$$\frac{\dot{n}_1''}{D_{12}} + \frac{\dot{n}_2''}{D_{21}} = - \left( \frac{dC_1}{dy} + \frac{dC_2}{dy} \right) \quad (6.24)$$

(6.21) and (6.22) yield the equality of diffusion coefficients in a binary mixture

$$D_{12} = D_{21} \quad (6.25)$$

This is only valid for a binary mixture.

## 6.3 Mass transfer in flows

In this section mass transfer through diffusion based on a concentration gradient, as previously introduced, is extended to the three-dimensional case.

If the fluid is a mixture of  $n$  different components, as in the previous example, and not a single pure substance, the convective mass transfer can be overlaid by mass transfer by diffusion caused by a concentration, pressure or temperature gradient.

If a differential volume, as shown in figure 6.4, is regarded, then the mean flow velocity  $\vec{w}$ , which is averaged over all components, can differ from the mean value of the flow velocities  $w_{xi}, w_{yi}, w_{zi}$  of each component  $i$ , due to diffusion processes.<sup>3</sup>

---

<sup>3</sup>Of course other phenomenon can cause a deviation of velocities, e.g. solid particles in an accelerated flow, due to inertial forces. These effects are not part of this consideration.

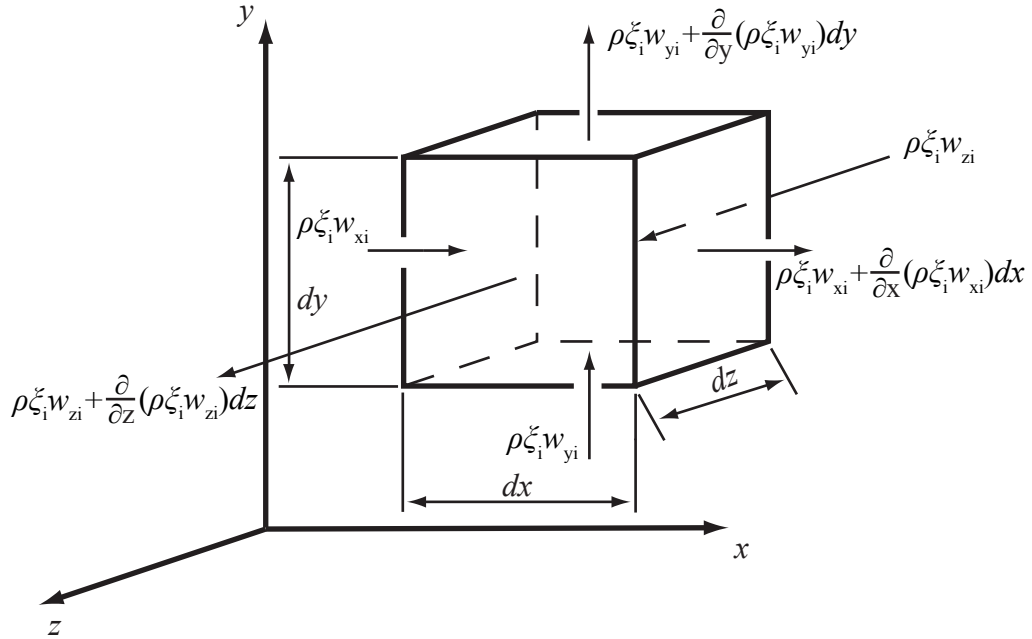


Figure 6.4: Substance balance at the control volume

There are different definitions of the mean velocity. In this case the mean velocity is defined as the mass centre velocity:

$$\vec{w} = \begin{pmatrix} w_x \\ w_y \\ w_z \end{pmatrix} = \frac{1}{\rho} \sum_{i=1}^n \rho \xi_i \begin{pmatrix} w_{xi} \\ w_{yi} \\ w_{zi} \end{pmatrix} \quad (6.26)$$

with the fluid density  $\rho$  in kg/m<sup>3</sup> and  $\xi_i$  as mass fraction of component  $i$  within the mixture.

For the balance of molar flows the volume cell  $dV = dx dy dz$  is regarded again. The mass of substance  $i$  within the volume is  $\xi_i \rho dV$ , and its temporal alteration is  $\partial(\xi_i \rho)/\partial t$ . The temporal alteration of mass can be defined by the mass flows through the six surfaces of the volume cell  $dV$ :

$$\begin{aligned}
\frac{\partial(\xi_i \rho)}{\partial t} dV &= \rho \xi_i w_{xi} dy dz - \left[ \rho \xi_i w_{xi} + \frac{\partial}{\partial x} (\rho \xi_i w_{xi}) dx \right] dy dz \\
&+ \rho \xi_i w_{yi} dx dz - \left[ \rho \xi_i w_{yi} + \frac{\partial}{\partial y} (\rho \xi_i w_{yi}) dy \right] dx dz \\
&+ \rho \xi_i w_{zi} dxdy - \left[ \rho \xi_i w_{zi} + \frac{\partial}{\partial z} (\rho \xi_i w_{zi}) dz \right] dxdy \\
&= -dV \left[ \frac{\partial}{\partial x} (\rho \xi_i w_{xi}) + \frac{\partial}{\partial y} (\rho \xi_i w_{yi}) + \frac{\partial}{\partial z} (\rho \xi_i w_{zi}) \right]
\end{aligned} \tag{6.27}$$

To describe mass flow by diffusion, terms like diffusion velocity and **diffusion stream density** are used. Here, the diffusion velocity is defined as the difference between the mean particle velocity  $\vec{w}_i = (w_{xi}, w_{yi}, w_{zi})$  and the mass centre velocity  $\vec{w} = (w_x, w_y, w_z)$ . The diffusion stream density  $\vec{j}_i''$  is to be understood as the related mass flow of component  $i$  ( $\text{kg}/\text{m}^2\text{s}$ ):

$$\vec{j}_i'' = \rho \xi_i (\vec{w}_i - \vec{w}) \tag{6.28}$$

The sum of all diffusion stream densities has to dissolve according to equation (6.26) and definition (6.28)

$$\sum_{i=1}^n \vec{j}_i'' = \sum_{i=1}^n \rho \xi_i (\vec{w}_i - \vec{w}) = 0 \tag{6.29}$$

As early as 1885, Fick empirically found the law for the diffusion stream density  $\vec{j}_i''$  (Fick (1855)), that is named after him, which states, that the diffusion stream density is proportional to the concentration gradient:

$$j_{xi}'' = -\rho D \frac{\partial \xi_i}{\partial x} \tag{6.30}$$

Putting the definition of diffusion stream velocity (6.28) into equation (6.27) yields

$$\frac{\partial(\xi_i \rho)}{\partial t} = - \left[ \frac{\partial}{\partial x} (\xi_i \rho w_x + j_{xi}'') + \frac{\partial}{\partial y} (\xi_i \rho w_y + j_{yi}'') + \frac{\partial}{\partial z} (\xi_i \rho w_z + j_{zi}'') \right] \tag{6.31}$$

This equation can be partially differentiated and rewritten assuming constant density and using the continuity equation. This yields the following conservation equation for component  $i$  (the index  $i$  is left out hereafter):

$$\rho \frac{\partial \xi}{\partial t} + \rho u \frac{\partial \xi}{\partial x} + \rho v \frac{\partial \xi}{\partial y} + \rho w \frac{\partial \xi}{\partial z} + \frac{\partial j''}{\partial x} + \frac{\partial j''}{\partial y} + \frac{\partial j''}{\partial z} = 0 \tag{6.32}$$

Using Fick's law (6.30) yields

$$\rho \frac{\partial(\xi)}{\partial t} + \rho u \frac{\partial \xi}{\partial x} + \rho v \frac{\partial \xi}{\partial y} + \rho w \frac{\partial \xi}{\partial z} - \frac{\partial}{\partial x} \left( \rho D \frac{\partial \xi}{\partial x} \right) - \frac{\partial}{\partial y} \left( \rho D \frac{\partial \xi}{\partial y} \right) - \frac{\partial}{\partial z} \left( \rho D \frac{\partial \xi}{\partial z} \right) = 0 \quad (6.33)$$

In the stationary case assuming constant properties and introducing the Schmidt-number  $\text{Sc} = \frac{\eta}{\rho D}$  yields the simplified form

$$\rho u \frac{\partial \xi}{\partial x} + \rho v \frac{\partial \xi}{\partial y} + \rho w \frac{\partial \xi}{\partial z} = \frac{\eta}{\text{Sc}} \left( \frac{\partial^2 \xi}{\partial x^2} + \frac{\partial^2 \xi}{\partial y^2} + \frac{\partial^2 \xi}{\partial z^2} \right) \quad (6.34)$$

which can be rendered dimensionless analogous to the energy equation in the convection section, introducing reference values. If these values are defined as follows:

$$x^* \equiv \frac{x}{L}; y^* \equiv \frac{y}{L}; z^* \equiv \frac{z}{L}; u^* \equiv \frac{u}{u_\infty}; v^* \equiv \frac{v}{u_\infty}; w^* \equiv \frac{w}{u_\infty}; \xi^* \equiv \frac{\xi - \xi_w}{\xi_\infty - \xi_w} \quad (6.35)$$

this leads to the dimensionless conservation equation

$$u^* \frac{\partial \xi^*}{\partial x^*} + v^* \frac{\partial \xi^*}{\partial y^*} + w^* \frac{\partial \xi^*}{\partial z^*} = \frac{1}{\text{Re Sc}} \left( \frac{\partial^2 \xi^*}{\partial x^{*2}} + \frac{\partial^2 \xi^*}{\partial y^{*2}} + \frac{\partial^2 \xi^*}{\partial z^{*2}} \right) \quad (6.36)$$

which leads to the fact, that the related concentration field has to be dependent on the dimensionless location variables and the characteristic numbers  $\text{Re}$  and  $\text{Sc}$ :

$$\xi^* = f(x^*, y^*, z^*, \text{Re}, \text{Sc}) \quad (6.37)$$

The analogy to heat transfer is apparent again. In section 4, convection:

$$T^* = f(x^*, y^*, z^*, \text{Re}, \text{Pr}) \quad (6.38)$$

was valid for the dimensionless temperature field.

### 6.3.1 Examples for transient diffusion

Regarding a one-dimensional transient problem, equation (6.33) can be simplified to

$$\rho \frac{\partial \xi}{\partial t} + \rho u \frac{\partial \xi}{\partial x} = \frac{\partial}{\partial x} \left( \rho D \frac{\partial \xi}{\partial x} \right) \quad (6.39)$$

If in addition, convection is neglected, this yields the following differential equation, which is known as "Fick's second law".

$$\rho \frac{\partial \xi}{\partial t} = \frac{\partial}{\partial x} \left( \rho D \frac{\partial \xi}{\partial x} \right) \quad (6.40)$$

This equation has a similar structure as equation (3.69) from chapter 3.5.2 and therefore can be solved in an analogue way.

## 6.4 Transition laws in mass transfer

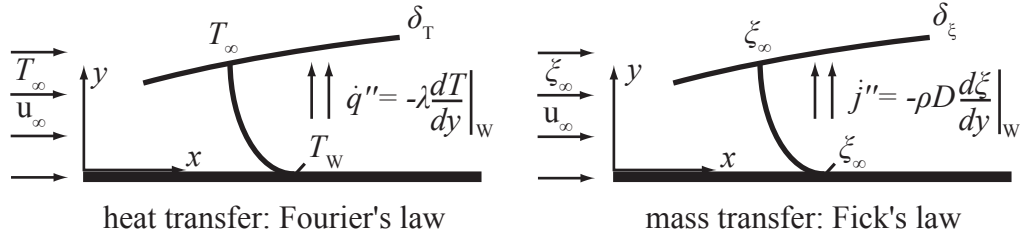


Figure 6.5: Analogy between heat and mass transfer

Similar to the heat transfer coefficient  $\alpha$  introduced in heat transfer, which linked heat flux  $\dot{q}''$  and the temperature difference between the wall temperature  $T_W$  and the surrounding  $T_\infty$

$$\dot{q}'' \equiv \alpha(T_W - T_\infty) \quad (6.41)$$

in mass transfer a material transfer coefficient  $g$  can be defined:

$$j''_A \equiv g(\xi_W - \xi_\infty) \quad (6.42)$$

To find a characteristic number for this transition coefficient it's useful to visualise the definition of the heat transfer coefficient once more. There, heat flux was determined drawing a balance using the local temperature gradient right next to the wall. Making  $T^* = \frac{T}{T_\infty - T_W}$  and  $y^* = \frac{y}{L}$ <sup>2</sup> dimensionless yielded

$$\dot{q}''_W = -\lambda \frac{\partial T}{\partial y} \Big|_{y=0} = -\lambda \frac{T_\infty - T_W}{L} \frac{\partial T^*}{\partial y^*} \Big|_{y^*=0} \quad (6.43)$$

<sup>2</sup>L resembles a characteristic length in the regarded problem

Comparing equation (6.41) and (6.43) the dimensionless Nusselt number was introduced

$$\frac{\alpha L}{\lambda} \equiv \text{Nu} = \left. \frac{\partial T^*}{\partial y^*} \right|_{y^*=0} = f(\text{Re}, \text{Pr}) \quad (6.44)$$

although for this number, for different cases, correlations of the following form exist:

$$\text{Nu} = C \text{ Re}^m \text{ Pr}^n \quad (6.45)$$

The same approach is used for the material transfer coefficient. For the diffusive material stream density, Fick's law is applied with reference values:

$$j''_A = -\rho D \left. \frac{\partial \xi}{\partial y} \right|_{y=0} = -\rho D \frac{\xi_\infty - \xi_W}{L} \left. \frac{\partial \xi^*}{\partial y^*} \right|_{y^*=0} \quad (6.46)$$

Comparing this equation to the material transfer coefficient already introduced in equation (6.42) yields the characteristic material transfer number, the Sherwood number  $\text{Sh}$ :

$$\frac{gL}{\rho D} \equiv \text{Sh} = \left. \frac{\partial \xi^*}{\partial y^*} \right|_{y^*=0} = f(\text{Re}, \text{Sc}) \quad (6.47)$$

Sherwood numbers can also be rewritten using characteristic numbers for material transfer

$$\text{Sh} = C \text{ Re}^m \text{ Sc}^n \quad (6.48)$$

Because the type of the mass conservation equation and the energy equation match, in case of similar boundary conditions, the constant  $C$  and the exponents  $m$  and  $n$  of both characteristic number relationships have to be equal.

Table 6.2: 1-D balance, no convection, constant material properties

heat transfer	mass transfer	momentum transfer
$\frac{\partial T}{\partial t} = \lambda \frac{\partial^2 T}{\partial x^2}$	$\rho \frac{\partial \xi_i}{\partial t} = D \rho \frac{\partial^2 \xi_i}{\partial x^2}$	$\frac{\partial u}{\partial t} = \nu \frac{\partial^2 u}{\partial x^2}$

### 6.4.1 Analogy between heat and mass transfer

A comparison of the characteristic numbers between heat and mass transfer shows that:

$$\frac{\text{Sh}}{\text{Nu}} = \left( \frac{\text{Sc}}{\text{Pr}} \right)^n \quad (6.49)$$

and hence

$$\frac{g}{\alpha/c_p} = \left( \frac{\text{Sc}}{\text{Pr}} \right)^{n-1} \quad (6.50)$$

For gases the Prantl and Schmidt number are almost identical. In this case a simple connection between the mass and heat transfer coefficient can be derived as an approximation, also known as Lewis' law:

$$\frac{g}{\alpha/c_p} = 1 \quad \text{Lewis' law (for gases)} \quad (6.51)$$

#### 6.4.2 Solving the one-dimensional transient heat conduction and diffusion problem respectively

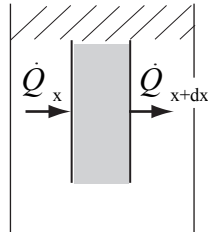


Figure 6.6: Transient heat conduction

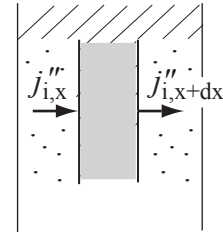


Figure 6.7: Transient diffusion

The energy conservation equation used to determine the temperature profile of transient heat conduction in a half-infinite plate (left-hand side) and the mass transfer equation for component  $i$  regarding mere diffusion to determine the concentration field (right-hand side) are almost identical. Hence hereafter these two problems are described and solved concurrent to demonstrate the similarity of the solutions.

$$\frac{\partial T}{\partial t} = \frac{\lambda}{\rho c_p} \frac{\partial^2 T}{\partial x^2}$$

$$\rho \frac{\partial \xi_i}{\partial t} = \rho D \frac{\partial^2 \xi_i}{\partial x^2}$$

Transforming both equations yields

$$\frac{\partial T}{\partial t} = \frac{\lambda}{\rho c_p} \frac{\partial^2 T}{\partial x^2}$$

$$\frac{\partial \xi_i}{\partial t} = D \frac{\partial^2 \xi_i}{\partial x^2}$$

with the following boundary conditions

$$T(t=0, x) = T_o$$

$$\xi_i(t=0, x) = \xi_{i,o}$$

$$T(t > 0, x=0) = T_u$$

$$\xi_i(t > 0, x=0) = \xi_{i,u}$$

$$T(t > 0, x \rightarrow \infty) = T_o$$

$$\xi_i(t > 0, x \rightarrow \infty) = \xi_{i,o}$$

Introducing an overtemperature and a dimensionless concentration, as well as a coefficient  $a$

$$\theta^* = \frac{T - T_o}{T_u - T_o}, \quad a = \frac{\lambda}{\rho c_p}$$

$$\theta^* = \frac{\xi_i - \xi_{i,o}}{\xi_{i,u} - \xi_{i,o}}, \quad a = D$$

eventually yields the same second order differential equation

$$\frac{\partial \theta^*}{\partial t} = a \frac{\partial^2 \theta^*}{\partial x^2} \quad (6.52)$$

using the transformed boundary conditions

$$\theta^*(t > 0, x \rightarrow \infty) = 0$$

$$\theta^*(t > 0, x = 0) = 1$$

$$\theta^*(t = 0, x) = 0$$

and the substitution

$$\eta \equiv \frac{x}{\sqrt{4at}} \quad (6.53)$$

the equation can be transformed into an ordinary differential euqation

$$\frac{\partial^2 \theta^*}{\partial \eta^2} = 2\eta \frac{\partial \theta^*}{\partial \eta} \quad (6.54)$$

its solution

$$\theta^* = 1 - \operatorname{erf}(\eta)$$

or

$$\theta^* = 1 - \operatorname{erf}\left(\frac{x}{\sqrt{4at}}\right)$$

respectively is valid for the temperature- as well as for the concentration field. A retransformation leads to the normal form with dimensions

$$\frac{T - T_o}{T_u - T_o} = 1 - \operatorname{erf}\left(\frac{x}{\sqrt{4\frac{\lambda}{\rho c_p}t}}\right) \quad \frac{\xi_i - \xi_{i,o}}{\xi_{i,u} - \xi_{i,o}} = 1 - \operatorname{erf}\left(\frac{x}{\sqrt{4Dt}}\right)$$

Figure 6.8 and 6.9 qualitatively show the profiles. The heat flux at the wall can be derived from the temperature gradient

$$\dot{q}''|_{x=0} = -\lambda \frac{dT}{dx}\Big|_{x=0} = \frac{\lambda}{\sqrt{\pi at}} (T_u - T_o) = \sqrt{\frac{\lambda c_p \rho}{\pi t}} (T_u - T_o) \quad (6.55)$$

The following equation is valid for the diffusion stream of component  $i$  at the surface

$$j_i''|_{x=0} = \frac{\rho D}{\sqrt{\pi Dt}} (\xi_{i,u} - \xi_{i,o}) \quad (6.56)$$

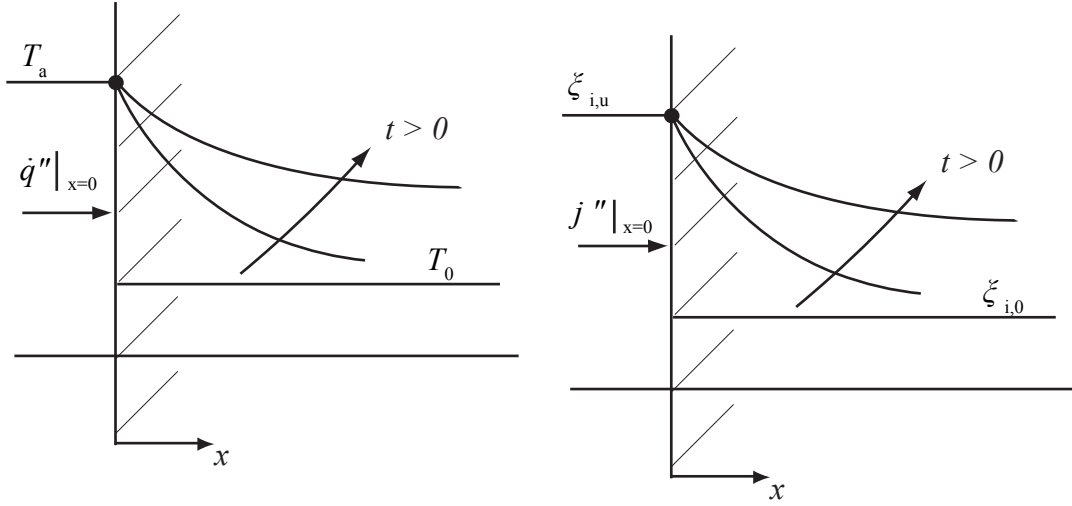


Figure 6.8: Temperature field

Figure 6.9: Concentration field

## 6.5 Evaporation at a liquid surface

The mechanism of a vaporous mass flow emerging from the surface of a liquid A into a gas mixture consisting of components A and B is called evaporation. This kind of mass transfer is driven by diffusion, i.e. diffusive resistances are determining. In contrast vaporisation is a process where the vapour component merges into a pure vapour-phase, hence diffusion resistances are irrelevant.

Hereafter, an evaporating mass flow is regarded, assuming, that component B from the gas mixture does not overflow into the liquid phase, hence the liquid surface is semipermeable. This process is described as single-sided diffusion in literature (see Mersmann (1986)).

Figure 6.10 shows this system. Here it is assumed, that the concentration of component A is permanently constant at position L, in simple terms  $\xi(L) = 0$  is valid. Furthermore the phase boundary permanently stays at  $x = 0$ , due to a constant mass flow that cancels out the evaporation. In this steady state

$$\frac{\partial \xi_A}{\partial t} = \frac{\partial \xi_B}{\partial t} = 0 \quad (6.57)$$

is valid. A balance at the phase boundary for the mass flow of component B leads to  $\dot{m}_B''(x = 0) = 0$ , because component B does not dissolve in the liquid. Because in the area  $0 < x < L$  no cross flow occurs,  $\dot{m}_B''(0 < x < L) = 0$  is valid. For the evaporating component A, mass flow can be introduced as in section 6.3 using the effective velocity of the particles  $w_A$ , the desity and the mass fraction  $\xi$  of component A.

$$\dot{m}_A'' = w_A \rho \xi_A \quad (6.58)$$

As the effective particle velocity is a superposition of the mass centre velocity  $w$  and the diffusion stream  $j''_A$  (see equation (6.28)), the mass flow of A is

$$\dot{m}_A'' = w\rho\xi_A + j''_A \quad (6.59)$$

A similar relationship can be derived for component B. Because the surface is impermeable for component B, as stated earlier, the mass flow is zero.

$$\dot{m}_B'' = w_B\rho\xi_B = w\rho\xi_B + j''_B = 0 \quad (6.60)$$

The total mass flow is the sum of part mass flows

$$\dot{m}'' = \dot{m}_A'' + \dot{m}_B'' = w\rho\xi_A + j''_A + w\rho\xi_B + j''_B \quad (6.61)$$

With the requirement that the sum of diffusion flows equals zero from equation (6.29), and  $\xi_A + \xi_B = 1$  yields

$$\dot{m}'' = \dot{m}_A'' + \dot{m}_B'' = w\rho \quad (6.62)$$

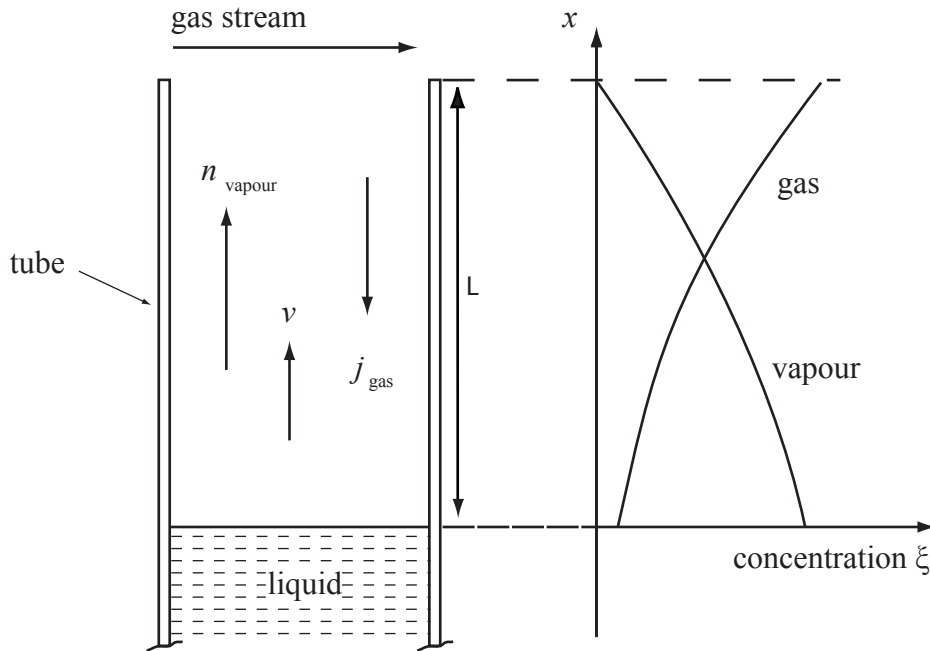


Figure 6.10: Stefan-stream

Applying this to equations (6.62) and (6.59), the total mass flow, as well as the mass flow of component A is:

$$\dot{m}'' = \dot{m}_A'' = \underbrace{\frac{1}{1 - \xi_A}}_F j_A'' \quad (6.63)$$

Apparently the net mass flow is larger than the diffusion flow by a factor F, the **Stefan-factor**. This factor takes into account that the surface is only permeable for the evaporating component ("semipermeable wall") and as a result the diffusive mass flow of component B driven by the concentration gradient towards the wall has to be compensated by a convective mass flow.

Expressing the mass flow  $j_A''$  according to (6.42) by the mass transfer coefficient and concentration difference yields:

$$\dot{m}_A'' = g \frac{\xi_{A,W} - \xi_{A,\infty}}{1 - \xi_{A,W}} \quad (6.64)$$

Or in dimensionless form:

$$\frac{\dot{m}_A''}{\rho u_\infty} = \frac{Sh}{Re \cdot Sc} \underbrace{\frac{\xi_{A,W} - \xi_{A,\infty}}{1 - \xi_{A,W}}}_B \quad (6.65)$$

B is the driving potential for mass transfer.

### 6.5.1 Determining the mass transfer coefficient

With the previous solution of the evaporation problem at an open surface (6.64), the mass flow could only be determined, if the concentration gradient at the surface was known. Now the mass flow should be determined using the concentrations at the surface  $\xi(x = 0)$  and at  $\xi(x = L)$ .

To begin with, the diffusion stream from equation (6.63) can be expressed by Fick's law.

$$\dot{m}'' = \dot{m}_A'' = -\frac{1}{1 - \xi_A} \rho D \frac{\partial \xi_A}{\partial x} \quad (6.66)$$

Because the mass flow is constant at every position  $x$ , the equation above can be analysed at  $x = 0$  (at the surface).

$$\dot{m}''|_0 = \dot{m}_A''|_0 = -\frac{1}{1 - \xi_{A,0}} \rho D \left( \frac{\partial \xi_A}{\partial x} \right)_0 \quad (6.67)$$

Putting this mass flow into equation (6.59), regarding equation 6.62 yields:

$$\dot{m}_A'' = -\rho D \frac{\partial \xi_A}{\partial x} - \frac{\xi_A}{1 - \xi_{A,O}} \rho D \left( \frac{\partial \xi_A}{\partial x} \right)_O \quad (6.68)$$

Differentiating this equation after  $x$  leads to

$$\frac{\partial \dot{m}_A''}{\partial x} = -\rho D \left[ \frac{\partial^2 \xi_A}{\partial x^2} + \frac{1}{1 - \xi_{A,O}} \left( \frac{\partial \xi_A}{\partial x} \right)_O \frac{\partial \xi_A}{\partial x} \right] = 0, \quad (6.69)$$

Whereat the derivation equals zero due to the constant mass flow. To solve this differential equation, the boundary conditions shall be defined. Because of the second order differential equation it is necessary to define two boundary conditions. For  $x = 0$  (at the phase boundary), the mass fraction can be described, e.g. by Raoult's law. Hence the mass fraction,  $\xi_O$  is assumed to be known. Furthermore the mass fraction in the free-flow at the position  $x = L$  with  $\xi(L) = 0$  is known. The differential equation above (6.69) can be rewritten in a dimensionless form by using suitable reference values. Defining  $\phi = x/L$  and  $\theta = \xi_A/\xi_{A,O}$  yields the boundary conditions:

$$\text{BC1: for } \phi = \frac{0}{L} = 0, \theta = \frac{\xi_{A,O}}{\xi_{A,O}} = 1 \text{ applies} \quad (6.70)$$

$$\text{BC2: for } \phi = \frac{L}{L} = 1, \theta = \frac{0}{\xi_{A,O}} = 0 \text{ applies} \quad (6.71)$$

With this transformation and by introducing the constant

$$\Psi = -\frac{\xi_{A,O}}{1 - \xi_{A,O}} \left( \frac{\partial \theta_A}{\partial \phi} \right)_O \quad (6.72)$$

The following differential equation

$$\frac{\partial^2 \theta}{\partial \phi^2} - \Psi \frac{\partial \theta}{\partial \phi} = 0 \quad (6.73)$$

can be solved analytically. Introducing these dimensionless variables in equation (6.67) yields the mass flow

$$\dot{m}'' = \dot{m}_A'' = \frac{\rho D}{L} \Psi \quad (6.74)$$

In order to solve this differential equation,  $\frac{\partial \theta}{\partial \phi}$  is substituted by  $K$ , which simplifies (6.73) to

$$\frac{\partial K}{\partial \phi} = \Psi K \quad (6.75)$$

This equation is solved by separation of variables.

$$K = e^{\Psi\phi + c_1} \quad (6.76)$$

Resubstituting  $K$  and integrating a second time yields

$$\theta = \frac{1}{\Psi} e^{\Psi\phi + c_1} + c_2 \quad (6.77)$$

Using both boundary conditions and transforming the equation yields:

$$\theta = \frac{e^{\Psi\phi} - e^\Psi}{1 - e^\Psi} \quad (6.78)$$

By Differentiating this equation after  $\phi$  and evaluating the derivation at  $\phi = 0$  (at the wall), this gradient can be put into equation (6.72). This leads to the following relationship

$$e^\Psi = \frac{1}{1 - \xi_{A,O}} \text{ oder: } \Psi = \ln \left( \frac{1}{1 - \xi_{A,O}} \right) \quad (6.79)$$

Which yields the mass flow from equation (6.74) with units

$$\dot{m}'' = \dot{m}_A'' = \frac{\rho D}{L} \ln \left( \frac{1}{1 - \xi_{A,O}} \right) \quad (6.80)$$

As expected the mass flow proceeds in positive x-direction, because the concentration decreases in x-direction. Furthermore the concentration profile can be indicated:

$$\ln \left( \frac{1 - \xi_A}{1 - \xi_{A,O}} \right) = \frac{x}{L} \ln \left( \frac{1}{1 - \xi_{A,O}} \right) \quad (6.81)$$

It should be pointed out, that the concentration profile is logarithmic and not linear. This profile derives from convection, which in turn is caused by diffusion. With the definition of a mass transfer coefficient  $g^*$ , that already takes the Stefan-stream into account, in case of evaporation at an open surface, can be determined as

$$g^* = \rho \frac{D}{L} \frac{1}{\frac{\xi_{A,O}}{\ln(\frac{1}{1 - \xi_{A,O}})}} \quad (6.82)$$

The analogy to heat transfer should here be pointed out once more. In case of mere heat conduction, i.e. no convection, the Nusselt number is one. In the case that has just been regarded there was also no forced stream from outside, so in case of mere diffusion, the Sherwood number also equals one. With equation (6.47) this leads to a mass transfer coefficient of  $g = \frac{\rho D}{L}$ . Comparing this to (6.82) shows that a second term was added. This term is known as "high flux correction", because it considers

the diffusion driven convection that appears. This is the factor by which the mass transfer increases compared to mere diffusion.

---

# Literature

- [Bayley u. a. 1972] BAYLEY, F. J. ; OWEN, J. M. ; TURNER, A. B.: *Heat Transfer*. William Clowes & Sons, Ltd., London, 1972
- [Blasius 1908] BLASIUS, H.: Grenzschichten in Flüssigkeiten mit kleiner Reibung. In: *Z. Math. Phys.* 56 (1908), S. 1–37
- [Carlslaw u. Jaeger 1948] CARLSLAW, H. S. ; JAEGER, J. C.: *Conduction of Heat in Solids*. Clarendon Press, Oxford, 1948
- [Croft u. Lilley 1977] CROFT, D. R. ; LILLEY, D. G.: *Heat Transfer Calculations Using Finite Difference Equations*. Appl. Sci. Publ. Ltd., London, 1977
- [Einstein 1905] EINSTEIN, Albert: Über die von der molekularkinetischen Theorie der Wärme geforderte Bewegung von in ruhenden Flüssigkeiten suspendierten Teilchen. In: *Annalen der Physik* 322 (1905), Nr. 8, S. 549–560
- [Fick 1855] FICK, Adolf: On liquid diffusion. In: *Phil. Mag. and Jour. Sci.* 10 (1855), S. 31–39
- [Heisler 1947] HEISLER, M.P.: Temperature Charts for Induction and Constant Temperature Heating. In: *Trans. ASME* (1947), S. 227–236
- [Holman 1976] HOLMAN, J. P.: *Heat Transfer*. 4. McGraw-Hill Book Company, 1976
- [Jakob 1949] JAKOB, M.: *Heat Transfer*. John Wiley & Sons, New York, 1949
- [Jischa 1982] JISCHA, M.: *Konvektiver Impuls-, Wärme- und Stoffaustausch*. Friedr. Vieweg & Sohn, Braunschweig, 1982
- [Kestin u. a. 1961] KESTIN, J. ; MAEDER, P. F. ; WANG, H. E.: Influence of turbulence on the transfer of heat from plates with and without a pressure gradient. In: *International Journal of Heat and Mass Transfer* 3 (1961), Nr. 2, 133 – 154. [http://dx.doi.org/DOI:10.1016/0017-9310\(61\)90076-X](http://dx.doi.org/DOI:10.1016/0017-9310(61)90076-X). – DOI DOI: 10.1016/0017-9310(61)90076-X. – ISSN 0017-9310
- [Lienhard 2008] LIENHARD, John H. ; LIENHARD, John H. (Hrsg.): *A Heat Transfer Textbook, Third Edition*. Phlogiston Press, Cambridge Massachusetts, 2008
- [McAdams 1954] MCADAMS, W. H.: *Heat Transmission, 3rd Ed.* McGraw-Hill Publishing Company, London, 1954

- [Mersmann 1986] MERSMANN, A. ; MERSMANN, A. (Hrsg.): *Stoffübertragung*. Springer, Berlin, 1986
- [Ostrach 1953] OSTRACH, S.: An Analysis of Laminar Free Convection Flow and Heat Transfer about a Flat Plate Parallel to the Direction of the Generating Body Force. In: *NACA Rep. 1111* (1953)
- [Pohlhausen 1921] POHLHAUSEN, K.: Zur näherungsweisen Integration der Differentialgleichung der laminaren Grenzschicht. In: *ZAMM - Journal of Applied Mathematics and Mechanics / Zeitschrift für Angewandte Mathematik und Mechanik* 1 (1921), Nr. 4
- [Rohsenow u. Harnett 1973] ROHSENOW, W. M. ; HARNETT, J. P.: *Handbook of Heat Transfer*. McGraw-Hill Book Company, New York, 1973
- [Schlichting u. Gersten 2006] SCHLICHTING, H. ; GERSTEN, K.: *Grenzschichttherorie*. Springer, Berlin, 2006
- [Schneider 1955] SCHNEIDER, P.J.: *Conduction Heat Transfer*. Addison-Wesley Publishing Comp., 1955
- [Whitaker 1974] WHITAKER, S.: *Fundamental Principles of Heat Transfer*. Pergamon Press Inc., New York, 1974
- [Whitaker 1976] WHITAKER, S.: *Fundamental Principles of Heat Transfer*. Pergamon Press Inc., New York, 1976
- [Whitaker 1977] WHITAKER, Stephen: *Fundamental Principles of Heat Transfer*. Pergamon Press Inc., New York, 1977
- [Witte 1974] WITTE, U.: *Dampferzeugertechnik*. Vulkan-Verlag, Essen, 1974

---

# Appendix

## Material properties

Table 1: Metals at 20°C

	$\rho$ $10^3 \frac{kg}{m^3}$	$c$ $\frac{kJ}{kgK}$	$\lambda$ $\frac{W}{mK}$	$a$ $10^{-6} \frac{m^2}{s}$
Aluminium	2,70	0,888	237	98,80
Lead	11,34	0,129	35	23,90
Chromium	6,92	0,440	91	29,90
Iron	7,86	0,452	81	22,80
Gold	19,26	0,129	316	127,20
Copper	8,93	0,382	399	117,00
Magnesium	1,74	1,020	156	87,90
Manganese	7,42	0,473	21	6,00
Molybdenum	10,20	0,251	138	53,90
Sodium	9,71	1,220	133	11,20
Nickel	8,85	0,448	91	23,00
Platinum	21,37	0,133	71	25,00
Silver	10,50	0,235	427	173,00
Titanium	4,50	0,522	22	9,40
Wolfram	19,00	0,134	173	67,90
Zinc	7,10	0,387	121	44,00
Tin, white	7,29	0,225	67	40,80
Bronze	8,80	0,377	62	18,70
Cast iron	7,80	0,540	42...50	10...12
Carbon steal ( $< 0,4\%C$ )	7,85	0,465	42...50	12...15
Cr-Ni-steal (X12CrNi 18,8)	7,80	0,500	15	3,80

Table 2: Non-metal solids at 20°C

	$\rho$ $10^3 \frac{kg}{m^3}$	$c$ $\frac{kJ}{kgK}$	$\lambda$ $\frac{W}{mK}$	$a$ $10^{-6} \frac{m^2}{s}$
Acrylglass (Plexiglas)	1,18	1,44	0,184	0,108
Asphalt	2,12	0,92	0,7	0,36
Concrete	2,1	0,88	1	0,54
Ice (0°C)	0,917	2,04	2,25	1,203
Soil, coarse gravel	2,04	1,84	0,52	0,14
Soil, Sand, dry	1,65	0,8	0,27	0,2
Soil, Sand, wet	1,75	1	0,58	0,33
Soil, clay	1,45	0,88	1,28	1
Glass, window	2,48	0,7	0,87	0,5
Glass, mirror	2,7	0,8	0,76	0,35
Glass, quartz	2,21	0,73	1,4	0,87
Glass wool	1,2	0,66	0,046	0,58
Gypsum	1	1,09	0,51	0,47
Granite	2,75	0,89	2,9	1,18
Cork	0,19	1,88	0,041	0,115
Marble	2,6	0,8	2,8	1,35
Mortar	1,9	0,8	0,93	0,61
Paper	0,7	1,2	0,12	0,14
Polyethylene	0,92	2,3	0,35	0,17
Polytetrafluorehylene	2,2	1,04	0,23	0,1
PVC	1,38	0,96	0,15	0,11
Porcelain (95°C)	2,4	1,08	1,03	0,4
Hard coal	1,35	1,26	0,26	0,15
Pine wood (radial)	0,415	2,72	0,14	0,12
Plaster	1,69	0,8	0,79	0,58
Bricks	1,6...1,8	0,84	0,38...0,52	0,28...0,34

Table 3: Liquids at 1 bar

	$T$	$\rho$	$c_p$	$\lambda$	$\nu$	$a$	$Pr$
	$^{\circ}C$	$10^3 \frac{kg}{m^3}$	$\frac{kJ}{kgK}$	$\frac{W}{mK}$	$10^{-6} \frac{m^2}{s}$	$10^{-6} \frac{m^2}{s}$	-
Nitrogen	-190	0,861	1,988	0,161	0,321	0,0939	3,42
Water	0	0,9998	4,218	0,561	1,793	0,133	13,48
	20	0,9982	4,181	0,598	1,004	0,1434	7,001
	40	0,9922	4,177	0,631	0,658	0,1521	4,3280
	60	0,9832	4,184	0,654	0,475	0,1591	2,983
	80	0,9718	4,197	0,67	0,365	0,1643	2,221
	99,63	0,9586	4,216	0,679	0,295	0,168	1,757
aqueous organic. solution	non- so- 21%	-10	1,187	3,312	0,528	4,02	0,136
NaCl							
Benzene	20	0,879	1,738	0,154	0,74	0,101	7,33
Methanol	20	0,792	2,495	0,22	0,737	0,111	6,57
Fuel Oil	20	0,819	2	0,116	1,82	0,0709	25,7
	100	0,766	2,38	0,104	0,711	0,0572	12,4
Mercury	20	13,55	0,139	9,3	0,115	4,9	0,023

Table 4: Gases at 1 bar

	$T$	$\rho$	$c_p$	$\lambda$	$\nu$	$a$	$Pr$
	$^{\circ}C$	$\frac{kg}{m}$	$\frac{kJ}{kgK}$	$10^{-3} \frac{W}{mK}$	$10^{-6} \frac{m^2}{s}$	$10^{-6} \frac{m^2}{s}$	-
Air	-200	5,106	1,186	6,886	0,979	1,137	0,8606
	-100	2,019	1,011	16,2	5,829	7,851	0,7423
	0	1,275	1,006	24,18	13,52	18,83	0,7179
	20	1,188	1,007	25,69	15,35	21,47	0,7148
	40	1,112	1,007	27,16	17,26	24,24	0,7122
	80	0,9859	1,01	30,01	21,35	30,14	0,7083
	100	0,9329	1,012	31,39	23,51	33,26	0,707
	200	0,7356	1,026	37,95	35,47	50,3	0,7051
	400	0,517	1,069	49,96	64,51	90,38	0,7137
	600	0,3986	1,116	61,14	99,63	137,5	0,7247
	800	0,3243	1,155	71,54	140,2	191	0,7342
	1000	0,2734	1,185	80,77	185,9	249,2	0,7458
Steam	100	0,5896	2,042	25,08	20,81	20,83	0,999
	200	0,4604	1,975	33,28	35,14	36,6	0,96
	400	0,3223	2,07	54,76	75,86	82,07	0,9243
	600	0,2483	2,203	79,89	131,4	146,1	0,8993
	800	0,2019	2,343	107,3	199,9	226,8	0,8816
	1000	0,1702	2,478	163,3	280	323,2	0,8665
Hydrogen	0	0,0886	14,24	176	95	139	0,68
	50	0,0748	14,36	202	126	188	0,67
	100	0,0649	14,44	229	159	244	0,65
Carbon dioxide	0	1,95	0,829	14,3	7,1	8,86	0,8
	50	1,648	0,875	17,8	9,8	12,3	0,8
	100	1,428	0,925	21,3	12,4	16,1	0,8
Helium	27	0,1625	5,193	155,7	122,6	184,5	0,655

Table 5: Binary diffusion coefficients

Composition	<i>T</i>	<i>D</i>
	<i>K</i>	$10^{-4} \frac{m^2}{s}$
Air- <i>CO</i> <sub>2</sub>	276	0,144
	317	0,179
Air- <i>C</i> <sub>2</sub> <i>H</i> <sub>5</sub> <i>OH</i>	313	0,147
Air- <i>He</i>	276	0,632
Air- <i>H</i> <sub>2</sub> <i>O</i>	313	0,292
<i>CO</i> <sub>2</sub> - <i>H</i> <sub>2</sub> <i>O</i>	307	0,201
<i>He</i> - <i>H</i> <sub>2</sub> <i>O</i>	352	1,136
<i>H</i> <sub>2</sub> - <i>H</i> <sub>2</sub> <i>O</i>	307	0,927
<i>CH</i> <sub>4</sub> - <i>H</i> <sub>2</sub> <i>O</i>	352	0,361

Table 6: Diluted aqueous solutions

Composition	<i>T</i>	<i>D</i>
	<i>K</i>	$10^{-9} \frac{m^2}{s}$
<i>CH</i> <sub>4</sub> - <i>H</i> <sub>2</sub> <i>O</i>	275	0,85
	333	3,55
<i>CO</i> <sub>2</sub> - <i>H</i> <sub>2</sub> <i>O</i>	298	2
<i>CH</i> <sub>3</sub> <i>OH</i> - <i>H</i> <sub>2</sub> <i>O</i>	288	1,26
<i>C</i> <sub>2</sub> <i>H</i> <sub>5</sub> <i>OH</i> - <i>H</i> <sub>2</sub> <i>O</i>	288	1
<i>O</i> <sub>2</sub> - <i>H</i> <sub>2</sub> <i>O</i>	298	2,4
<i>N</i> <sub>2</sub> - <i>H</i> <sub>2</sub> <i>O</i>	298	2,6
<i>H</i> <sub>2</sub> - <i>H</i> <sub>2</sub> <i>O</i>	298	6,3

Table 7: Emissivity ( $\varepsilon$ ) of various solids $(\varepsilon_n)$  : in normal direction of the surface $(\varepsilon)$  : total emissivity

Surface	T K	$(\varepsilon_n)$	$(\varepsilon)$	Surface	T K	$(\varepsilon_n)$	$(\varepsilon)$
<b>1. Metals</b>							
Aluminum, plain	443	0,039	0,049	Zinc. highly polished	500	0,045	
- , polished	373	0,095			600		0,055
- , heavily oxidized	366	0,2		Iron Plate, galvanized			
	777	0,31		- , plain	301	0,228	
Aluminum Oxide	550	0,63		- , gray oxidized	297	0,276	
	1100	0,26		Tin. non oxidized	298		0,043
	1089	0,052			373	0,05	
Chromium, polished	423	423	423	<b>2. Non-Metals</b>			
Gold, highly polished	500	0,018		Asbestos	296	0,96	
Copper, polished	293	0,03		- , paper	311	0,93	
- , struck	293	0,037			644	0,94	
- , black oxidized	293	0,78		Roofing felt	294	0,91	
- , oxidized	403	0,76		Gypsum	293	0,8 - 0,9	
Inconel, rolled	1089		0,69	Glass	293	0,94	
- , sandblasted	1089		0,79	Quarz /7 mm thick)	555	0,93	
Iron and Steel,					1111	0,47	
- , polished	700	0,144		Rubber	293	0,92	
	1300	0,377		Holz,			
- , sanded	293	0,242		- , Beech	343	0,94	0,91
Cast iron, polised	473	0,21		Ceramics			
Cast steal, polished	1044	0,52		White $AL_2O_3$	366		0,9
	1311	0,56		Carbon,			
Iron sheet				not oxidized	298	0,81	
- , heavy rusty	292	0,685			773	0,79	
- , rolled	294	0,657		- , Fibers	533	0,95	
Cast iron,				- , Graphite	373	0,76	
oxidized at 866 K	472	0,64		Corundum rough	353	0,85	0,84
	872	0,78		Coating, Colors:			
Steal,				Oil Paint, black	366	0,92	
oxidized at 866 K	472	0,79		- , green	366	0,95	
	872	0,79		- , red	366	0,97	
Messing, not oxidized	298	0,035		- , white	373	0,925	
	373	0,035		Coating, white			
- , oxidized	473	0,61		- , flat black	353	0,935	0,97
	873	0,59		Bakelite Coating	353	0,93	
Nickel, not oxidized	298	0,045		Mennig Color	373		
	373	0,06		Radiator (acc. to VDI-74) 373	0,925		
	873	0,478		Enamel. white on iron	292	0,897	
- , oxidized	473	0,37		Marble			
Platinum	422	0,022		- light gray. polished	273-366	0,9	
	1089	0,123		Paper	273	0,92	
Mercury,					366	0,94	
not oxidized	298	0,1		Porcelain, white	295	0,924	
	373	0,12		Clay, glassy	298	0,9	
Silver, polished	311	0,022		- , flat	298	0,93	
	644	0,031		Water	273	0,95	
Wolfram	298		0,024	Ice. smooth with water	273	0,966	0,92
	1273		0,15	- , rough surface	273	0,985	
	1773		0,23	Bricks. red	273-366		0,93

## Bessel function

### Error function

$$\operatorname{erf}(\eta) = \frac{2}{\sqrt{\pi}} \int_{\xi=\eta}^{\xi=o} e^{-\xi^2} d\xi$$

complimentary error function

$$\operatorname{erfc}(\eta) = 1 - \operatorname{erf}(\eta) = \frac{2}{\sqrt{\pi}} \int_{\xi=\eta}^{\xi=\infty} e^{-\xi^2} d\xi$$

characteristics

$$\operatorname{erf}(\infty) = 1 \quad \operatorname{erf}(-\eta) = -\operatorname{erf}(\eta) \quad \frac{d}{d\eta} [\operatorname{erf}(\eta)] = \frac{2}{\sqrt{\pi}} e^{-\eta^2}$$

Table 1:

$\eta$	$erf(\eta)$	$erfc(\eta)$	$\frac{2}{\sqrt{\pi}}e^{-\eta^2}$
0	0	1	1,128
0,05	0,0564	0,944	1,126
0,1	0,112	0,888	1,117
0,15	0,168	0,832	1,103
0,2	0,223	0,777	1,084
0,25	0,276	0,724	1,06
0,3	0,329	0,671	1,031
0,35	0,379	0,621	0,998
0,4	0,428	0,572	0,962
0,45	0,475	0,525	0,922
0,5	0,52	0,48	0,879
0,55	0,563	0,437	0,834
0,6	0,604	0,396	0,787
0,65	0,642	0,378	0,74
0,7	0,678	0,322	0,691
0,75	0,711	0,289	0,643
0,8	0,742	0,258	0,595
0,85	0,771	0,229	0,548
0,9	0,797	0,203	0,502
0,95	0,821	0,179	0,458
1	0,843	0,157	0,415
1,1	0,88	0,12	0,337
1,2	0,91	0,09	0,267
1,3	0,934	0,066	0,208
1,4	0,952	0,048	0,159
1,5	0,966	0,034	0,119
1,6	0,976	0,024	0,087
1,7	0,984	0,016	0,063
1,8	0,989	0,011	0,044
1,9	0,993	0,007	0,03
2	0,995	0,005	0,021

Table 2: Bessel functions

x	$I_0(x)$	$I_1(x)$	$2/\pi \cdot K_0(x)$	$2/\pi \cdot K_1(x)$
0	1	0	$\infty$	
0,2	1,01	0,1005	1,116	3,041
0,4	1,0404	0,204	0,7095	1,391
0,6	1,092	0,3137	0,495	0,8294
0,8	1,1665	0,4329	0,3599	0,5486
1	1,2661	0,5652	0,268	0,3832
1,2	1,3937	0,7147	0,2028	0,2768
1,4	1,5534	0,8861	0,1551	0,2043
1,6	1,75	1,0848	0,1197	0,1532
1,8	1,9896	1,3172	$0,9290 \times 10^{-1}$	0,1163
2	2,2796	1,5906	0,7251	$0,8904 \times 10^{-1}$
2,2	2,6291	1,9141	0,5683	0,6869
2,4	3,0493	2,2981	0,447	0,533
2,6	3,5533	2,7554	0,3527	0,4156
2,8	4,1573	3,3011	0,279	0,3254
3	4,8808	3,9534	0,2212	0,2556
3,2	5,7472	4,7343	0,1757	0,2014
3,4	6,7848	5,6701	0,1398	0,1592
3,6	8,0277	6,7028	0,1114	0,1261
3,8	9,5169	8,1404	$0,8891 \times 10^{-2}$	$0,9999 \times 10^{-2}$
4	11,302	9,7595	0,7105	0,7947
4,2	13,443	11,706	0,5684	0,6327
4,4	16,01	14,046	0,4551	0,5044
4,6	19,093	16,863	0,3648	0,4027
4,8	22,794	20,253	0,2927	0,3218
5	27,24	24,336	0,235	0,2575

Table 3: Bessel-Funktionen 1. und 2. Art,  $5 \leq x \leq 10$ 

x	$I_0(x)$	$I_1(x)$	$2/\pi \cdot K_0(x)$	$2/\pi \cdot K_1(x)$
5	27,24	24,336	0,235	0,2575
5,2	32,584	29,254	0,1888	0,2062
5,4	39,009	35,182	0,1518	0,1653
5,6	46,738	42,328	0,1221	0,1326
5,8	56,038	50,946	$0,9832 \times 10^{-3}$	0,1064
6	67,234	61,342	0,792	$0,8556 \times 10^{-3}$
6,2	80,718	73,886	0,6382	0,6879
6,4	96,962	89,026	0,5146	0,5534
6,6	116,54	107,31	0,4151	0,4455
6,8	140,14	129,38	0,335	0,3588
7	168,59	156,04	0,2704	0,2891
7,2	202,92	188,25	0,2184	0,2331
7,4	244,34	227,18	0,1764	0,188
7,6	294,33	274,22	0,1426	0,1517
7,8	354,69	331,1	0,1153	0,1424
8	427,56	399,87	$0,9325 \times 10^{-4}$	$0,9891 \times 10^{-4}$
8,2	515,59	483,05	0,7543	0,7991
8,4	621,94	583,66	0,6104	0,6458
8,6	750,46	705,38	0,4941	0,522
8,8	905,8	852,66	0,4	0,4221
9	1.093	1.030,90	0,3239	0,3415
9,2	1.320,70	1.246,70	0,2624	0,2763
9,4	1.595,30	1.507,90	0,2126	0,2236
9,6	1.927,50	1.824,10	0,1722	0,181
9,8	2.329,40	2.207,10	0,1396	0,1465
10	2.815,70	2.671,00	0,1131	0,1187